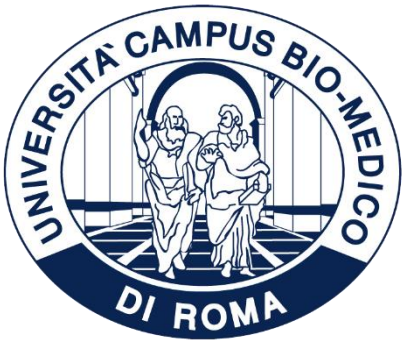

UNIVERSITÀ CAMPUS BIO-MEDICO DI ROMA

DEPARTMENTAL FACULTY OF ENGINEERING

Ph.D. Course in Science and Engineering for Humans and Environment
Curriculum Bioengineering

XXXVII Cycle

Development of new technological solutions in Otorhinolaryngology: from respiratory monitoring to prevention of otological disorders.

Coordinator
Prof. Giulio Iannello

Supervisors
Prof. Manuele Casale
Prof. Emiliano Schena

Ph.D. Candidate
Lucrezia Giorgi

Contents

List of Figures

List of Tables

List of Acronyms

Acronym	Definition
AASM	American Academy of Sleep Medicine
AHI	Apnea-Hypopnea Index
AI	Artificial Intelligence
BH	Zephyr^{tm} Bioharness 3.0
BMI	Body Mass Index
DL	Deep Learning
ECG	Electrocardiography
ENT	Ear, Nose, And Throat
ESS	Epworth Sleepiness Scale
FFT	Fast Fourier Transform
HL	Hearing Loss
HSAT	Home Sleep Apnea Test
LOA	Limits of Agreements
MAE	Mean Absolute Error
MAPE	Mean Absolute Percentage Error
ML	Machine Learning
MOD	Mean of Difference
NIHL	Noise-Induced Hearing Loss
NTC	Negative Temperature Coefficient
OSA	Obstructive Sleep Apnea
PAT	Peripheral Arterial Tone
PPE	Personal Protection Equipment
PSG	Polysomnography
QB	Quiet Breathing
RMS	Root Mean Square
RR	Respiratory Rate
SD	Standard Deviation
SFM	Smart Face Mask
SNHL	Sensorineural Hearing Loss
UA	Upper Airways
WB	Wheatstone Bridge

Abstract

The integration of engineering and medicine is driving significant advancements in healthcare, with innovations enhancing diagnosis and treatment guided by a patient-centered care view. In otorhinolaryngology, where complex anatomy and diverse disorders pose challenges, technological progress in minimally invasive techniques and precision tools have improved patient outcomes.

The present Ph.D. dissertation aims to present the results of developing novel technological solutions in the otorhinolaryngology field, addressing key challenges in monitoring respiratory and sleep-related breathing disorders and the prevention of otological disorders. The solutions presented in this thesis were validated in real-life settings or under controlled conditions that mimic real-world scenarios.

The first chapter of the thesis introduces the three otorhinolaryngological diseases considered during the Ph.D. work, such as respiratory disease, sleep-related breathing disorders, and noise-induced hearing loss.

Chapter 2 presents the design and development of a smart face mask for unobtrusive respiratory monitoring. The smart face mask device integrates two temperature sensors and is able to detect the respiratory rate of the subjects. The face mask was validated in static and dynamic conditions to replicate possible real-world scenarios. The results demonstrated high accuracy in estimating respiratory rate in static and dynamic conditions, both during quiet breathing and tachypnoea.

The third chapter focuses on a non-invasive system for detecting obstructive sleep apnea by analyzing snoring sounds. The study introduces an algorithm that identifies apnea events caused by airway obstruction based on snoring sound patterns. The algorithm was tested on healthy subjects and patients, showing promising results as a potential screening tool.

Chapter 4 introduces a novel protective earplug to mitigate the impact of high-frequency sounds from medical instruments while minimally affecting speaking frequencies. Among the professionals affected by this disease, the device was tested on 20 dental professionals during an 8-hour workday. The results showed positive feedback on the ability to communicate with patients and colleagues and on the noise attenuation.

The last chapter summarizes the study conducted during the Ph.D. by reporting the main findings and future applications in everyday clinical practice.

1 Innovations in Otorhinolaryngology: Clinical needs and opportunities

1.1 New device in Otorhinolaryngology: Clinical needs and opportunities for technological innovation

Otorhinolaryngology, commonly referred to as ENT (Ear, Nose, and Throat), is a specialized medical field dedicated to the diagnosis and treatment of disorders affecting different anatomical districts, such as the ear, nose, throat, head, and neck. For this reason, otolaryngologists treat various medical issues, from balance disorders and ear infections to nasal congestion, diseases that affect the upper respiratory tract, and voice disorders. The specialty is defined by complex anatomy and often difficult surgical access, and professionals in this field have embraced this challenge by continually striving for the least invasive means possible for the precise articulation of this anatomy. Indeed, this field has continuously evolved through technological advancements, ranging from early light-assisted tools to contemporary techniques such as endoscopy, microscopy, and robotic surgery. These innovations have significantly enhanced visualization and precision, enabling less invasive approaches and improved patient outcomes.

Despite these advancements, the diagnosis of ENT conditions often relies on conventional tools such as otoscopy and endoscopy, which are heavily dependent on the practitioner's technical skills and subjective judgment. This can lead to variability in diagnostic accuracy, highlighting the urgent need for more objective and reliable diagnostic methods.

The diagnosis of ENT diseases is typically conducted through a medical interview and an otoscopic or endoscopic examination, performed daily by otolaryngologists and general practitioners as part of routine care. However, it has been noted that the diagnosis using these common tools is susceptible to misdiagnosis due to the reliance on the technical skills and experience of the physician, as well as the subjective bias of the observer [1]. This highlights the need for more objective and accurate diagnostic tools for ENT

healthcare. Continued research into innovative technologies and sustainable practices remains essential to bridge the gap between resource-rich centers and underserved communities worldwide. Indeed, ENT diseases are highly prevalent in the population. As an example, according to the World Health Organization (WHO), deafness and hearing loss (HL) are widespread and found in every region and country. Currently, more than 1.5 billion people (nearly 20% of the global population) live with HL; 430 million of them have disabling HL. It is expected that by 2050, there could be over 700 million people with disabling HL. Many of the impacts of HL can be mitigated through early detection and interventions. These include specialized education programs and sign language instruction for young children and their families. Assistive technologies, including hearing aids, cochlear implants, and hearing protection devices, can help people prevent and deal with HL at any age. People may also benefit from speech therapy, aural rehabilitation, and other related services [2].

Another common type of disorder is upper airway (UA) disorder, a condition that affects the ability to breathe and is caused by an acute infection, which involves the upper respiratory tract, including the nose, sinuses, pharynx, larynx, or trachea. Symptoms of UA disorders may include difficulty breathing, chronic dry cough, nasal obstruction, sore throat, tonsillitis, sinusitis, otitis media, and the common cold. Lastly, it is important to know that respiratory disease can also occur during the night. These are called Sleep-Related Breathing Disorders and encompass a spectrum of chronic conditions ranging from snoring, UA resistance syndrome, Obstructive Sleep Apnea (OSA), and central sleep apnea. Their prevalence is very high, ranging from 3.1% for UA resistance syndrome (4.4% in women and 1.5% in men) [3] to a higher percentage for OSA with approximately one billion individuals affected worldwide (24% of men and 9% of women) [4], [5]. Though the prevalence of central sleep apnea is lower than OSA, both conditions often coexist, and patients can exhibit features of both states [6]. Also, the prevalence of central sleep apnea tends to increase with age and is higher in the elderly population above 65 [7]. This can be explained by the relatively increased chemo responsiveness in the elderly population, which is prone to developing central apnea, particularly during non-rapid eye movement (NREM) sleep [8].

1.2 Main Otorhinolaryngological Pathologies

1.2.1 Upper Airways Respiratory Disorders

The respiratory system is composed of the airways, which are hollow structures responsible for air passage, enabling its transport from the external environment, and the lungs, parenchymal organs that perform hematosis (the exchange of oxygen and carbon dioxide between blood and air).

The airways are commonly divided into UAs, which include the nose, the nasal portion of the pharynx, the larynx, and the lower airways, consisting of the trachea and bronchial branches (Figure 1).

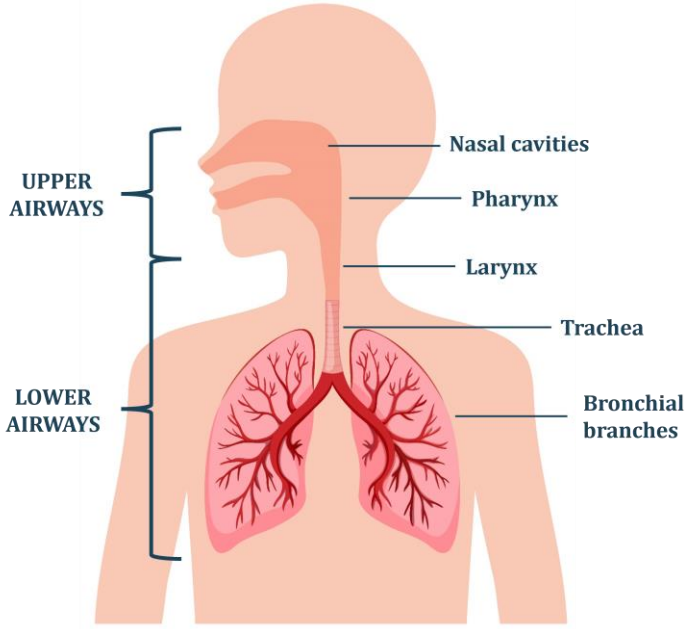

Figure 1: Anatomy of the upper and lower airways.

Otorhinolaryngology primarily addresses conditions affecting the UA. For this reason, the following discussion will introduce the anatomy and physiology of the nose and the mechanics of respiration.

The nasal cavities, shown in Figure 2, represent the primary filtration system of the airways, preventing the inhalation of harmful and toxic particles that could damage the lower respiratory tract. Beyond their respiratory and olfactory functions, nasal cavities play a critical role in filtering, warming, and humidifying inhaled air before it reaches the

lower airways. Anatomically, the nasal cavities can be divided into three parts: the vestibule, the olfactory region, and the respiratory region.

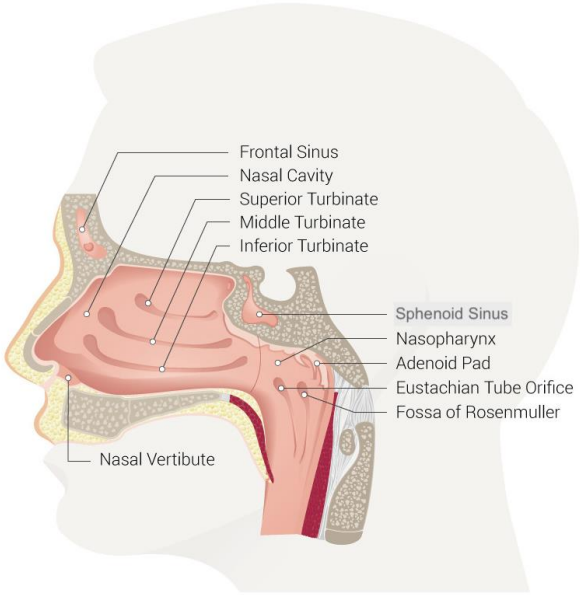

Figure 2: Anatomy of the nasal cavity, including the frontal sinus, superior turbinate, middle turbinate, inferior turbinate, sphenoid sinus, nasopharynx, adenoid pad, eustachian tube orifice, fossa of Rosenmuller, and nasal vestibule [9].

The nasal vestibule, located at the most anterior part of the nasal cavities inside the nostrils, has a surface area of approximately 0.60 cm^2 in adults. The vestibule contains vibrissae, hair-like structures that trap inhaled particles. Posterior to the vestibule lies the respiratory region, accessed through the atrium. This region is subdivided into three sections separated laterally by the superior, middle, and inferior turbinates. The respiratory nasal mucosa consists of pseudostratified epithelium of columnar, mucus-containing goblet cells and basal cells, supported by a lamina propria rich in blood vessels. The olfactory region is located in the upper portion of the nasal cavities, extending to the septum and lateral walls. Like the respiratory mucosa, the olfactory mucosa is composed of pseudostratified epithelium but includes specialized cells with olfactory receptors critical for odor perception.

The nose serves as the entryway to the respiratory system. Inspired air is channeled into a laminar flow by the structures of the nasal valve and muscles. Indeed, the nasal cavity contains a series of fissures formed between the walls and turbinates, between the septum and turbinates, and among the turbinates themselves. In this way, the fissures force the airflow to be laminar. This laminar flow is further modulated by

microturbulence created by the turbinates and meat along the lateral nasal wall, enhancing the contact between the airflow and the mucosal surface. This spiral motion brings the air into close contact with the mucosa, which is richly vascularized and contains valve-like structures between arteries and veins that regulate blood flow. This process mimics a radiator's function: air moves through these structures, warms up, becomes lighter, and rises, creating a continuous circulation driven by the pressure difference between the external environment and the nasal cavity. The primary purpose of this complex system is to warm and humidify inspired air, ensuring it reaches the lungs at a temperature close to blood temperature. This prevents excessive heat loss through respiration. Humidification also protects the integrity of the mucosa, as dryness could foster bacterial growth and infections. Properly functioning mucosa warms the air, humidifies it, and induces vortical airflow that helps trap airborne particles. These particles, often laden with bacteria or allergens, are driven to the periphery of the vortex and captured by the mucosa, preventing them from reaching deeper into the respiratory system. Increased blood flow causes the mucosa to swell, reducing the available cavity space. For instance, during a cold, inflammation increases blood flow, mucosal swelling, and reduced cavity space, resulting in nasal congestion.

If the mucosa’s functions are impaired, the lower airways become more vulnerable to pollution and infections. Chronic conditions, such as rhinitis or persistent colds, can lead to mucosal atrophy, as seen in chronic allergies, further compromising respiratory protection [10].

People can come into contact with hazardous substances in various situations, from air pollution in large cities to exposure to particles in specific work environments. These substances include volatile organic compounds, vitreous fibers, chemicals, metals, respirable dust (such as silica and coal mine dust), fumes, vapors, gases, and contagious pathogenic materials. Exposure to these respiratory sensitizers has been linked to several respiratory conditions, including rhinitis, asthma, chronic obstructive pulmonary disease, and irritation of mucous membranes [11], [12]. Additionally, it can cause restrictive illnesses like pulmonary fibrosis, pneumoconiosis, and malignancies, including lung cancer and mesothelioma. The risk of exposure to chemical and biological risks and work-related disease incidence is highly concentrated in four occupational groups: technicians, operators, agricultural workers, and workers in elementary occupations [11], [12]. Also, recently, great attention has been given to the problem of environmental pollution, especially in large cities, which subjects people to serious health problems [13]. Indeed, research has shown that exposure to air pollution has

several negative consequences for health. Short-term exposure can lead to hospital admissions caused by respiratory and/or cardiovascular diseases, days of restricted activity, absence from work or school, and acute symptoms such as cough, asthma, and dyspnea [13]–[15]. Prolonging exposure can affect the functioning of the autonomic nervous system, the immune system, and the antioxidant system. This can cause systemic inflammation, respiratory and cardiovascular disease, lung cancer, and chronic obstructive pulmonary disease. Also, exposure to such agents increases the possibility of adverse birth outcomes, such as preterm birth, lower birth weight, and post-natal infant mortality [13], [15], [16].

Awareness of this topic has undoubtedly increased with the advent of the COVID-19 pandemic. Since then, attention to respiratory diseases has grown significantly, leading to more preventive measures, such as monitoring for potential respiratory illnesses and protection through face masks. In fact, the importance of keeping track of respiratory parameters as indicators of a subject's health status is becoming increasingly recognized. Among these, respiratory rate (RR) has been shown to provide information about patients' clinical deterioration. Indeed, an abnormal RR can predict potential clinically severe events such as readmission to an intensive care unit, adverse cardiac events, pneumonia, pulmonary embolism, obstructive sleep apnea, and overdose. Moreover, because relative changes in RR are greater in magnitude than blood pressure and heart rate, they appear to be a better discriminator in identifying patients at high risk of cardiopulmonary deterioration. In addition, RR responds to various stressors and can indicate pain, emotional and environmental stress, and cognitive load. Not related to the clinical field, RR detection can also be used to detect the presence of respiration and as an indicator of physical exertion and fatigue associated with exercise tolerance [17], [18]. Some examples of applications of RR monitoring are summarized in Figure 3.

Various technologies are available to measure RR, depending on the specific application, the measurement requirements, and the user needs. However, none of them is widely available and enables accurate and continuous RR monitoring across multiple settings. It is essential to develop a non-intrusive, comfortable, and reliable solution that ensures accurate measurement without causing discomfort to the user. Such a system should be applicable in both clinical and non-clinical environments, facilitating remote patient monitoring, early detection of respiratory conditions, and seamless integration into daily activities.

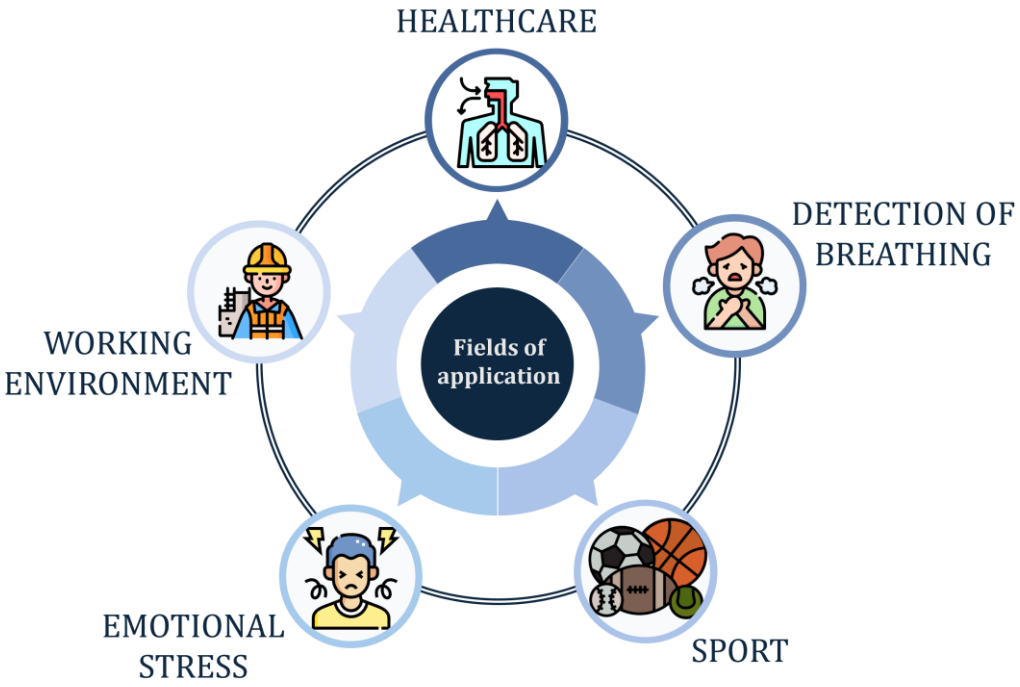

Figure 3: Fields of application of RR monitoring.

1.2.2 Sleep-Related Breathing Disorders

Sleep-related breathing disorders encompass a spectrum of chronic conditions, including snoring, upper airway resistance syndrome, OSA, and central sleep apnea.

The most common disorder is snoring, a vibratory sound that appears during the inspiratory and sometimes the expiratory phase of the respiratory cycle. The sound is caused by pharyngeal tissue vibration due to airflow through a narrowed airway. During sleep, the relative atonia of the upper airway dilator muscles induces narrowing and increased resistance at this level. Consequently, airflow becomes turbulent, and the pharyngeal tissues vibrate as the air passes through. More specifically, snoring is characterized by oscillations of the soft palate, pharyngeal walls, epiglottis, and tongue [19]. To better understand the impact of pharyngeal anatomy on airflow, the upper airway can be modeled as a Starling resistor. As shown in Figure 4, the pharynx is treated as a collapsible conduit located between the rigid upstream structure of the nasal cavity and the rigid downstream structure of the trachea. During inspiration, if the pressure at the level of the trachea (P_t) falls below the surrounding tissue pressure (P_{st})—due to either excessive inspiratory effort or elevated P_{st}—an obstruction forms, leading to flow limitation. This obstruction prevents the nasal cavity pressure (P_{nc}), typically equal to atmospheric pressure, from decreasing in response to the drop in P_t. Consequently, despite further decreases in tracheal pressure, the airflow remains constant and is determined only by the difference between the upstream pressure and surrounding tissue pressure. According to the Starling resistor model, snoring occurs during flow limitation when $P_{nc} > P_{st} > P_t$. If P_{nc} drops below P_{st}—commonly due to a further increase in P_{st}—airflow ceases, resulting in apnea ($P_{st} > P_{nc} > P_t$) [20], [21].

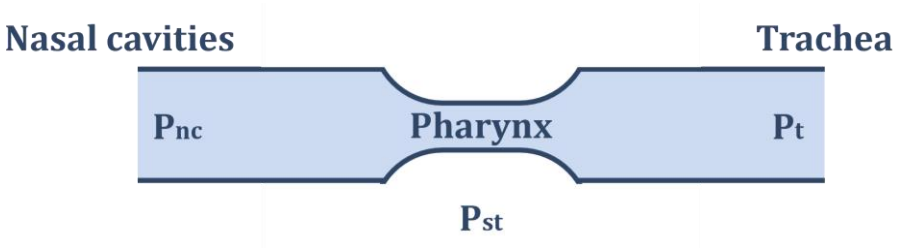

Figure 4: Modelling upper airways as Starling resistor.

However, models based on the Starling resistor have the major limitation of not including the mechanical characteristics, muscle activity, and functional anatomy of the airway walls, which also contribute to the collapse [22].

Loud snoring is the primary clinical characteristic of OSA. Patients with OSA commonly exhibit loud snoring, with a typical snoring pattern that includes 4–5 loud noises followed by silence (apnea), resumed breathing, and further noise, often accompanied by choking or gasping sounds. This symptom usually shows up more when lying down or right after drinking alcohol. However, occasionally, snoring might not be as noticeable, even in severe sleep apnea cases. Additionally, there is mounting evidence that, even in the absence of OSA, snoring may contribute to daytime sleepiness. Daytime sleepiness is a hallmark symptom resulting from hypoxemia and REM sleep fragmentation and is often reported during activities requiring sustained attention, such as driving. Tools such as the Epworth Sleepiness Scale (ESS) quantify the propensity to fall asleep in specific scenarios [23]. Other symptoms include fatigue, excessive night sweating, morning headaches, unrefreshing sleep, nasal obstruction, anxiety, social withdrawal, and decreased libido. This could be explained by either UA inflammation brought on by vibrations in the pharynx caused by snoring or by UA resistance, which is characterized by episodes of increased respiratory effort followed by arousals and daytime sleepiness. The term simple snorer is used to define snorers without any apneic events. The total snoring index is defined as the number of snore events in any body position (prone, supine, left, right, and upright) per hour of sleep [24].

Also, snoring every night can lead to fragmented sleep, reducing overall sleep quality and causing daytime fatigue, irritability, and decreased cognitive function. Moreover, snoring has been associated with multiple subclinical markers of cardiovascular pathology, including elevated blood pressure, increased carotid-intima-media thickness, stenosis, and atherosclerosis. These effects could partly reflect mechanical stress imposed by snoring vibrations on the UA in combination with a range of shared risk factors for OSA and cardiovascular disease, such as obesity and a sedentary lifestyle [25], [26].

OSA is a clinical condition characterized by intermittent, partial, or complete collapse of the UA during sleep, resulting in sleep fragmentation, hypoxemia, and excessive daytime sleepiness. The OSA syndrome encompasses a spectrum of severity, ranging from simple snoring without significant oxygen desaturation to severe cases with over 60–70 apneic episodes per hour and oxygen desaturation levels as low as 50%. While the precise mechanism of obstruction is not fully understood, it is known that oropharyngeal muscle hypotonia and the increase in negative pressure generated by the diaphragm and

intercostal muscles lead to a physiological reduction in upper airway patency, particularly at the level of the tongue base and pharyngeal walls [27].

OSA is also a significant risk factor for systemic conditions, particularly cardiovascular and endocrinological disorders [28]. The pathophysiology of OSA is multifactorial, involving a reduction in the size of the upper airways due to anatomical or functional abnormalities (e.g., obesity or craniofacial structural changes) [29] and increased pharyngeal collapsibility caused by impaired neuromuscular compensation and the absence of protective pharyngeal reflexes during sleep [30]. Upper airway collapse may be complete, leading to obstructive apnea (defined as airflow reduction >90% with persistent respiratory effort), or partial, leading to hypopnea (defined as ventilation reduction >30% with oxygen desaturation >3% or microarousals) [31]. These microarousals, lasting 3–15 seconds, are not perceived by the patient but cause REM sleep fragmentation. Intermittent hypoxia plays a key role in the pathophysiology of apnea, hypopnea, and their consequences, including excessive daytime sleepiness [32], cardiovascular comorbidities [33], and increased all-cause mortality, particularly in severe OSA [34]. Diagnosis relies on polysomnography, the gold-standard method [35]. This technique records the frequency of apnea events accompanied by arousal or a decrease in oxyhemoglobin saturation of ≥3%. Based on these observations, the apnea-hypopnea index (AHI) is calculated. Factors that may influence AHI levels include neck adiposity, age, alcohol consumption, certain medications, fluid balance, thyroid disorders, and body position [36].

Epidemiological studies estimate that the prevalence of OSA in the general population aged 30–60 years is 24% in men and 9% in women [37]. A recent study reported nearly 1 billion cases worldwide [4], raising significant public health concerns (Figure 5). Risk factors include obesity, age, and sex, alongside ethnicity, family history, and lifestyle habits such as alcohol consumption and smoking [38], [39].

According to a recent epidemiological study in Italy, there are 12,329,614 patients affected by moderate to severe OSA (27% of the population) and an overall prevalence of more than 24 million people aged from 15 to 74 years old (54% of the population). However, only 460,000 patients with moderate to severe OSA are diagnosed (4% of the estimated prevalence) and 230,000 treated (2% of the estimated prevalence), suggesting a substantial gap in the diagnostic and treatment workflow [40].

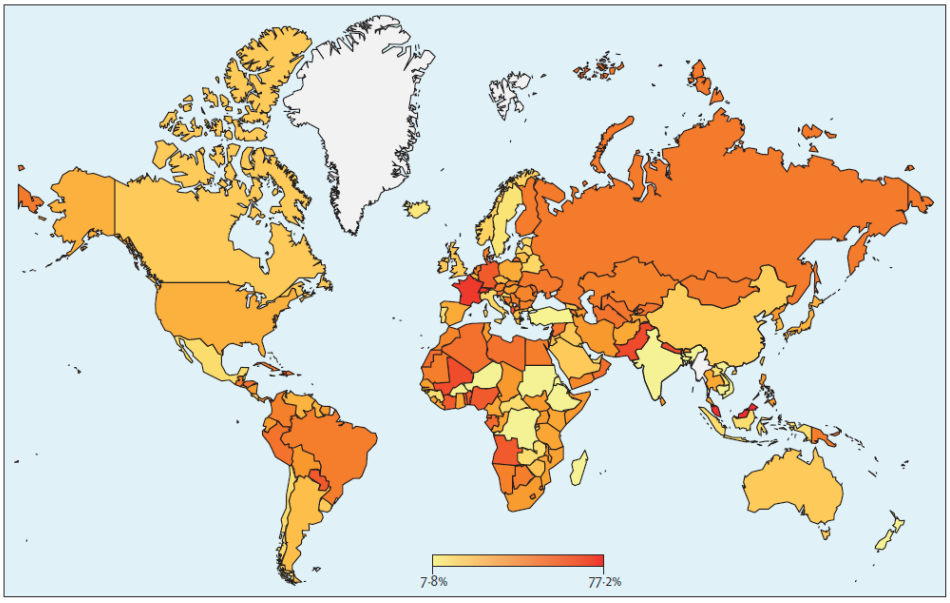

Figure 5: Global heat map of estimated prevalence of obstructive sleep apnea (AHI five or more events per h) for each country [4].

The risk of OSA correlates with body mass index (BMI) and increases with excess adipose tissue, which narrows the upper airways. Obesity can also reduce vital capacity, disrupt ventilation-perfusion ratios, and limit lung and chest wall movement [41]. Consequently, countries with high obesity rates report a higher incidence of OSA [42].

Although OSA can occur at any age, its prevalence tends to increase with age, plateauing after 65 years [34], [41], [43]. The male sex is an independent risk factor for OSA, with a male-to-female prevalence ratio of approximately 1.5:1 [44]. The reasons for this disparity remain partially understood.

Currently, the gold standard diagnostic method is the full-night Polysomnography (PSG), which requires the following measurements: electroencephalogram (EEG), electrooculogram (EOG), electrocardiogram (ECG) or heart rate, chin electromyography (EMG), airflow, arterial oxygen saturation, and respiratory effort [45]. However, the full PSG is highly costly due to the numerous measures required, the need for specialized staff, and the full-time night occupation of the laboratory. Alternatively, unattended tests, called Home Sleep Apnea Tests (HSATs), have been recently proposed [46]. Many insurance companies agree to the use of HSAT for OSA diagnosis since the Centers for Medicare and Medicaid Services declared in 2008 that the use of home testing is reimbursable [47], [48]. HSATs do not require sleep laboratories, are easier to perform, are less expensive, and are widely available. Some examples of HSAT devices available on the market are shown in Figure 6.

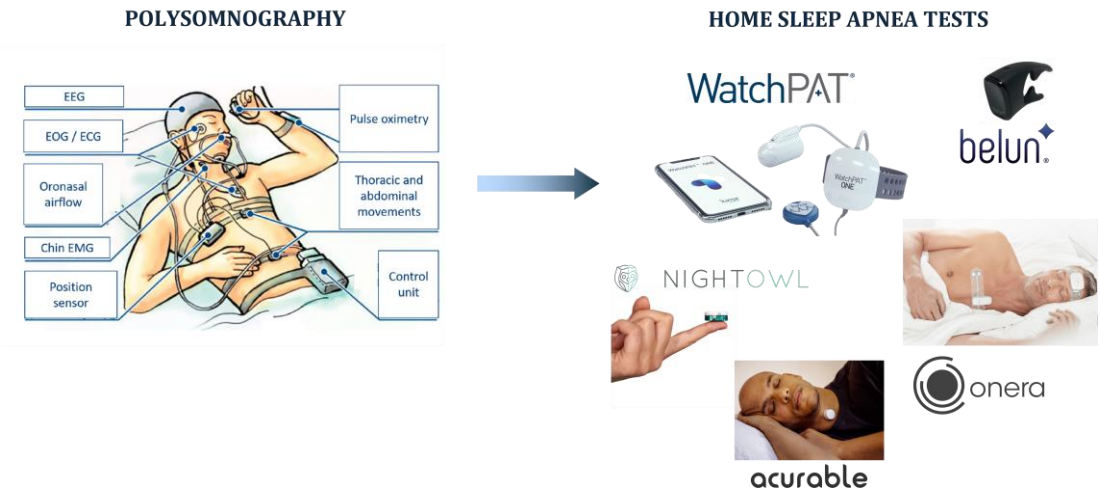

Figure 6: Transition from complete polysomnography (PSG) to home sleep apnea tests (HSAT). The figure shows some examples of HSAT devices available on the market.

Their introduction has indeed shortened the waiting list; however, this disorder remains highly underdiagnosed and undertreated. Therefore, new solutions are needed to increase the sample of the general population to be diagnosed and treated. In light of these challenges, a clinical prediction model that can accurately identify patients who are most likely to benefit from PSG has to be developed. Such a model should aim to exclude a diagnosis of OSA when the probability is low, establish the likelihood before considering PSG, and prioritize patients requiring PSG based on the probability of a positive outcome.

1.2.3 Otological Disorders

The ear is the primary organ of hearing and plays a fundamental role in everyday life, as sounds provide humans with a wealth of information. For example, sounds such as an alarm, a falling and breaking object, or a ringing alarm clock are crucial in alerting us to danger. Hearing is vital in hazardous situations and essential for communication, a fundamental aspect of human social interaction. The use of language involves a rapid and sophisticated analysis of sounds: sound waves reach the ears, are transformed into electrochemical signals, and are sent to the brain's auditory area. Subsequently, the language comprehension area, known as Wernicke's area, processes these sounds. Syllables are combined into words, and words into sentences, which are then synthesized into concepts within the brain's frontal cognitive areas. These concepts are further elaborated to enable the speaker to respond. This entire process occurs seamlessly, thanks to the auditory system - a continuously active structure that facilitates activities we often take for granted.

The human ear is composed of three main parts, as shown in Figure 7:

- Outer ear: Its function is to capture sound waves and transmit them to the tympanic membrane. It consists of the auricle and the external auditory canal, each fulfilling specific roles in sound transmission.
- Middle ear: Responsible for transmitting mechanical energy from the vibrations of the tympanic membrane to the inner ear. It includes the tympanic cavity, mastoid system, and Eustachian tube. The tympanic cavity is a biconcave lens-shaped cavity whose lateral wall, formed by the tympanic membrane, separates the outer ear from the middle ear. The tympanic cavity houses the three ossicles - malleus, incus, and stapes - linked by movable joints and anchored to the cavity walls by small ligaments. The malleus is attached to the tympanic membrane, and the base of the stapes adheres to the oval window, a small opening separating the middle ear from the inner ear. Sound waves set the tympanic membrane in motion, and the ossicular chain amplifies and transmits these vibrations to the inner ear. The mastoid system comprises bony cells in the mastoid process of the temporal bone, with the largest cell connecting to the tympanic cavity. The Eustachian tube, a bony and cartilaginous canal, links the middle ear to the nasopharynx and maintains equal pressure on both sides of the tympanic membrane, enabling optimal vibration.

- Inner ear: This consists of a series of cavities within the temporal bone forming the bony labyrinth, including the vestibule (a central cavity), three semicircular canals, and the cochlea. The cochlea is the most critical element of the inner ear. It is a conical mass of bony tissue containing a spiral canal housing the membranous cochlear duct, which includes the organ of Corti and auditory receptors. The cochlear duct is divided into three spaces: the cochlear duct proper or scala media in the center, the scala vestibuli above, and the scala tympani below. These compartments are filled with fluid—endolymph in the cochlear duct and perilymph in the scala vestibuli and scala tympani. Sound vibrations transmitted via the ossicles to the oval window generate fluid waves in the cochlea, initiating the mechanical deflection of the basilar membrane and signal transduction. The basilar membrane exhibits tonotopic organization, where each portion responds to specific frequencies: distal regions are sensitive to low frequencies, while proximal regions respond to higher frequencies (Figure 8). This organization is mirrored in the auditory cortex, where regions are mapped to specific frequencies.

Sound waves reach the cochlea as mechanical vibrations, which are converted into electrochemical signals by the hair cells contained in the basilar membrane, specialized receptors for signal transduction. The electrical signals generated by hair cells trigger neurotransmitter release, propagating action potential in the auditory nerve.

Cochlear stimulation occurs via two mechanisms:

- Air conduction: Sound travels through the outer and middle ear to the cochlea. This is the primary physiological mechanism for hearing.
- Bone conduction: Vibrations transmitted through the skull directly stimulate the cochlea. Under normal conditions, bone conduction contributes minimally to hearing due to impedance differences between air and cranial bone.

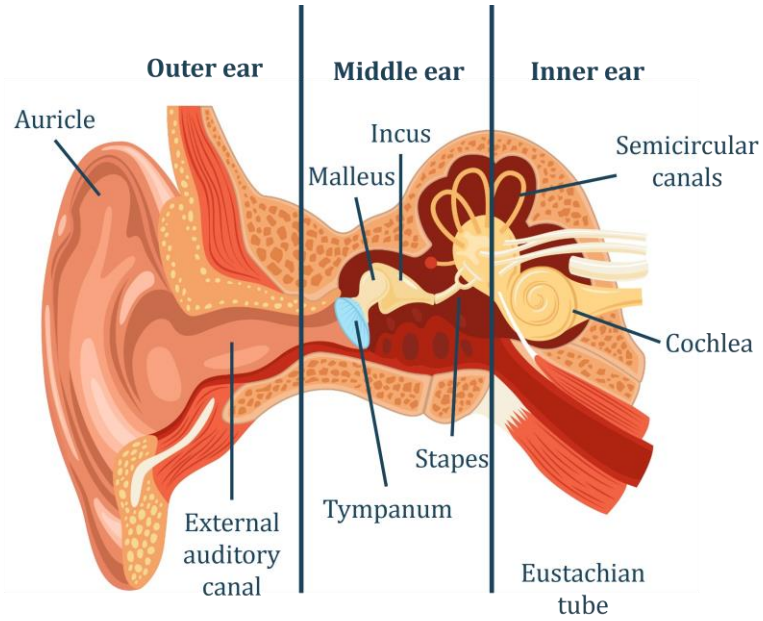

Figure 7: Anatomy of the ear.

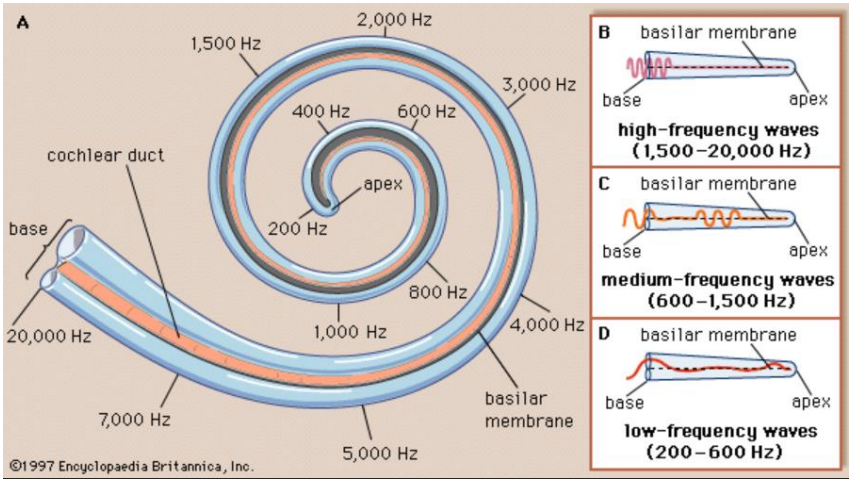

Figure 8: Tonotopic organization of the cochlea: each portion responds to specific frequencies, the distal regions are sensitive to low frequencies, while proximal regions respond to higher frequencies.

HL is a reduction in auditory capacity due to damage to one or more components of the auditory system. It may affect one ear (unilateral) or both (bilateral). According to the World Health Organization, 466 million people worldwide, including 34 million children, suffer from HL [49].

HL can be classified as:

1. **Conductive HL**: Impairment in sound transmission through the outer or middle ear, with intact sensory systems. Causes include outer ear anomalies, otitis media, or otosclerosis.
2. **Sensorineural HL (SNHL)**: Damage to the inner ear structures, often due to noise-induced hair cell degeneration. This is the most common form of age-related HL (presbycusis). The risk factors underlying SNHL can be classified into four major categories: Cochlear aging, environmental factors such as noise exposure, ototoxic drugs, socioeconomic factors, genetic factors like gender, race, and specific genetic predispositions, and concomitant comorbidities (hypertension, diabetes, stroke, and smoking) [50].
3. **Mixed HL**: Combined conductive and sensorineural impairments, often associated with damage to the auditory pathways or cortex.

It is known that prolonged exposure to intense noise can cause Noise-induced HL (NIHL). Noise generated by machinery in factories and workshops, motorized traffic, household appliances, sound amplification systems, and airplanes landing and departing from airports has reached intolerable levels in nearly all industrialized cities. The characteristic anatomical-pathological lesions of NIHL are localized in the neuroepithelium of the organ of Corti, where initial degeneration and eventual disappearance of hair cells can be observed. Outer hair cells are affected first and more significantly than inner hair cells. The extent and severity of the damage are proportional to noise intensity and exposure duration, while the location of the lesions corresponds to the frequency of the traumatic sound. High-frequency sounds cause lesions in the basal turn, while low-frequency sounds affect the apical region of the cochlea. When the noise has a broad sound spectrum, as is usually the case, lesions predominantly localize to a segment of the basal turn of the cochlea.

NIHL is a sensorineural type initially confined to frequencies around 4,000 Hz. It later progresses to involve higher frequencies and, subsequently, medium and low frequencies. Two distinct mechanisms have been identified: metabolic intoxication and mechanical trauma. Metabolic intoxication is an imbalance between metabolic (energy

production) and catabolic (waste disposal) processes, leading to insufficient energy production and toxic product accumulation. Mechanical trauma can occur in two forms. With very high and impulsive intensity levels (e.g., explosive sounds), membrane structures of the cochlear partition may rupture, and intercellular connections may break. At lower intensity levels, specific cochlear regions experience intense mechanical stimulation of hair structures, leading to earlier and more preferential permanent lesions in these areas. This type of HL is often accompanied by tinnitus. If the noise was not excessively intense or the exposure duration was not too prolonged, a complete recovery of auditory function can occur, referred to as auditory fatigue. However, if certain intensity or duration limits are exceeded or if noise exposures occur before full recovery is achieved, permanent damage is established. In its initial stages, HL is typically unnoticed; the only subjective sign may be difficulty hearing doorbells or the ticking of a watch. Even in the early stages, tonal audiometry reveals a characteristic "dip" centered around 4,000 Hz. In more severe or advanced cases, the "dip" deepens and widens, first towards higher frequencies and then towards lower ones [51], [52].

NIHL has significant social implications, as it is often associated with occupational activities conducted in noisy environments. Occupational exposure to loud, repeated, and prolonged noise is the most common cause. For the same noise intensity, intermittent and discontinuous noise is less harmful than continuous and uniform noise, while impulsive noise is more damaging. Although most cases of NIHL are linked to specific occupational activities, some are associated with recreational activities, such as hunting, shooting, motocross, and frequenting nightclubs, where the intensity of music is often damaging to the ear. Habitual nightclub attendees, even young ones, frequently exhibit hearing deficits.

The diagnosis is relatively straightforward when the characteristic "dip" at 4,000 Hz is observed and corroborated by a history of exposure to intense noise. From a therapeutic perspective, unfortunately, NIHL is irreversible. Hearing aids can be recommended in cases of advanced HL, particularly when medium and low frequencies are also affected, impeding social interactions. For this reason, it is important to act from the preventive side. Individual prevention involves using hearing protectors capable of attenuating noise intensity; even a reduction of 10 to 20 dB is sufficient in most cases to significantly decrease the risk of noise-induced hearing damage [53].

Hearing Personal Protection Equipment (PPE) can be divided into two groups: those that attenuate airborne noise (headphones and inserts or earplugs) and those that also attenuate sound transmission through bone conduction, enveloping all or part of the

head of the exposed individual, such as acoustic helmets or headsets. Currently, the most commonly used hearing PPE are (Figure 9):

- Passive earmuffs: they consist of rigid ear cups designed to fit around or cover the auricle, applying pressure to the head. These cups are internally lined with sound-absorbing material to enhance noise attenuation. The edges of the ear cups are equipped with cushioned seals, typically filled with liquid or foam, to create an airtight closure against the head. They can be secured in place using either a headband or a mounting system attached to a protective helmet. Passive earmuffs are commonly employed in environments such as construction sites and manufacturing facilities to provide effective hearing protection.
- Active earmuffs: headphones that automatically adjust their level of protection based on ambient sound intensity. These devices reproduce external sounds at reduced levels while attenuating higher-intensity noises through a gain control function. Additionally, they can include active noise control systems that neutralize unwanted sounds by superimposing inverse waveforms. Many active earmuffs are also equipped with integrated radio communication systems, enabling the transmission and reception of audio signals when connected to a transceiver. These earmuffs are particularly used in military applications, shooting ranges, and aviation, where precise sound management and communication are critical.
- Earplugs: these devices are designed to be inserted into the external auditory canal. They are available in various shapes and materials, offering a range of options to suit individual preferences. Musicians and concert staff frequently use earplugs in order to protect their hearing from prolonged exposure to high decibel levels while still being able to hear the music and communicate.
- Acoustic helmets or headsets: these are rigid devices that cover a significant part of the head and external ear, reducing sound propagation through bone conduction as well. They are used in mining, heavy industry, and construction. While common hearing protection devices provide good protection, they can completely isolate the user from the surrounding environment, increasing workplace risks related to the perception of acoustic signals and hindering effective and comfortable communication with colleagues.

Figure 9: Types of hearing personal protective equipment.

However, the primary drawback of these PPEs is that they attenuate all sounds indiscriminately, including typical speech frequencies. This can create significant communication difficulties among workers and other individuals, often leading to the abandonment of these devices [54]. To address this issue, commercially available electronic headphones with controlled attenuation feature adjustable amplification for speech frequencies and an electronic system that limits impulsive noises to 82 dBA. However, integrating this electronic regulation mechanism significantly increases the cost of these devices, which typically range between €500 and €1000.

For this reason, it is essential to develop lower-cost solutions that not only protect hearing from excessive noise but also facilitate communication with others and prevent the sense of isolation that can arise from wearing headphones that excessively cancel surrounding sounds.

1.3 Ph.D. Candidate Contribution

The present Ph.D. dissertation focuses on the development of novel technological solutions in otorhinolaryngology, addressing key challenges in monitoring respiratory and sleep-related breathing disorders and preventing otological diseases. The research aimed to design and develop innovative systems that address important clinical needs in the field. These solutions were validated either in real-life settings or under conditions that mimic real-world scenarios.

The thesis is organized into three main sections, following the structure presented in the introduction:

- Chapter 2 presents a smart face mask for unobtrusive respiratory monitoring. This chapter details the design, development, and validation of the device on healthy subjects. The device is based on temperature sensors and is able to detect the respiratory rate of the subjects. The validation included static and dynamic conditions to replicate the possible real-world scenarios.
- Chapter 3 focuses on a non-invasive system for detecting OSA using snoring sound analysis. The study introduces an algorithm that identifies apnea events caused by airway obstruction based on snoring sound patterns. The algorithm was tested on healthy subjects and patients, showing promising results as a potential screening tool.
- Chapter 4 describes the design and development of a protective earplug to mitigate the impact of high-frequency sounds from medical instruments while minimally affecting speaking frequencies. The device was validated through experimental testing, including a specific use case involving dentists and their staff, to assess its efficacy in reducing exposure to harmful noise levels.

Lastly, Chapter 5 summarizes the key contributions and findings of the present dissertation and outlines potential future developments in the field.

This dissertation underscores the important role of technological innovation in addressing unmet clinical needs in otorhinolaryngology and paving the way for more patient-centric healthcare tools.

2 Wearable Systems for Physiological Respiratory Monitoring

2.1 State of the art in smart technologies for monitoring respiratory disorders

Filtering face masks are, among many occupational fields, the most widely used personal protective equipment. Healthcare workers are their biggest users, especially with the persistence of the COVID-19 pandemic [55]. However, the mandatory use of face masks is not limited to the hospital setting but also extends to all those categories of workers who are in contact with substances dangerous to health [11], [56]. These include volatile organic substances, vitreous fibers, chemicals, metals, respirable dust (including silica and coal mine dust), fumes, vapors, gases, and contagious pathogenic materials. Exposure to these respiratory sensitizers has been linked to several respiratory conditions, including rhinitis, asthma, chronic obstructive pulmonary disease, and irritation of mucous membranes [11], [12]. This broad use of masks has led to their exploitation as wearable solutions for respiratory monitoring [57]–[59]. In fact, the importance of keeping track of respiratory parameters as indicators of a subject's health status is becoming increasingly recognized. Among these, respiratory rate (RR) has been shown to provide information about patients' clinical deterioration. Indeed, an abnormal RR can predict potential clinically severe events such as readmission to an intensive care unit, adverse cardiac events, and overdose. Moreover, because relative changes in RR are greater in magnitude than blood pressure and heart rate, it appears to be a better discriminator in identifying patients at high risk of cardiopulmonary deterioration. In addition, RR responds to various stressors and can indicate pain, emotional and environmental stress, physical, fatigue, and cognitive load [17], [18].

Various technologies are available to measure RR, depending on the specific application, the measurement requirements, and the user needs. It has been shown that RR can be extracted from different sources such as airflow, respiratory sounds, air temperature, air humidity, respiratory-induced chest wall movements, and cardiac activity [18], [60]. Flowmeters are most used in clinical practice because of their high accuracy, sensitivity,

and response frequency [60]. However, these sensors need to be exposed to the air inhaled and exhaled by the subject, and consequently, their measurement is usually quite intrusive. Like them, temperature and humidity sensors are typically placed at the level of the nostrils and/or lips and are intrinsically obtrusive. Indeed, as discussed in Chapter 1.2.1, the inhaled air is warmed and humidified by the internal nasal mucosa, ensuring it reaches the lungs at a temperature close to blood temperature. Consequently, the exhaled air is warmer during breathing, and the temperature difference between the inhaled and the exhaled air can reach about 15°C [61]. Also, the amount of water vapor differs from inhaled and exhaled airflow. Therefore, they can estimate RR from the difference in temperature and humidity between exhaled and inhaled air [60]. However, the small size of the sensing element partially mitigates their intrusiveness. These sensors generally allow recording of the respiratory waveform over time and the RR analysis on a breath-by-breath basis.

The encumbrance problem is partially overcome with microphones, cardiac signals (electrocardiography and photoplethysmography), and strain and movement sensors. These do not need direct contact with inhaled/exhaled air, so they can easily be embedded in wearable devices and integrated into clothes and garments. However, acoustic approaches remain susceptible to background noise and subject activity unrelated to breathing, while the others are very sensitive to movement unrelated to the breathing activity [60]. Physical activities cause movements that can cause artifacts on the sensor's output even at low speeds, for example, while walking. Their frequency contents are in the range of 0.5 Hz – 1.40 Hz, which, unfortunately, is partially overlapped with the frequency range of respiration [62], [63]. For this reason, mitigating these artifacts in estimating RR is essential.

Among all the possible solutions, the functioning and the small size of temperature sensors allow them to be easily integrated into face masks to give mechanical stability to the sensor and reduce the sensitivity to body movements. Based on this principle, thermistors can be a feasible solution since their output is an electrical resistance highly sensitive to temperature. Therefore, the changes in airflow temperature between inspiration and expiration allow the detection of these two respiratory phases and, consequently, the period of both phases and RR. These sensors can be used to measure the respiratory signal in both adults and infants due to their small size, low intrusiveness, and proper response time [18], [60], [64].

Several authors have chosen thermistors to monitor respiratory parameters in the literature, integrating them in oxygen face masks or other support near the mouth and

nostrils [64]–[69]. Other authors also mounted different types of sensors on surgical face masks to evaluate respiratory parameters (Figure 10). The proposed solutions were based on different sensors, such as respiratory sensing triboelectric nanogenerator [57], [70], textile-based capacitive sensor [58], graphene oxide-based radiofrequency identification sensor [71], Fibre Bragg Grating (FBG)-based soft sensor [59], paper-based electrical respiration sensor [72]. They all showed devices with good performances, demonstrating the feasibility of using face masks as support for RR monitoring.

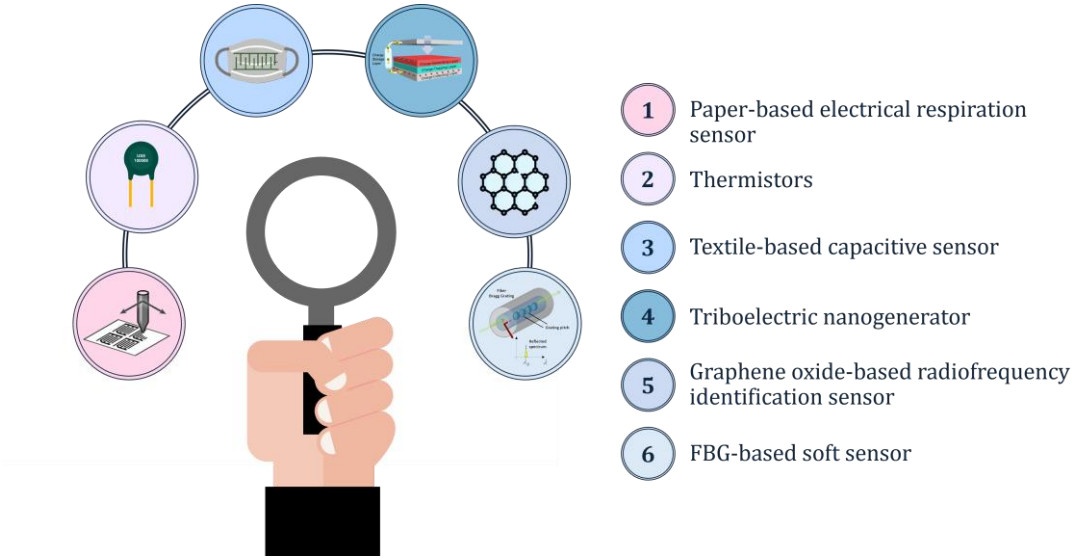

Figure 10: Examples of sensors integrated into surgical face masks to detect RR.

Several authors have explored the use of thermistors to monitor RR. Among them, Lerman et al. [65] proposed a solution using three thermistors, two positioned close to the mouth/nose within a disposable oxygen face mask and one outside the mask to measure and adjust for the ambient temperature. The estimation of the RR was evaluated by comparing the results obtained from the experimental mask with a capnography. For two minutes, the investigator, in sync with a metronome, breathed at steady rates of 7.5 bpm – 60 bpm. They demonstrated that the device could measure the respiratory rate accurately over a broad range with the thermistors mounted on the face mask.

Differently, other studies made the subjects breathe at their own rhythm. Sifuentes et al. [73] tested their solution on 23 healthy volunteers by placing a thermistor near the nostrils of each subject and comparing it with a piezoelectric sensor. Subjects breathed firstly at a fixed rate and secondly freely. In this latter condition, they performed the Bland-Altman analysis and found the lowest mean of difference (MOD) and limits of

agreements (LOA) compared to the other studies. Turnbull et al. [69] tested a prototype for testing pediatric RR, composed of a mouthpiece, a lower flap to stabilize the device in the mouth, and an upper lip flap with two thermistors integrated at the nasal outlet to detect the temperature wave of exhaled air. The instrument was tested firstly on healthy adult volunteers and then on Congolese hospitalized children. Adults were asked to breathe at a specific rate while children breathe at their rhythm. Compared to capnography, they found a MOD and LOA of -0.5 ± 4.7 bpm in adults and 1 ± 19 bpm in children. The authors stated that the device can accurately measure the RR in healthy adults and children and facilitate the diagnosis of pneumonia by community health workers in low-income and middle-income countries. Hurtado et al. [74] presented a non-invasive system with a temperature sensor between the nose and the mouth. Under spontaneous breathing, the mean RR difference between the respiratory monitor and visual counting was 0.4 bpm. Lastly, Dawood et al. [75] presented a portable, affordable respiratory rate measurement device. To record the patients' breathing patterns based on the temperature variations, a thermistor was connected to a nebulizer mask. Over a range of different ambient temperatures (cold, room temperature, and hot), breathing rates (slow, normal, and fast), breathing depths (shallow, normal, and deep), and breathing orifices (nasal and oral), the integrated system showed a modest average error of 5.6%. At the time of development, the entire cost was less than €40. Table 1 summarizes the results found in the literature.

As a potential application of this technology, several authors have explored the use of RR in the Intensive Care Unit. Firstly, Qudsi and Gupta, in 2013 [60], presented a nebulizer mask with an embedded thermistor. They tested it to measure RR and to activate an alarm when the patient was not breathing, showing good results in a simulated environment (within 5% of the actual respiration rate). Similar to them, Rao and Sudarshan [67] mounted a thermistor on a mask to monitor RR. Also, they set an upper and lower threshold limit, and a warning alert is activated if the RR crosses them. Veerabhadrappa et al. [66] designed a system that includes electrocardiography (ECG), pulse oximetry to measure arterial blood saturation, and a thermistor to monitor RR and body temperature. They tested the device on 100 volunteers, showing that all the parameters increased in stressful conditions compared to normal conditions. This system can be used for remote patient monitoring. However, these studies only assessed the feasibility of the solution but did not confirm their results, comparing them with a reference system.

In this study, a smart face mask (SFM) was developed using two thermistors to estimate RR. The performances were first evaluated on healthy subjects by comparing the RR calculated by the SFM with those obtained using a reference system (Zephyr™ BioHarness 3.0, commercialized by Medtronic) [76]. This preliminary assessment conducted in static condition (i.e., sitting) showed promising results. For this reason, a second study enrolling new healthy subjects (8 volunteers) was performed focusing on the performance of the SFM in estimating RR in a second static condition with the subject standing and a dynamic one while walking. This analysis faced the more challenging conditions which are prone to potential inaccuracies related to motion artifacts. Therefore, this investigation allowed the understanding of the potential application of the proposed SFM in different scenarios which can be experienced during a broader spectrum of daily life activities [77].

Table 1: Summary of Literature Review of studies that use thermistors to detect RR.

First author (year)	Type and number of sensors	Subjects	Reference system	Protocol	Results
Lerman (2016) [65]	Two thermistors	3 healthy subjects	capnography	The investigator breathed at constant rates of ~7.5-60 bpm for 2 min	MOD: -0.17 bpm lLOA: -2.15 bpm uLOA: 1.8 bpm
Sifuentes (2016) [73]	One thermistor	23 healthy subjects	piezoelectric sensor	Two procedures: "Controlled Breathing," where subjects breathe following a baseline, and "Free Breathing," where subjects breathe at their rhythm.	MOD: 0.017 bpm lLOA: -0.286 bpm LOA: 0.320 bpm
Turnbull (2018) [69]	Two thermistors Output data of the sensors transmitted by a cable to a laptop computer	23 hospitalized children	visual counting	hospitalized children breathe at their own rhythm for 1 min.	MOD: -6.8 bpm lLOA: -59 bpm uLOA: 39 bpm
	Two thermistors Output data of the sensors transmitted to standalone LED screen	10 healthy adults 42 hospitalized children	capnography	Healthy adult volunteers breathe at a fixed rate. Hospitalized children breathe at their own rhythm.	Adults MOD: -0.5 bpm lLOA: -5.2 bpm uLOA: 4.2 bpm Children MOD: 1 bpm lLOA: -18 bpm uLOA: 20 bpm
Hurtado (2020) [74]	Temperature Sensor (number not specified)	20 healthy subjects	visual counting	All subjects lay down on a stretcher in the supine position and perform the following protocol: 1) Breathe through their nose for one minute following a metronome at 6, 8 and 10 bpm. 2) The same protocol repeated for oral breathing 3) Breathe spontaneously during 10 min.	1) MOD: 0.1 bpm lLOA: -0.4 bpm uLOA: 0.7 bpm 2) MOD: -1.6 bpm lLOA: -7.6 bpm uLOA: 4.4 bpm 3) MOD: 0.4 bpm lLOA: -0.5 bpm uLOA: 1.3 bpm
Dawood (2022) [75]	One thermistor	5 healthy subjects	visual counting	All the subjects breathed from 30 to 60 s in the following conditions: - Temperature: Cold (<10 °C), Room (23–25 °C), Hot (>28 °C) - Rate: Slow (<16 bpm), Normal (16–20 bpm), Fast (>20 bpm) - Breath depth: Shallow, Normal, Deep - Orifice: Nasal, Oral	Average error: 5.6%

lLOA – lower limit of agreement; uLOA – upper limit of agreement

2.2 Development of a smart face mask

2.2.1 Working principle

The principle behind the functioning of the thermistors is a variation of the resistance with the temperature. They can be divided into two categories: the Negative Temperature Coefficient (NTC) thermistors, where resistance decreases with the increase of the temperature, and the Positive Temperature Coefficient thermistors, where resistance increases with the increase of the temperature [78].

In the proposed SFM, were used two nominally identical NTC thermistors. The input-output relationship is described by:

$$R(T) = R_0 * e^{\left[\beta\left(\frac{1}{T}-\frac{1}{T_0}\right)\right]} \quad (1)$$

Where β is a constant depending on the thermistor material, and R_0 is the thermistor's resistance at the reference temperature T_0, usually 25 °C [78]. In Figure 11 is shown the relationship between the temperature and the resistance of the chosen thermistor.

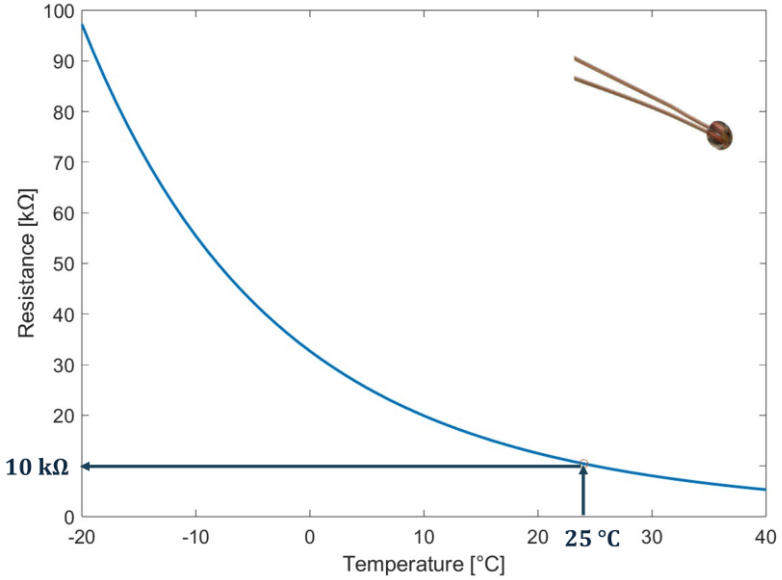

Figure 11: Temperature-resistance relationship. At 25 °C, the resistance is equal to 10 kΩ.

2.2.2 Design and Fabrication

The thermistors' output was transduced into a voltage signal using a Wheatstone bridge (WB). Since WB is known to be balanced when the product of the resistances on the opposite branches is equal, considering four resistors with resistance value R, three of them fixed and one variable (its resistance change is ΔR), the WB output of the quarter-bridge configuration ($\Delta e_{1/4}$) is:

$$\Delta e_{1/4} \approx e_1 \frac{\Delta R}{4R} \tag{2}$$

With e_1 voltage supply.
The WB can be designed in a half-bridge configuration, with two variable resistances on opposite branches. Considering that the two resistances experienced an identical change (i.e., ΔR), the output of the WB ($\Delta e_{1/2}$) is:

$$\Delta e_{1/2} \approx e_1 \frac{\Delta R}{2R} = 2\Delta e_{1/4} \tag{3}$$

The relationships reported in (2) and (3) highlight that the half-bridge configuration allows the sensitivity of the quarter-bridge configuration to be doubled. Therefore, we proposed a solution using two thermistors (G10K3976, Measurement Specialties, Inc., a TE Connectivity Company) positioned on opposite branches of a WB to improve the sensitivity of the whole measuring chain. The half-bridge configuration used for the SFM is shown in Figure 12, where R_{x1} and R_{x2} represent the resistance of the two thermistors. The two fixed resistors (R_{WB}) were chosen at 10 kΩ to balance the bridge since this is the resistance value of the thermistors at 25 °C, as shown in Figure 11. The bridge output ($\Delta e_{1/2}$) is amplified by an INA122P instrumental amplifier with a gain of 5. This amplification value was an optimal trade-off to increase the output amplitude while avoiding the amplifier's saturation. The WB and the INA122P are powered by 5 V using the M5Stick PLUS ESP32-PICO by M5Stack Technology. The same device is used to acquire the output of the amplifier (ΔV_{OUT}) and send it via Bluetooth to a PC for analysis.

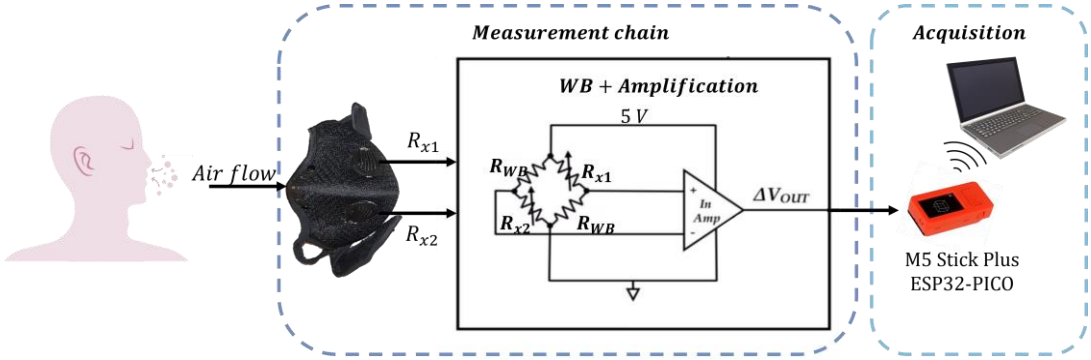

Figure 12: Schematic representation of the experimental circuit. Rx1, Rx2: resistance of the two thermistors. RWB: fixed resistors. In Amp: instrumental amplifier.

2.2.3 Data analysis

The data collected by the SFM and the reference system, the Zephyr™ BioHarness 3.0 (BH), were processed by the software MATLAB® by MathWorks. For both signals, the estimation of the RR values was performed as follows:

- A digital band-pass filter was applied using the Butterworth filter design function and then the *filtfilt* function that performs the zero-phase forward and reverse digital filtering. The signal was band-pass filtered between 0.01 Hz and 1.5 Hz to remove frequency components unrelated to the breathing activity.
- The signal was segmented into windows matching the trial duration to synchronize the two devices and select the portion of the signal to be analyzed.
- The peak detection was obtained using the function *findpeaks* on each window on the normalized waveforms, manually setting each subject's minimum peak distance and the minimum peak height. The two waveforms show an opposite trend in time (Figure 13) due to the nature of the two systems: the chest strap is strained during inspiration following the chest expansion, so the BH output increases, while the output of the SFM decreases during inspiration. For this reason, the SFM waveform was inverted before applying the function *findpeaks.*
- The calculation of instantaneous RR (i.e., RR^i) was performed by dividing the distance between the $(i+1)^{th}$ and the i^{th} peak by the sampling frequency (Equation 1) and then dividing 60 by the previous result (Equation 2). This way, RR is expressed in breaths per minute (bpm).

$$T_i = \frac{t_{i+1} - t_i}{f_s} \quad (1)$$

$$RR^i = \frac{60}{T_i} \quad (2)$$

Where t_i and t_{i+1} is the time of, respectively, ith and (i+1)th peak, and f_s the sampling frequency (25 Hz for the BH, ~100 Hz for SFM).

Figure 14 shows an example of the analysis of signals deriving from the SFM and the BH. The RR values of the two phases (i.e., Quiet Breathing - QB and tachypnoea) were averaged to obtain the mean RR value ($\overline{RR}_{SFM}^{QB}$ and $\overline{RR}_{SFM}^{T}$ for the proposed system and $\overline{RR}_{BH}^{QB}$ and $\overline{RR}_{BH}^{T}$ for the reference BH).

The performance of the SFM was obtained through the Bland-Altman analysis [79], with a resulting plot of the differences between methods ($RR_{BH} - RR_{SFM}$) against the mean between the value obtained from the two systems ($(RR_{BH} - RR_{SFM})/2$). Also, for the feasibility assessment the Mean Absolute Percentage Error (MAPE) for each test was calculated, according to the following equation:

$$MAPE\ [\%] = \frac{1}{n}\sum_{i=1}^{n}\left|\frac{RR_{SFM,i} - RR_{BH,i}}{RR_{BH,i}}\right| * 100 \quad (3)$$

In addition to this, in the second test, the Mean Absolute Error (MAE) was also calculated:

$$MAE\ [bpm] = \frac{\sum_{i=1}^{n}|RR_{SFM,i} - RR_{BH,i}|}{n} \quad (4)$$

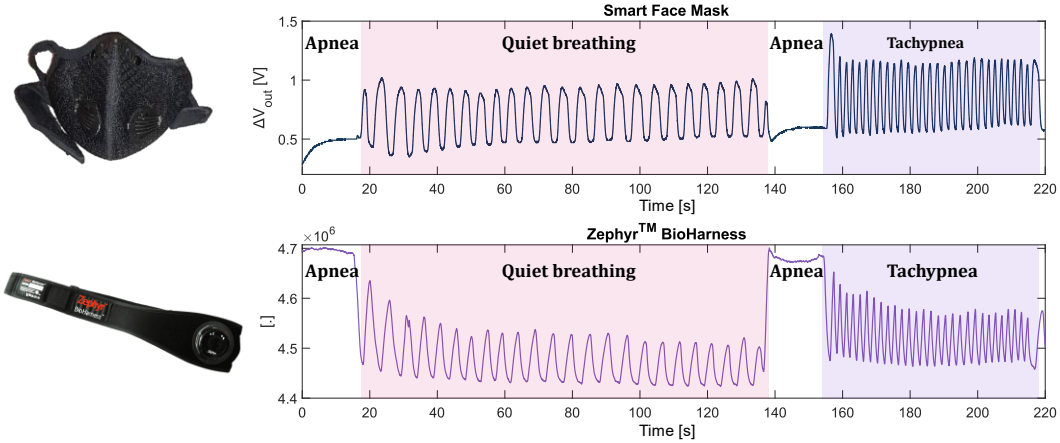

Figure 13: Signal deriving from SFM and BH.

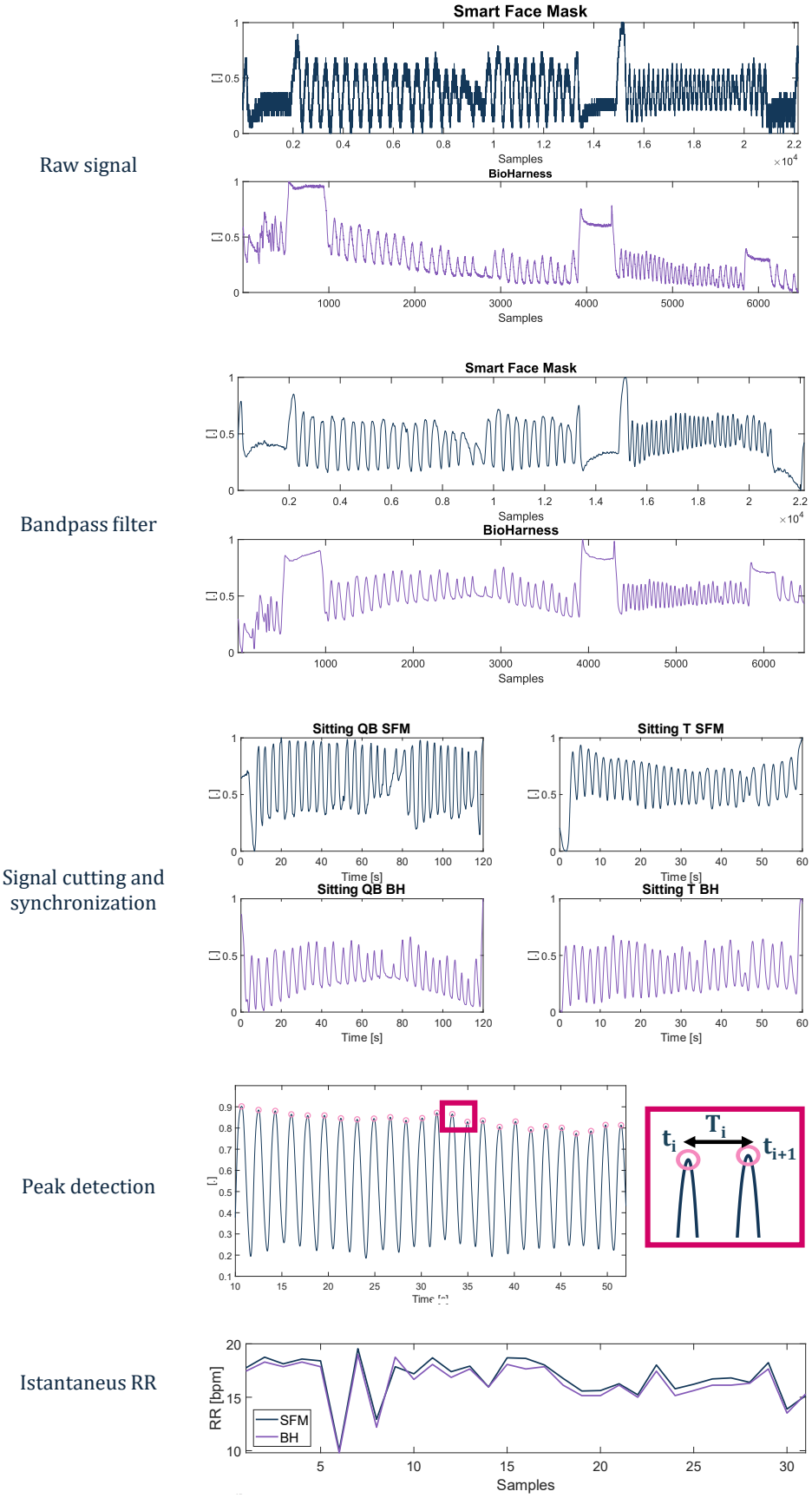

Figure 14: Example of analysis of the SFM and BH signals.

2.3 Validation of the smart face mask

2.3.1 Feasibility assessment of the smart face mask

2.3.1.1 Experimental protocol

In this study, six healthy volunteers (5 men and 1 woman, 26.0 ± 7.4 years old) were enrolled to assess the feasibility of the proposed system in estimating RR. Each volunteer wore the SFM and the reference BH, as shown in Figure 15 and performed the following protocol while sitting:

- 15 s apnea followed by 120 s QB;
- 15 s apnea followed by 60 s tachypnoea.

The apnea stage was performed to synchronize the outputs of the two devices: the SFM with the BH.

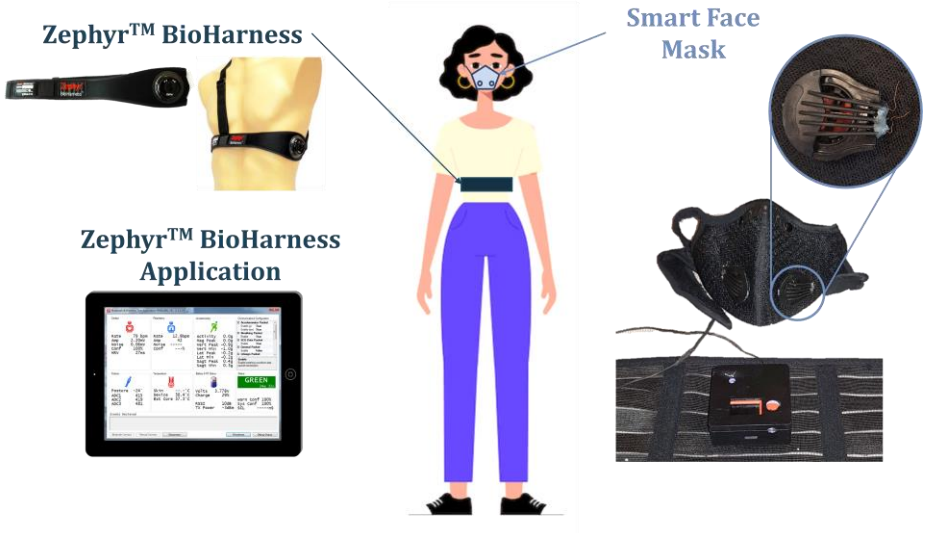

Figure 15: Experimental set-up: the subject wears the Zephyr BioHarness, shown on the left with its graphic interface, and the Smart Face Mask, on the right. The Smart Face Mas is connected to the M5Stick. The thermistors are inserted into the two valves.

2.3.1.2 Results

From the analysis of the signals acquired by the SFM and the BH, the mean RR for each subject was obtained both in the QB and tachypnoea stages. Then, the MAPE was calculated for each subject at each stage: for QB, the MAPE values range from 1.44% to 4.29%, and for the tachypnoea, from 0.95% to 4.20%. The detailed results for each subject are reported in Table 2.

To assess the agreement between the two measures, the Bland-Altman analysis has been performed with its resulting plot. The graphs obtained from this analysis (Figure 16 and Figure 17) showed a horizontal line corresponding to the MOD, and two lines centred at MOD ± 1.96 * SD (Standard Deviation - SD). In particular, for QB, we obtained 0.05±1.46 bpm, while for the tachypnoea 0.18±3.54 bpm.

Table 2: Mean RR for each subject estimated by the ZephyrTM BioHarness (BH) and the Smart Face Mask (SFM) and corresponding Mean Absolute Percentage Error (MAPE).

Sbj	$\overline{RR}$ [bpm] during Quiet Breathing			$\overline{RR}$ [bpm] during Tachypnoea		
	SFM	BH	MAPE	SFM	BH	MAPE
#1	11.92	11.95	2.04 %	17.41	17.36	2.94 %
#2	22.12	22.13	2.60 %	28.30	28.45	4.20 %
#3	14.79	14.77	4.29 %	65.82	65.99	2.94 %
#4	19.33	19.51	1.44 %	28.09	28.58	3.59 %
#5	11.92	11.94	2.66 %	28.80	28.89	0.95 %
#6	25.05	25.08	2.47 %	36.66	36.84	1.50 %

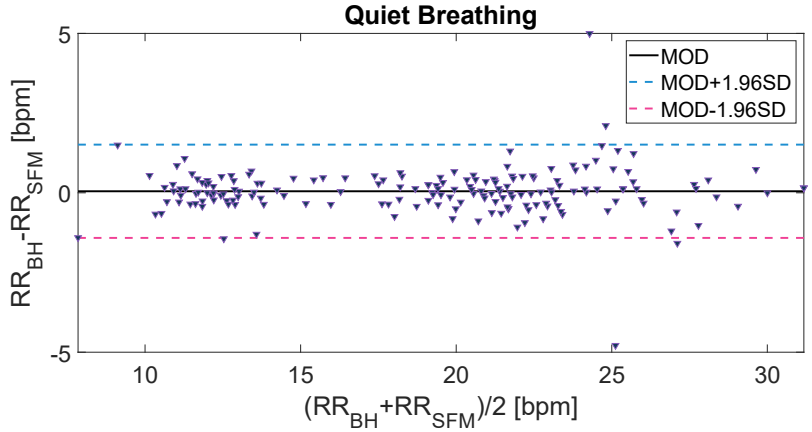

Figure 16: Bland-Altman plot comparing the RR measured by BH and by SFM in the quiet breathing stage.

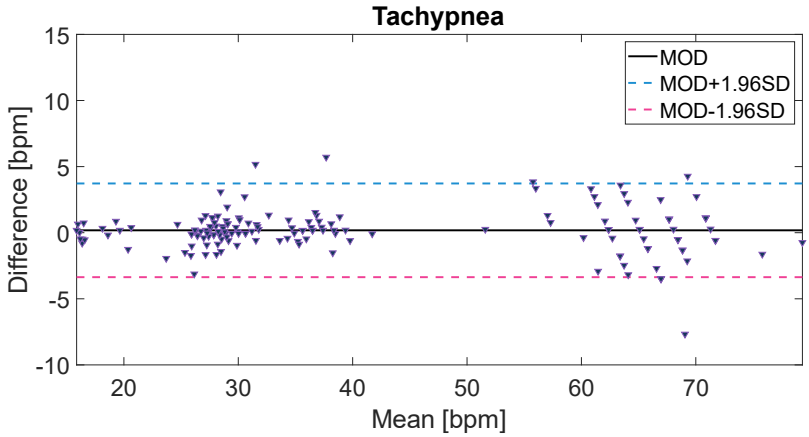

Figure 17: Bland-Altman plot comparing the RR measured by BH and SFM in the tachypnoea stage.

2.3.2 Validation in static and dynamic conditions

2.3.2.1 Experimental protocol

In this study, eight healthy volunteers (2 men and 6 women, 27.6 ± 3.9 years old) were enrolled to assess the feasibility of the proposed system in estimating RR in static and dynamic conditions.

To assess the performance of the SFM, the subjects were asked to wear the SFM and the reference system BH, as previously done in the first analysis (Figure 15). The SFM was tested in three conditions: sitting, standing, and walking. In the first two conditions, the subjects performed 120 s of QB and 60 s of tachypnoea, while for the last 120 s of QB. At the beginning and the end of each test, the subjects performed 15 s of apnea. The apnea stage was performed to synchronize the outputs of the SFM with the BH. Figure 18 shows a schematic representation of the protocol, an example of signals for the first two conditions, and an example of the walking test.

For each subject, the signals acquired by the SFM and the BH were analyzed, and mean RR in the QB and tachypnoea stages for the sitting and standing conditions and in the QB for the walking condition were obtained. To perform the analysis, the signal was divided into windows corresponding to the duration of the trial. Indeed, for the sitting and standing tests, the signal was divided into two windows: 120 s for the analysis of the QB stage and 60 s for the study of the tachypnoea stage, starting from the end of the apnea. For the walking test, the signal was cut in one window of 120 s for the analysis of the QB stage. The results are reported in Table 3 and described in the following paragraphs for each condition.

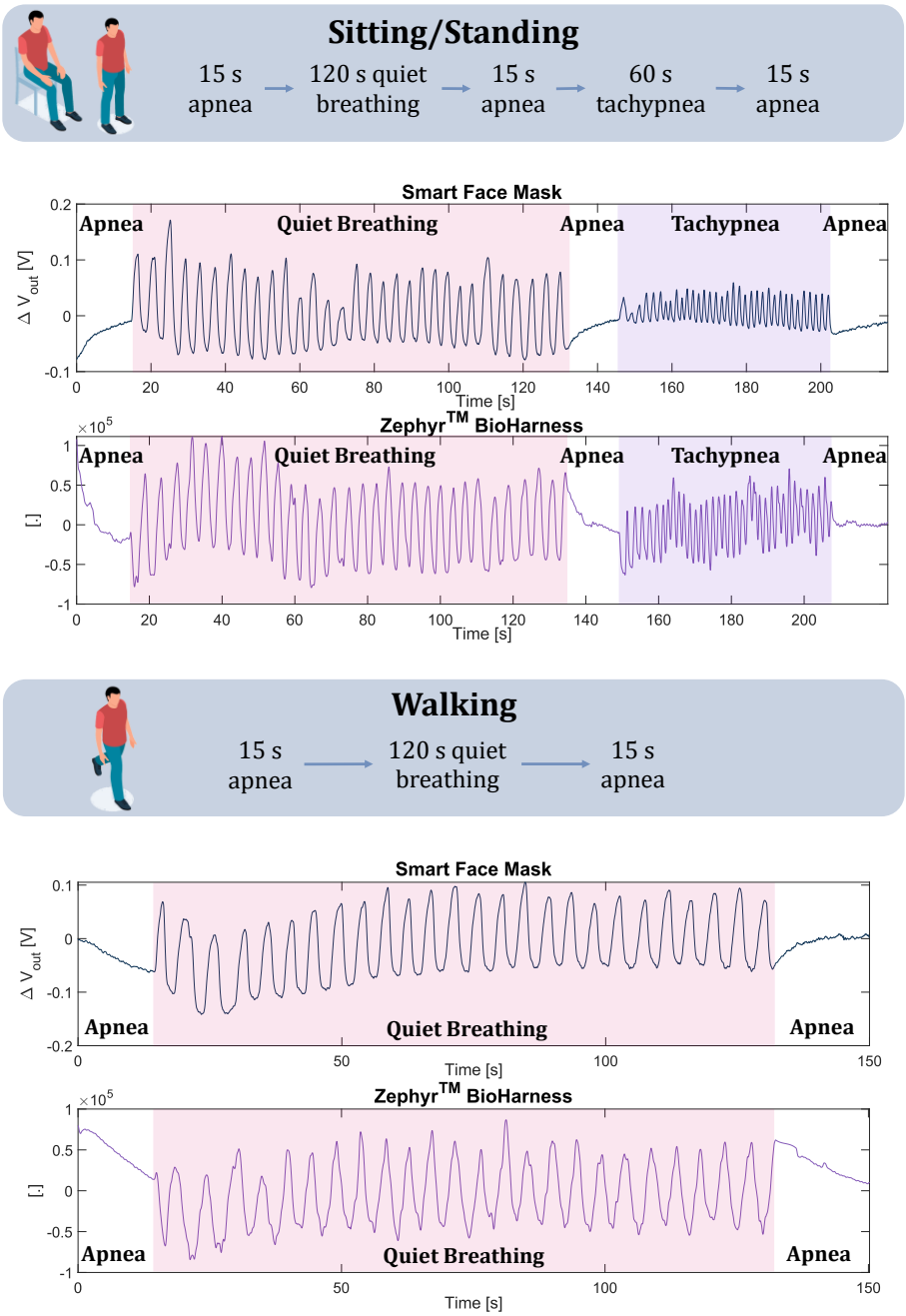

Figure 18: Schematic representation of the protocol followed by the subjects with an example of the signal deriving from the sitting/standing test and one from the walking test.

2.3.2.2 Results - Sitting

While sitting, the MAE values ranged from 0.46 bpm to 0.97 bpm in QB and from 0.83 bpm to 5.46 bpm when performing tachypnoea. The corresponding MAPE found in QB ranged from 2.8% to 5.6% and from 2.8% to 11.9% during tachypnoea. Figure 19 shows the resulting Bland-Altman plot, where a different colour represents each subject. During the QB stage, all the subjects had RRs ranging between 10 bpm and 20 bpm, with a MOD±LOA of 0.40 ± 1.97 bpm. During tachypnoea, almost all subjects breathed with RRs of 23 bpm to 47 bpm, while subjects 1 and 5 showed RRs higher than everyone else (more than 40 bpm). This results in a higher MOD±LOA of 1.13 ± 7.38 bpm.

2.3.2.3 Results - Standing

Similar to the sitting position, while standing, the MAE values ranged from 0.47 bpm to 1.05 bpm in QB, with corresponding MAPE from 2.8% to 6.5%. Compared to the sitting condition, better results were found during tachypnoea, with MAE ranging from 0.85 bpm to 3.10 bpm and MAPE from 3.0% to 7.5%.

From the Bland-Altman analysis, a MOD±LOA was found of 0.50 ± 1.58 bpm in QB and 1.02 ± 4.70 bpm in tachypnoea. Figure 20 shows the Bland-Altman plot. In this case, during QB, subject 6 showed RRs higher than the other subjects, with values closer to a tachypnoea stage (more than 20 bpm). Similarly, during tachypnoea, subject number 5 showed higher RR values compared to all the other subjects who showed RRs lower than 50 bpm.

2.3.2.4 Results - Walking

While walking, the MAE values ranged from 0.43 bpm to 1.56 bpm, with a corresponding MAPE of 3.9% to 9.9%. From the Bland Altman plot (Figure 21), it can be noticed that almost all subjects had an RR lower than 22 bpm, except for subject 7, who showed RRs ranging from 20 bpm to 33 bpm. A MOD±LOA was found at 0.50±2.75 bpm.

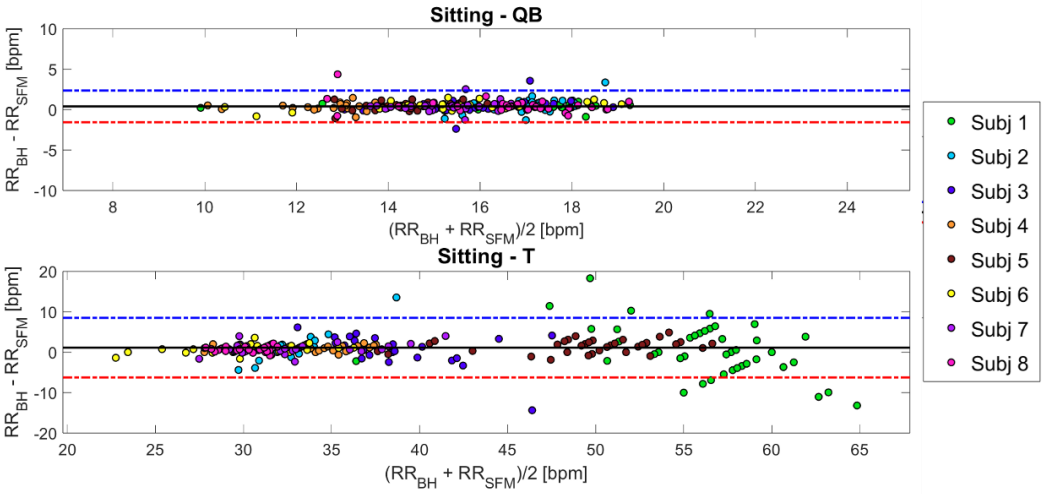

Figure 19: Bland-Altman plot in sitting condition. The black horizontal line corresponds to the mean of the differences (MOD); the blue and red dotted lines represent the Limit of Agreement (LOA). QB: Quiet Breathing; T: Tachypnoea

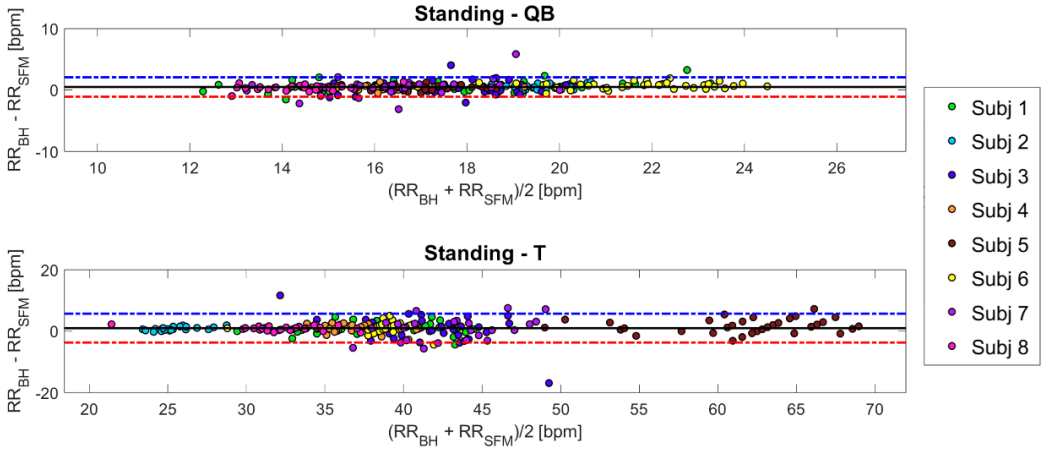

Figure 20: Bland-Altman plot in standing condition. The black horizontal line corresponds to the mean of the differences (MOD); the blue and red dotted lines represent the Limit of Agreement (LOA). QB: Quiet Breathing; T: Tachypnoea

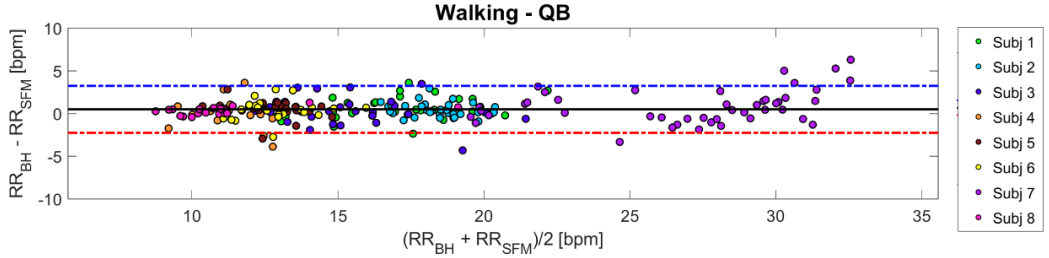

Figure 21: Bland-Altman plot in walking condition. The black horizontal line corresponds to the mean of the differences (MOD); the blue and red dotted lines represent the Limit of Agreement (LOA). QB: Quiet Breathing

Table 3: Mean RR, MAE, and MAPE of the subjects for each position in quiet breathing and tachypnoea. QB: Quiet Breathing; T: Tachypnoea

Subj		Sitting		Standing		Walking
		QB	T	QB	T	QB
S1	$\overline{RR}_{SFM} \pm SD\ [bpm]$	16.81±1.98	55.91±4.43	17.76±3.10	40.36±4.13	17.07±2.61
	$\overline{RR}_{BH} \pm SD\ [bpm]$	16.42±1.97	54.19±8.45	17.27±2.76	39.28±3.99	16.48±2.23
	$MAE\ [bpm]$	0.46	5.46	0.82	1.73	1.07
	$MAPE$	2.8%	11.9%	4.8%	4.5%	6.5%
S2	$\overline{RR}_{SFM} \pm SD[bpm]$	17.30±1.12	33.45±3.03	19.83±0.79	25.85±1.52	18.66±1.11
	$\overline{RR}_{BH} \pm SD[bpm]$	16.75±0.70	32.25±0.69	19.24±0.73	25.02±1.20	18.15±1.26
	$MAE\ [bpm]$	0.78	2.04	0.59	0.85	0.70
	$MAPE$	4.7%	6.3%	3.1%	3.4%	3.9%
S3	$\overline{RR}_{SFM} \pm SD\ [bpm]$	16.04±1.63	37.73±3.94	17.79±1.61	41.86±3.04	15.55±2.28
	$\overline{RR}_{BH} \pm SD[bpm]$	15.65±1.43	37.15±5.23	17.4±1.51	41.32±4.98	15.19±2.64
	$MAE\ [bpm]$	0.57	2.41	0.89	3.00	1.23
	$MAPE$	3.7%	6.3%	5.3%	7.5%	8.3%
S5	$\overline{RR}_{SFM} \pm SD\ [bpm]$	12.91±1.13	34.76±2.72	16.09±1.09	37.23±1.88	11.43±1.23
	$\overline{RR}_{BH} \pm SD[bpm]$	12.55±1.09	33.79±2.56	15.66±1.10	36.35±2.27	11.35±1.43
	$MAE\ [bpm]$	0.48	1.01	0.47	1.25	1.12
	$MAPE$	3.8%	3.0%	3.0%	3.5%	9.9%
S7	$\overline{RR}_{SFM} \pm SD\ [bpm]$	14.63±1.06	50.31±4.51	17.26±0.93	62.42±5.51	13.21±0.96
	$\overline{RR}_{BH} \pm SD[bpm]$	14.19±0.86	48.73±4.10	16.84±0.88	60.81±5.19	12.75±1.20
	$MAE\ [bpm]$	0.57	1.89	0.47	2.08	0.87
	$MAPE$	4.0%	3.9%	2.8%	3.4%	7.1%
S8	$\overline{RR}_{SFM} \pm SD\ [bpm]$	15.72±2.20	31.06±3.41	21.92±1.67	39.29±2.00	12.98±1.56
	$\overline{RR}_{BH} \pm SD\ [bpm]$	15.22±1.97	30.22±2.96	21.18±1.62	38.06±2.05	12.59±1.35
	$MAE\ [bpm]$	0.59	1.06	0.77	1.61	0.91
	$MAPE$	3.9%	3.5%	3.7%	4.2%	7.4%
S9	$\overline{RR}_{SFM} \pm SD[bpm]$	15.57±1.02	33.00±3.88	16.80±1.96	43.46±4.39	27.05±4.45
	$\overline{RR}_{BH} \pm SD[bpm]$	15.17±0.92	32.18±3.29	16.29±1.51	41.88±3.18	26.22±3.91
	$MAE\ [bpm]$	0.53	1.14	1.05	3.10	1.56
	$MAPE$	3.5%	3.5%	6.5%	7.4%	5.9%
S10	$\overline{RR}_{SFM} \pm SD[bpm]$	16.88±1.55	30.77±1.31	14.60±0.99	32.53±2.73	10.75±1.24
	$\overline{RR}_{BH} \pm SD[bpm]$	16.74±2.79	30.06±1.29	14.24±0.88	31.69±2.94	10.43±1.00
	$MAE\ [bpm]$	0.97	0.83	0.47	0.92	0.43
	$MAPE$	5.6%	2.8%	3.4%	3.0%	4.0%

2.4 Discussion and Conclusion

The SFM was composed of an antipollution sports mask that can be reusable by replacing the internal active carbon filter, ensuring prolonged and sustainable use. Furthermore, the chosen thermistor is characterized by a hermetically sealed glass package, as indicated in the datasheet, making it suitable for deployment in humid environments. The use of this technology was chosen because of its high sensitivity, reliability, and quick response time. Also, the resolution is sufficient to distinguish the temperature differences between inspiratory and expiratory flows. Sifuentes et al. [73], who examined the capabilities of a thermistor and a piezoelectric sensor, verified these findings. They exhibited an NTC thermistor mounted in a Wheatstone quarter-bridge configuration with a precision of 0.2 °C. They also demonstrated that the system's response time of 0.8 s was sufficient for following the respiratory signal. Several authors have explored the use of thermistors to monitor RR and have shown promising results. As an example, some authors [66]–[68] used thermistors to measure RR and trigger an alarm in case of breathing cessation, demonstrating the possibility of using this technology in Intensive Care Unit applications. It can be used alone or incorporated with ECG, pulse oximetry for arterial blood saturation measurement, and body temperature monitoring. However, it is noteworthy that these studies primarily focused on the feasibility of the solutions and did not validate their findings by comparing them with a reference system.

These design considerations enhance the durability and adaptability of the SFM, making it well-suited for various conditions. Thermistors are, in fact, an economical and versatile option for managing respiratory health issues in resource-constrained settings [64], [68], [69]. This is especially relevant in low- and middle-income nations where chronic respiratory illnesses are common yet frequently untreated [80]–[82].

The developed SFM has an increased sensitivity by using two thermistors in a WB half-bridge configuration. This configuration is also important for the external temperature compensation which can influence the measurements. The experimental results confirmed the system's feasibility in estimating RR and are comparable to those in the literature, which integrate different types of sensors on surgical face masks to evaluate respiratory parameters.

The first assessment showed a maximum $\overline{RR}$ difference of 0.18 bpm in the QB stage and 0.49 bpm in the tachypnoea stage between the systems. The maximum MAPE found was 4.29% in the QB and 4.20% in the tachypnoea stage. During QB, we found a MOD of 0.05

bpm and a LOA amplitude lower than 3 bpm, while during tachypnoea we found a higher MOD (0.18 bpm) and LOA amplitude (7.08 bpm). This high LOA value is due to the high frequencies tested (> 60 bpm), which are more challenging to detect but also very uncommon in everyday life. Similarly, authors using the same technology found comparable results in terms of MOD (from -0.5 bpm to 1 bpm) and LOA (from 0.303 to 19 bpm)[65], [69], [73], [74].

When compared to other technologies, similar findings have been reported in the literature. For instance, an FBG-based sensor demonstrated a maximum discrepancy of -0.69 bpm and a MAPE of 2.88% [59]. Additionally, Simic et al. developed a textile-based capacitive sensor integrated into a face mask, offering a lightweight and portable solution with high response and recovery times, ensuring good reproducibility between tests [58]. Lastly, another study introduced a wireless smart face mask incorporating an ultrathin, self-powered pressure sensor, which exhibited high sensitivity to breathing airflow. Unlike respiratory rate measurements performed with non-embedded devices, this fully portable and wearable system enhances ease of use in daily life [83].The main limitation of the first study performed in this thesis regards the sample size since only six subjects were enrolled. Moreover, there was a need to test the feasibility of the SFM under more challenging scenarios (e.g., by simulating movements related to sports activities, occupational settings, or clinical procedures). For this reason, a second trial was performed to extend the first feasibility study.

The SFM was tested on eight new healthy subjects in two additional conditions to simulate different everyday life conditions. Static positions (sitting and standing) were selected to simulate occupational settings, such as a company worker's daily activities. Differently, the walking condition was performed to test the SFM in more challenging scenarios and to see if movements influence the detection of RR.

While walking, the maximum MAE obtained was 1.56 bpm, a little higher than QB in sitting and standing conditions but lower than the tachypnoea stage. These results confirmed that mounting sensors on face masks gives them mechanical stability, preventing the sensors from motion artifacts [60], [84]. The lower performance during tachypnoea in the static positions is due to the high frequencies tested (> 50 bpm), which are more challenging to detect but uncommon in everyday life. From the Bland-Altman analysis, our device showed performance comparable to those found in literature, with MOD lower than 0.5 bpm in QB and lower than 1.2 bpm in tachypnoea, and LOA lower than 2 bpm in QB and not higher than 7.4 bpm in tachypnoea. Indeed, a similar study showed MOD between -1.6 bpm to 1 bpm and LOA from 0.303 bpm to 19 bpm [65], [69],

[73]–[75]. However, a comparison can be made only in standing and sitting conditions since solutions based on thermistors have not yet been tested in dynamic situations. Also, only two studies analyzed high RR, making the subjects breathe at a fixed rate ranging from 0 to 60 bpm and breathing at a slow, normal, and fast rate. However, they did not distinguish the results based on the RRs, so comparing them with ours was not possible [65], [75].

Since only eight subjects were enrolled, the sample size is still the primary limitation source. However, it should be noted that the subjects were different from the ones that tested the SFM the first time. To strengthen the findings' generalizability and robustness, future research will take into account a larger and more varied cohort of participants. Furthermore, additional trials will be conducted to evaluate the SFM's viability in more demanding contexts, such as sporting activities, professional settings, or medical procedures. This will offer an extensive understanding of its potential and constraints under various real-world scenarios.

Lastly, it should be underlined that the tests were conducted indoors, minimizing the influence of external temperature variations. To fully assess the impact of environmental conditions on respiratory rate measurement, future tests should be performed outdoors under different temperature and humidity levels. This will allow for a better understanding of how these factors affect the performance of the mask’s thermistor-based sensing system and ensure its reliability across various real-world scenarios.

In conclusion, this study demonstrated the feasibility of using a thermistor-based SFM to monitor RR in different scenarios, such as in everyday life activities, in occupational settings, and in more dynamic situations like walking. More studies are needed, enrolling in a larger number of subjects and testing the SFM in more challenging scenarios.

3 Development of a non-invasive System for Detecting Obstructive Sleep Apnea

3.1 State of the art in smart technologies for monitoring sleep-related respiratory disorders

OSA is a frequent and underdiagnosed Sleep-Related Breathing Disorder that carries a risk of complications, increases mortality, and causes additional healthcare load. It is characterized by intermittent upper airway obstruction causing interruptions of breath (apneas) and reductions in breath amplitude (hypopneas) during sleep, lasting from 10 seconds to 60 seconds or even more [85]. Currently, the gold standard diagnostic method is the full-night PSG, which requires the EEG, the EOG, the ECG, airflow, arterial oxygen saturation, and respiratory effort [45]. However, because of the multitude of examinations needed, the specialized personnel required, and the laboratory's full-time night shift, the complete PSG is very expensive. As an alternative, unsupervised assessments, HSATs, have been suggested lately [46], which do not require sleep laboratories, are easier to perform, are less expensive, and are widely available. Although the waiting list has reduced since their introduction, this disorder is still extremely underdiagnosed and undertreated. To increase the number of individuals that can be diagnosed and treated, new approaches are therefore required. Given these difficulties, it is necessary to create a clinical prediction model that can precisely determine which patients are most likely to benefit from PSG. Also, the American Academy of Sleep Medicine (AASM) has recently emphasized the need for more reliable and systematic diagnostic methods beyond the AHI alone**.** To improve screening accuracy, these models leverage demographic, anthropometric, comorbidity, and symptom data [86].

Recent studies search for convenient and comfortable OSA screening options using objective techniques like wearable technology or subjective techniques like questionnaires such as STOP-Bang (Snoring, Tiredness, Observed apnea, high Blood Pressure) [87].

It is known that snoring is the most prevalent symptom of this condition, with a prevalence reaching up to 94% of OSA patients. For this reason, it's widely believed that

the worse the OSA, the louder and more frequent the snoring. Nonetheless, between 10% and 60% of people in the general population snore regularly, though most do not have OSA [88]. A few studies attempted to objectively examine the connection between the severity of OSA and snoring by analyzing the audio signal in the time and frequency domain. By characterizing the snoring acoustic features, the aim of these studies is to correlate the snoring with the AHI and so to screen patients with the probability of having OSA. With the advancement of Artificial Intelligence (AI) models in healthcare, new algorithms have been implemented to refine OSA screening strategies, aiming to enhance sensitivity and accuracy. These models are particularly effective in diagnosing and screening due to their ability to process vast amounts of data and identify patterns that may not be apparent to clinicians. For instance, Machine Learning (ML) algorithms have been used to analyze anthropometric measurements to predict the likelihood of OSA, while Deep Learning (DL) models like Convolutional Neural Networks (CNNs) have been extensively applied to interpret medical imaging, including radiographs and computed tomography scans, for detecting abnormalities and disease markers. Furthermore, the analysis of respiratory sounds using ML and DL techniques has shown promising results in diagnosing respiratory conditions, demonstrating the versatility and potential of these algorithms in enhancing early detection and accurate diagnosis across various medical conditions. With this aim, microphones have been widely used to detect breathing sounds, snoring sounds, and breathing pauses and analyze breathing cessation (quiet time) or breath reduction between breaths and/or snores, recovery breath gasp after apnea, and modulated breathing patterns.

In a study performed by Alshaer et al. [89], the potential respiratory events were classified as apnea if there was a flat segment between the side edges (ventilation) characterized by zeros or near-zero (<0.01) amplitude in the normalized potential respiratory events, the flat segment lasts at least 10 s, and the flat segment lies between periods of ventilation that have an amplitude close to baseline level. If these tests were not positive, they tested the respiratory events for identification of hypopnea by verifying the falling edge based on the assumption that hypopnea evolves as a gradual reduction in net airflow from the gradual collapse of the upper airway in the obstructive type or the gradual decrease in respiratory drive in the central type; width length greater than 10 s; and a depth of 0.5 for the starting peak and 0.8 for the end peak. This algorithm showed an accuracy of 81%, specificity of 64%, and sensitivity of 96% when compared with the AHI scored the mean PSG of three evaluators according to the AASM guidelines. The same authors [88] implemented a Random Forest (RF) classifier using as features:

periodicity, which detects periodic sounds resulting from vibration of tissues during snoring; signal energy, which is proportional to sound amplitude; ratio of frequencies bands above and below 400 Hz; flatness of the frequency spectrum; uniformity of the signal; and entropy, a measure of signal's uncertainty. They found a weak but significant correlation between the snoring index and AHI (r = .32, P < .0001) and a non-significant negative correlation with central AHI (r = −.14, P = .035). Also, Snoring Index showed a had modest positive and negative predictive values for OSA (0.63 and 0.62 on average, respectively) and good sensitivity but low specificity (0.91 and 0.31 on average, respectively) attributed to the large number of snorers without OSA.

Two public and one self-recorded dataset were fed to a deep CNN algorithm, which was trained to recognize respiration sounds in sleep sound signals and to detect them using a Linear Regression (LR) classifier to identify OSA patients from potential patients. Using PSG as a reference, the authors obtained an Area Under the Curve (AUC) ranging from 0.79 to 0.82 [90]. Similarly, the deep CNN model built by Le et al. [91] on the basis of PSG audio datasets, smartphone audio datasets synced with PSG, and a home noise data set to train the model to detect OSA reached an accuracy of 86%. The same model was used to classify OSA severity with a sensitivity and specificity of 85% and 84%. Using the same algorithm, the authors tested the performance of the model with sound recording using an Android phone and an iOS one. They demonstrated comparable sensitivity, specificity, and accuracy for OSA screening, being 93.3%, 94.4%, and 94.3% in severe OSA screening using the iOS phone and 92.9%, 94.3%, and 94.1% using the Android phone [92]. Especially in post-pandemic settings, several apps designed for at-home acoustic OSA screening have been developed, with the advantage of requiring no further hardware than a smartphone. Among them, the Deep Neural Network (DNN)-powered Firefly and Sleep Study Apps showed an AUROC curve of 0.84 to 0.92 in screening moderate-severe OSA [93], [94]. Both these apps are supported by Android and Apple smartphones. Bahr-Hamm et al. [95] combined the entropy of snoring sound, low-frequency ECG, and thoraco-abdominal effort-PSG signal entropy values as surrogate markers for OSA detection and OSA severity classification using a Support Vector Machine (SVM) algorithm. The best performances were obtained using snoring signal entropy and considering the second night. Lastly, Hajipour et al. [96] compared the performance of RF against LR as feature selection tools and classification approaches for wakefulness OSA screening using daytime tracheal breathing sounds. RF outperformed LR in terms of blind-testing accuracy, specificity, and sensitivity, showing a 3.5%, 2.4%, and 3.7%

improvement, respectively. However, the regularized LR appeared to be faster than the RF and resulted in a more efficient model.

Differently, by analyzing the characteristics in the time domain of the snoring sounds, a recent study [97] selected a group of healthy habitual snorers without other OSA symptoms and quantified snoring frequency and intensity in a single night. From the snoring sounds, they extracted: the snore latency, defined as the time from sleep onset to the first snore breath; snoring frequency, the percentage of inspiratory breaths during sleep with sound peaks ≥40 dB(A); the snoring intensity (mean peak inspiratory sound), which is the maximum sound produced during each inspiration; and the sound threshold for adverse health events. The authors point out that subjects without OSA had a snoring intensity below 53 dB(A) and a snoring frequency below 25%. With this study, they found that the frequency and severity of snoring affected the presence of OSA, indicating that the likelihood of having OSA increased with snoring sound levels.

Another interesting study [98] analyzed the snoring sound to extract: the Mel-Cepstability, a measure of the entire night spectrum's stability; the running variance, which quantifies the inter-snore variability of the snore's energy across the night; the Apneic Phase Ratio, defined as the relative number of snore groups with energy variance larger than a specific threshold; the Inter-Event Silence, such as for example the silence between 2 sound events; and the Pitch Density, a measure of the stability of the tissue's vibration frequency. According to their results, the inter-event silence was the most effective feature for predicting AHI when used alone. However, estimating AHI using this feature alone leads to poor AHI prediction. So, it is important to integrate all these five features together to create a multidimensional feature vector that has a strong correlation with the AHI.

Analyzing the frequency domain of snoring sounds, Azarbarzin et al. [99] extracted the average power, the zero crossing rate, the frequency of the spectral peak with the lowest frequency, the frequency of the peak with maximum power, and the spectral entropy. They reached an accuracy for 4-class classification of about 77.2%. However, in distinguishing between non-OSA (AHI < 5) and OSA (AHI > 5) snorers, the algorithm shows better performance (92.9% sensitivity, 100% specificity, and 96.4% accuracy).

Halevy et al. [100] explored the acoustic characteristics of hypopnea in order to discriminate it from apnea. For each apnea, hypopnea, and normal breath event, a 36-dimension feature vector was extracted, and then the most representative features were selected: the time signal amplitude, which varies between normal breathing segments and hypopnea and apnea events; the loud breath or snore at the end of apnea or a

hypopnea event to compensate for the lack of oxygen caused by the cessation of breathing; the autocorrelation function of the short-term energy sequence among hypopnea and normal breath events which tends to resemble a sine wave; the mean of the higher quartile of the frequency center of mass time derivative; and the duty cycle, computed as the area of the higher energy content divided by the area of the entire energy content of the event. To classify normal breath, apnea, and hypopnea, an accuracy of 84.7% was achieved while distinguishing between two classes (apneic events and normal breath events), the classifier achieved an accuracy of 93.4%.

Lastly, Levartovsky et al. [101] extracted from the detected breathing events four acoustic features: the sound intensity (dB), the event duration (s), the acoustic energy (dB × s), and the frequency center of mass (frequency centroid, Hz). They did not find significant differences in snoring intensity, duration, and energy between groups in both sexes at all sleep stages, while in all sleep stages, frequency centroid was elevated ($p < 0.01$) in men with OSA compared with men in the comparison group. The Pearson correlation analysis showed no association between AHI and mean breathing or mean snoring intensity, while the frequency centroid of breathing and snoring sounds correlated with AHI. The presented works are summarized in Table 4.

Based on these previous works, the aim of this study is to implement an algorithm that is able to extract respiratory events related to OSA in suspected subjects and evaluate the severity of this disease from the snoring sound. In this way, this method can be used as a simple and cost-effective screening tool.

Table 4: Overview of the state of the art studies.

Author (year)	N. of patients	Sound recording device	Algorithm	Features extracted
Ben-Israel et al. (2012) [98]	90	Non-contact directional condenser microphone placed 1 m above the bed	Custom algorithm	Mel-Cepstability; Running Variance; Apneic Phase Ratio; Inter-Event Silence; Pitch Density
Alshaer et al. (2013) [89]	50	Microphone embedded in the center of a loose-fitting face frame	Custom algorithm	Apneas: Flatness test; Width test; Depth tests Hypopneas: Falling edge (FE) test; Width test; Depth test
Azarbarzin et al. (2013) [99]	57	Microphone embedded in a chamber placed over the suprasternal notch of trachea	Custom algorithm	Average power; zero crossing rate; the frequency of the spectral peak with the lowest frequency; the frequency of the peak with maximum power; the spectral entropy
Halevi et al. (2016) [100]	44	Directional condenser microphone positioned 1 m above the subjects' head	SVM	Entropy, duty cycle; frequency center of mass, short-term energy
Levartovsky et al. (2016) [101]	121	Directional microphone positioned 1 m above the subjects' head	Custom algorithm	Sound intensity; event duration; acoustic energy; frequency center of mass
Alshaer et al. (2019) [88]	235	BresoDX device	RF	Periodicity; signal energy; the ratio of frequency bands; flatness of the frequency spectrum; uniformity of the signal; entropy
Hajipour et al., (2020) [96]	199	Sony ECM-77B microphone embedded in a chamber placed over the suprasternal notch of their trachea.	LR; RF	78 tracheal breathing sound features: sex, age, height, weight, body mass index (BMI), neck circumference, and Mallampati score
Luo et al., (2020) [90]	132	Microphone placed 1 m from the patients	deep CNN	Audio signal sets (Audioset and ESC-50) and data sets from potential patients (PSG and sleeping sound recordings). Sleeping sound signals are collected by a microphone (Model NT3, RODE, Sydney, Australia)
Sowho et al. (2020) [102]	162	Digital sound pressure level meter (DT-8851, Ruby Electronics, Saratoga, CA)	Custom algorithm	Snore latency; snoring frequency; Snoring intensity; Sound threshold for adverse health events
Tiron et al., (2020) [93]	248	Smartphone app	DNN	Active sonar detection of respiratory effort and movement; passive recording of breathing sounds
Romero et al., (2022) [94]	103	Smartphone placed next to the bed at head level.	DNN	Audio recording
Bahr-Hamm et al., (2023) [95]	86	PSG-embedded microphone placed on the neck	SVM	Snoring entropy

Le et al., (2023) [91]	1315	PSG microphone installed on the ceiling 1.7 m above the subject's head; smartphone microphone (LG G3, LG Electronics, Inc, Seoul, Republic of Korea) placed 1 m away from the subject	deep CNN	PSG audio data sets, smartphone audio data sets synced with PSG, and a home noise data set featuring 22500 noises
Han et al., (2024) [92]	101	iPhone 13 (Apple Inc) and Galaxy S20 (Samsung Electronics)	deep CNN	Recorded Breathing sounds

Support Vector Machine – SVM; Random Forest – RF; Linear Regression – LR; Convolutional Neural Network – CNN; Deep Neural Network - DNN

3.2 Derivations of Obstructive Sleep Apnea from Snoring Sound

The audio signal was collected using the audio recording application installed in a Samsung Galaxy Tab S7.

To detect the respiratory events (apneas and hypopneas) from the audio signal, the following analysis was carried out:

- A digital band-pass filter was applied using the Butterworth filter design function and then the *filtfilt* function that performs the zero-phase forward and reverse digital filtering. The signal was band-pass filtered between 150 Hz and 500 Hz to remove frequency components unrelated to snoring. To choose the cut-off frequencies, the signal was analyzed using the Fast Fourier Transform (FFT) to detect the dominant frequency components and the spectrogram to visualize how the frequency content varied over time. An example of the audio signal and the respective FFT and spectrogram is shown in Figure 22.
- To reduce the computational load, the signal was undersampled from 44100 Hz (original sampling frequency) to its half, 22050 Hz, and segmented into 30-minutes windows.
- The resampled signals of each window were processed to calculate their envelopes using a moving Root Mean Square (RMS) window (approximately 1.5 times the new sampling frequency), and the resulting envelopes were then normalized to a range between 0 and 1.
- The function *findpeaks* was applied on the normalized signals, manually setting each subject's minimum peak distance and the minimum peak height.
- To detect potential respiratory events, the distances between consecutive peaks were converted to time values. Apneas were defined as intervals lasting at least 10 s, with a maximum duration of 60 s set to exclude silences caused by the cessation of snoring. For each apnea interval, the difference between the peak value and the median signal value over the following 10 s was calculated and normalized. Apneas were flagged when this normalized difference exceeded 90%, indicating significant signal deviations during the apnea period.

An example of an analysis process on one signal is shown in Figure 23.

The results were expressed as the total number of respiratory events found by the analysis of the audio signal and from the reference system. In addition, the AHI index,

calculated by dividing the total number of respiratory events (apneas and hypopneas) by the total sleep time, was calculated to determine the degree of severity.

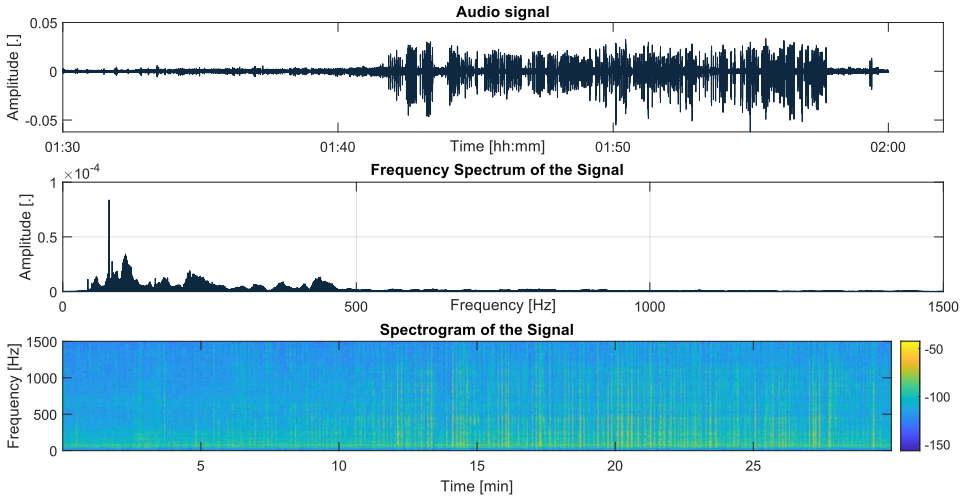

Figure 22: Segment of the audio signal and respective FFT and spectrogram.

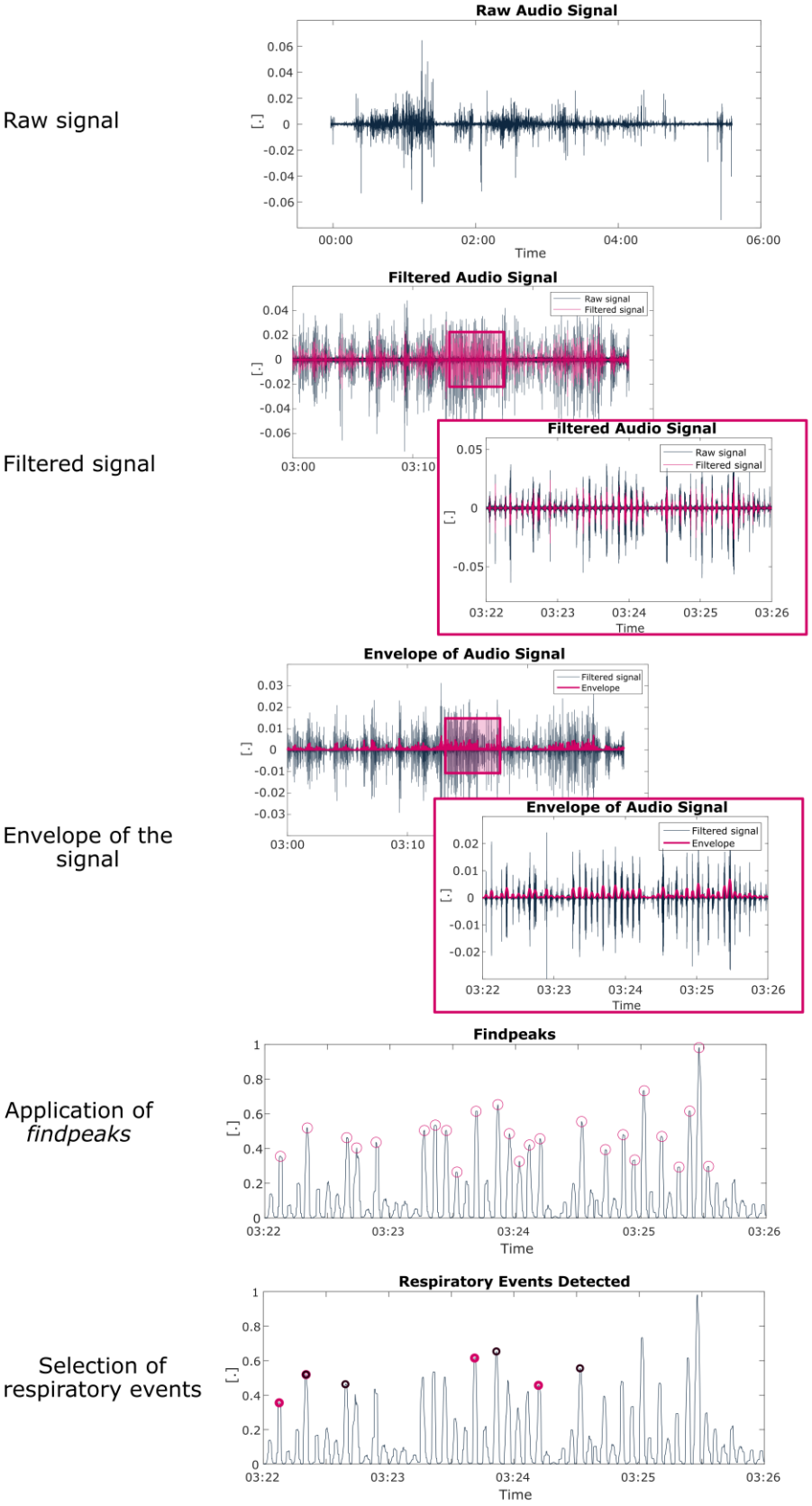

Figure 23: Data analysis step: the raw signal is filtered and enveloped. The findpeaks function is applied to the normalized signal. The start and end of the respiratory events are visualized in the last plot as a pink and black circle, respectively.

3.3 Experimental testing on subjects with suspected Obstructive Sleep Apnea

3.3.1 Reference system

As a reference system, the WatchPAT device (Itamar Medical Ltd., Caesarea, Israel) was chosen as it is widely used in clinical practice. The WatchPAT is worn on the patient's wrist, like a watch, and collects data based on changes in peripheral arterial tone (PAT). The PAT signal is a non-invasive measure of arterial pulsatile volume changes at the fingertip. A reduction in the PAT signal, accompanied by an accelerated pulse rate, reflects sympathetic activation, indicative of autonomic arousals and micro-arousals commonly associated with sleep apnea. The PAT algorithm integrates reductions in the PAT signal with oximetry desaturations to identify respiratory events. By the nature of the signal, the device detects respiratory events indirectly, recognizing them at their endpoints when the nervous system begins to respond to breathing difficulties.

In this way, it provides the following data: AHI, Respiratory Disturbance Index, Oxygen Desaturation Index, total sleep time, and sleep stage percentages. In addition, the WatchPAT device provides information about snoring and body position [15]. Also, the Central PLUS Module enables specific identification of Central Sleep Apnea and Percent of Sleep Time with Cheyne-Stokes Respiration. However, it is essential to notice that the WatchPAT cannot be used in the following cases: use of alpha-blockers, short-acting nitrates (less than 3 h before the study); permanent pacemaker: atrial pacing or VVI without sinus rhythm; and sustained non-sinus cardiac arrhythmias.

According to the last update of the clinical guidelines of the AASM [103], the severity of the disease is based on the AHI index, as reported in Table 5.

Table 5: Severity of OSA

Severity	**AHI**
Normal	<5 events/h
Mild OSA	5–14.9 events/h
Moderate OSA	15–29.9 events/h
Severe OSA	≥30 events/h

3.3.2 Experimental protocol

In this study, four subjects with suspected OSA (2 men and 2 women, aged 57 ± 23.71 years, range 24–80 years, BMI 23.27±2.29 kg/m^2) were enrolled to evaluate the algorithm's performance in detecting respiratory events.

Each volunteer underwent a home-based night study using the WatchPAT device (Itamar Medical Ltd., Caesarea, Israel) as the reference system, while simultaneously, a tablet recorded their snoring sounds throughout the night, as illustrated in Figure 24.

The subjects were instructed on how to position the WatchPAT and start the test. They were asked to activate both devices upon going to bed and to stop the audio recording upon waking. The WatchPAT automatically stops recording when removed from the body.

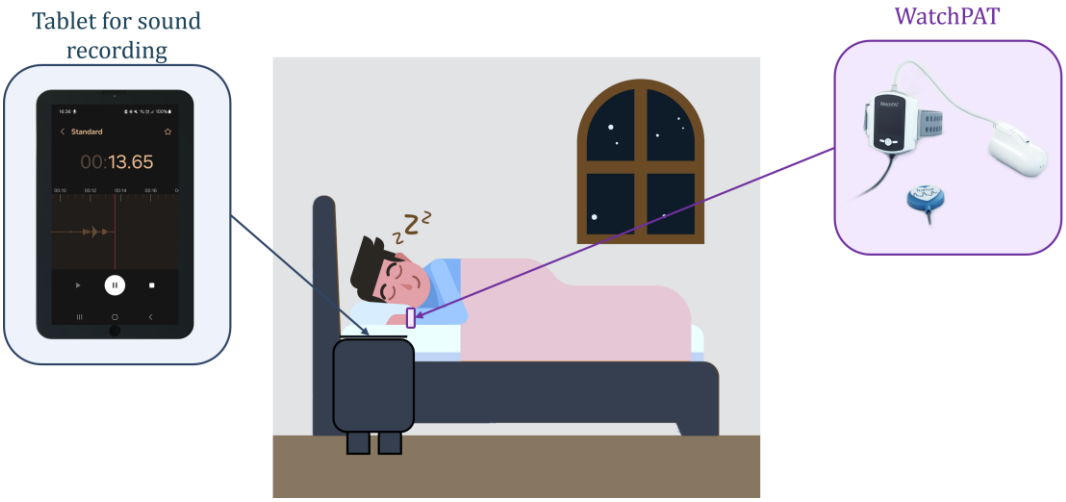

Figure 24: Experimental setup: the subject wore the WatchPAT and positioned the tablet close to the bed.

3.3.3 Results

To compare the results obtained from the audio signal with those from the reference system, the two signals were synchronized based on the start and end times of the recordings. However, due to the nature of the reference system, it was not possible to perfectly align the respiratory events detected by the two systems. Instead, the total number of events was evaluated.

From the analysis of the audio signal, the algorithm calculated the number of respiratory events, and the corresponding AHI index was determined. These results were then

compared to those obtained using the WatchPAT device. The founded results are shown in Figure 25.

For subjects 1, 2, and 4, the number of events detected differed by at most one event. Subjects 1 and 2 were correctly classified within the "normal" range, while subject 4 was accurately categorized in the "mild" range.

Subject 3, however, suffers from a severe form of sleep apnea, which includes central events that cannot be detected by the audio-based method. The difference between the two systems for this subject was 89 events. Despite this, when calculating the AHI, the index derived from the audio-based system was 47.8, placing it in the "severe" range, consistent with the AHI estimated by the WatchPAT.

A

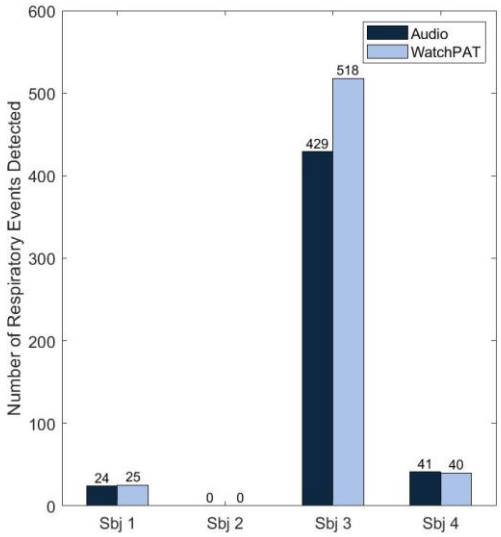

B

Subject	AHI [events/h]	
	Audio Signal	WatchPAT
#1	3.2	3.4
#2	0	0
#3	47.8	57.8
#4	7.6	7.4

Figure 25: ***A.*** *Comparison of the total number of respiratory events resulting from the analysis of the snoring sound and the WatchPAT for each subject.* ***B.*** *AHI index calculated by the two systems for each subject.*

3.4 Discussion and Conclusion

The prevalence of OSA is increasing globally, driven primarily by the rising rates of obesity, the principal risk factor for the condition. However, significant disparities exist in the diagnosis and management of OSA across countries, largely influenced by variations in healthcare infrastructure, public awareness, and the availability of specialized sleep medicine services.

For example, a population-based study in Singapore revealed limited awareness of OSA, with only 21.5% of participants familiar with the condition [104], while in a Canadian survey the authors reported better awareness of sleep apnea (56%) [105].

Big disparities among the countries also exist in the accessibility to attended or unattended PSG, the gold standard for OSA diagnosis. In Nigeria, for instance, fewer than 5% of teaching hospitals are equipped with sleep laboratories, and none have dedicated sleep disorder clinics [106]. However, expanding traditional diagnostic infrastructure alone is unlikely to address the global burden of OSA effectively. Even in high-income countries, where PSG is more readily available, patients often face long travel distances and wait times spanning months. Broader adoption of home-based diagnostic testing and telemedicine services may help mitigate these challenges [107], [108]. Also, since untreated OSA is associated with significant health consequences, early identification and intervention are fundamental. In this context, developing new and reliable screening tools is critical. Current clinical practice often relies on questionnaires to assess OSA risk, such as the Berlin Questionnaire, STOP-Bang, and the ESS. However, these tools are limited by varying levels of diagnostic performance.

This study aimed to develop a simple and cost-effective screening tool for OSA, utilizing snoring sounds as the primary diagnostic marker. Snoring is a common complaint among patients, many of whom are unaware that objective measures of snoring severity are strong predictors of concomitant OSA, even after adjusting for risk factors such as age and sex.

The findings of this study highlight the potential of an audio-based algorithm as a cost-effective and accessible method for OSA screening, offering a promising alternative to traditional approaches in clinical practice.

During sleep, upper airway resistance increases, leading to the amplification of air-pressure oscillations that are perceived as typical breathing sounds. These sounds can vary from quiet to very loud snoring (> 40 dB) in the same subject [101].

In this study, a non-contact microphone was chosen to record breathing and snoring sounds, as this approach allows for more natural sleep that is not influenced by the presence of cumbersome equipment. In contrast, previous studies in the literature have employed contact microphones taped to the nostrils or trachea or microphones embedded in face masks [88], [109], [110]. However, such methods can interfere with the subject's sleep, resulting in an inaccurate representation of a typical night.

One of the main challenges of an audio-based approach is background noise. Although nighttime environments are generally quieter than daytime, it remains crucial to exclude sounds originating from subject movement, bed partners, or external sources such as street traffic. These noises, which differ significantly from snoring, were filtered in the implemented algorithm using a band-pass filter, ensuring the accurate identification of snoring sounds.

The inability to precisely synchronize respiratory events between the audio-based system and the WatchPAT device is one of the study's primary challenges. This limitation stems from the nature of the PAT signal, which makes a derivative measurement and does not allow for precise prediction of apnea termination. Consequently, the comparison between the two systems was made by considering the total number of respiratory events detected by each system during the night.

The results of this study demonstrate the promising potential of the audio-based system for detecting respiratory events and estimating the AHI, particularly for patients with OSA severity ranging from normal to moderate. Indeed, in these subjects (number 1, 2, and 4), close agreement was found between the audio-based system and the reference WatchPAT device. However, the significant discrepancy observed in subject number 3 highlights the important limitation of the audio-based approach, which is its inability to detect central sleep apnea events, which are not associated with snoring or typical obstructive breathing patterns. However, this type of patient requires a more in-depth neurological assessment by undergoing a full PSG, including the EEG study. Despite this limitation, the AHI estimated by the audio system still accurately categorized the subject within the "severe" range, demonstrating robustness in identifying overall disease severity. Receiving such a result, the subject would still be encouraged to undergo more detailed evaluations and consult a physician to discuss potential treatment options. On the other hand, this method allows to exclude individuals with no significant respiratory pathology, such as simple snorers.

Several studies have assessed the effectiveness of different algorithms in distinguishing between OSA and non-OSA patients and in predicting disease severity. Alshaer et al. [89]

achieved an accuracy of 81%, a specificity of 64%, and a sensitivity of 96% by classifying a respiratory event as apnea if a flat segment between the side edges (ventilation) of at least 10 seconds was detected. Using a deep CNN model, Le et al. [91] achieved an accuracy of 86% in detecting OSA. The same model was applied to classify OSA severity, yielding a sensitivity of 85% and a specificity of 84%. The same authors also tested audio recordings obtained using both Android and iOS smartphones, demonstrating comparable sensitivity, specificity, and accuracy for OSA screening. Specifically, for severe OSA detection, the iOS-based approach achieved a sensitivity of 93.3%, a specificity of 94.4%, and an accuracy of 94.3%, while the Android-based method reached 92.9%, 94.3%, and 94.1%, respectively [92].

Azarbarzin et al. [99] analyzed the frequency domain of snoring sounds, extracting parameters such as average power, zero-crossing rate, the frequency of the spectral peak with the lowest frequency, the frequency of the peak with the highest power, and spectral entropy. Their algorithm achieved an accuracy of 77.2% in a four-class classification task. However, when distinguishing between non-OSA (AHI < 5) and OSA (AHI > 5) snorers, the model demonstrated superior performance, with a sensitivity of 92.9%, a specificity of 100%, and an accuracy of 96.4%.

These findings suggest that while this audio-based system may not replace comprehensive diagnostic tools, it holds significant promise as an accessible and cost-effective screening tool, particularly for OSA. Future improvements, such as incorporating these data with clinical and anthropometric data of the subject, could further enhance the diagnostic accuracy of this approach. In addition, none of the included participants had a snoring bed partner. This condition should be investigated to determine whether the proximity of the device to the study participant is sufficient to accurately distinguish their snoring or if it is possible to differentiate snoring based on, for example, frequency characteristics or distinct breathing patterns.

Lastly, given that the primary limitation of this research is the small sample size, future studies will aim to include a larger and more diverse cohort of participants to enhance the robustness and generalizability of the findings.

This study may be considered a first effort in implementing an algorithm able to detect respiratory events from snoring sounds and may be beneficial for the following research in developing useful screening tools for potential OSA patients.

4 Development of an Earplug for Protecting from Medical Instrument Sounds

4.1 State of the art in individual protective device for the prevention of Otorhinolaryngological disorders

HL from prolonged noise exposure is known as NIHL. It results from multifactorial damage to auditory structures following exposure to occupational, environmental, or recreational sources of loud sound. The duration and severity of NIHL depends on the extent and location of cellular damage, which correlates with the intensity and time of the sound stimulus.

For many years, it has been known that exposure to dangerous noise levels at work is related to the incidence of acquired HL [111]. Globally, disabling HL attributed to occupational noise is estimated to affect approximately 16% of adults, ranging from 7 to 21% across various geographic regions [112].

This recognition started the development and implementation of public health policies and early intervention and prevention initiatives. Workplaces across many industries, including manufacturing, utilities, transportation, the military, construction, agriculture, and mining, are required by law in many countries to control harmful noise exposures and implement hearing conservation programs. Various strategies are employed to limit noise exposure in the workplace to prevent occupational NIHL. These strategies include reducing noise at the source, implementing noise barriers, and dampening systems. Also, administrative actions can be taken, such as scheduling changes to limit the duration of noise exposure and implementing quiet zones. When noise levels cannot be reduced to acceptable standards, PPE becomes crucial [111], [113].

However, the main risk of these PPE is that they attenuate all sounds indiscriminately, affecting typical speech frequencies. This, of course, can generate difficulties in communication with other people and workers, so these devices are often abandoned [54]. Electronic headphones with controlled attenuation are commercially available, featuring adjustable amplification for speech frequencies (i.e., 500 Hz - 2000 Hz) and an

electronic system for limiting impulsive noises to 82 dBA. However, integrating the electronic regulation mechanism increases the device's costs. It is essential to note the absence of regulatory mandates obligating workers in this category to wear hearing PPE; instead, the decision remains discretionary for individuals. The high costs associated with these devices may potentially dissuade prospective buyers from acquiring them.

Recent studies evaluated the usability and effectiveness of PPE. Among these, Borell et al. [114] investigated the proper use, comfort, and fit of various PPE items—such as helmets, ear protectors, goggles, respiratory masks, gloves, protective clothing, and safety harnesses—used individually or in combination during construction work.

The usability tests indicated that single PPE items were generally effective and well-tolerated. However, combining multiple PPE items often resulted in minor discomfort, which progressively increased. For instance, wearing a helmet along with goggles and ear protectors led to poor fit, uncomfortable pressure at the temples, and potential obstruction of peripheral awareness. The study highlighted that ear protectors could isolate users from their environment, making them unable to hear co-workers or critical warnings, which poses a safety risk. However, certain ear protection devices are available that allow for the transmission of alarm signals and speech while still attenuating ambient noise. An example of these has been implemented by Madahana et al. [115] who developed a system for early monitoring of HL in mine workers. The system integrates a smartwatch and smart hearing muffs equipped with sound sensors to measure noise intensity and exposure frequency. Data collected by these devices is transmitted to a database, where machine learning algorithms—including logistic regression, support vector machines, decision trees, and Random Forest Classifier—analyze and categorize it into priority levels. Feedback is then sent to the worker's smartwatch, with extreme priority levels triggering vibrations to alert the worker of hazardous noise exposure. Preliminary results indicate that the decision tree algorithm achieved the highest accuracy, with an average testing accuracy of 91.25% and training accuracy of 99.79%. The system demonstrated effective performance in detecting noise levels, transmitting data to the database, and providing timely alerts to workers.

However, it is known that also healthcare workers are at risk of NIHL. As an example, the orthopedic operating theatre environment is characterized by excessive noise generated by power tools, plaster-cutting saws, bone-cutting saws, suction, and the striking of hammers, which generate noise as loud as 145 dB. These may result in impaired cognitive function, HL, and communication problems, which may cause surgical errors in the patient's care. According to the literature that is currently available, half of the staff

members who work in orthopedic theaters are more likely to experience different levels of NIHL [116].

Another study included employees from the clinical laboratory, front desk, central supply center, janitorial services, and clinic to evaluate their risk to develop HL. Based on the median occupational noise exposure, these participants were then divided into groups for high-noise exposure (HNE) and low-noise exposure (LNE). The HNE group had a significantly higher average noise exposure than the LNE group (70.4 dBA vs. 61.8 dBA). These numbers exceed the average hospital noise levels of 30 to 35 dB that are advised by the WHO. This study emphasizes the long-lasting range of noise-induced damage brought on by exposure at medium and high intensities [117].

Lastly, sound pressure levels from magnetic resonance imaging (MRI) usually exceed 85 dB and can occasionally peak at 120–130 dB. Therefore, it is necessary to reduce this acoustic noise to protect patients and staff. Additionally, MRI-generated noise is linked to patient anxiety and discomfort, which can exacerbate claustrophobic reactions and lead to exams being preemptively stopped. Also, the noise makes it difficult for staff to speak to the patient or provide verbal support during the examination [118].

In this context, this study aims to develop a new earplug that protects from high-frequency noise and amplifies speech frequencies. Moreover, this prototype has been tested in the context of healthcare personnel routinely working in a dental office chronically exposed to high-frequency noise sources.

4.2 Design and fabrication of the protective earplug

4.2.1 Working principle

The resonance effect is a phenomenon where a system naturally oscillates or vibrates at its resonant frequency, significantly amplifying its response. On the contrary, antiresonance occurs when a system exhibits a decrease in response at a specific frequency. The resonance-antiresonance principle offers a practical approach for achieving selective amplification and attenuation of a particular frequency range. Indeed, a resonant filter or circuit can be designed to amplify specific frequencies while attenuating frequencies outside that range. Among the different possible solutions, resonance tubes can be used as mechanical filters, achieving a similar effect through acoustic resonance. Modifying the tube's length makes it possible to tune it to resonate at frequencies within the desired range. Also, the tube's diameter can impact the resonance's quality and efficiency: a larger diameter tube generally allows for greater air volume and can result in more robust resonant responses, while a smaller diameter tube may exhibit higher frequencies and have a narrower resonance bandwidth [119].
In the application proposed in this study, the dimensions of the tube's parameters also need to meet the typical characteristics of an earplug: the diameter cannot be too small, or it could be obstructed by cerumen, and the dimensions of the earplug influence the length.

4.2.2 Device design and fabrication

In this study, we used a closed-end resonance tube with one end open and one closed. A good approximation is to consider the hole as an open-closed tube resonator: the side facing outward (open to the environment) allows sound to enter freely, while the side facing the ear (almost closed) transmits sound inward, but with an acoustic load provided by the ear. Indeed, the hole is not a perfectly closed tube but rather a conduit behaving more like a band-pass filter. Moreover, cavity resonances and potential interactions with the inner ear shift the amplification peak towards lower frequencies. The cavity resonances inside the ear modify the peak frequency, and coupling with the auditory canal creates a more complex system than a simple closed tube.

The protective earplug is designed to have a central part that is universal and closely resembles a real ear canal and concha, and the ear tips to customize it. This design allows for a highly comfortable ear protector that fits the ear better than standard ones, typically with simple shapes like cylinders or cones. Furthermore, the device has a hole that runs through the ear protector's entire length, allowing controlled sound passage from the outside to the inside of the ear. The hole is designed to attenuate harmful sounds and, at the same time, amplify essential sounds, such as human voices.

For this specific application, the hole diameter was chosen based on the resonance properties of a tube with a 1.8 mm internal diameter and 17 mm length. These dimensions were optimized to amplify speech frequencies (500 Hz - 1000 Hz) while attenuating high frequencies (4000 Hz - 6000 Hz) commonly produced by medical instrumentation.

The protective earplug was realized using a Resin Digital Light Processing (DLP) 3D printer (EnvisionTEC Perfactory) and made of acrylic resin, available in various colors. The ear tips used are made of silicone or neoprene. The earplug viewed from two opposite angles and worn by a subject is shown in Figure 26.

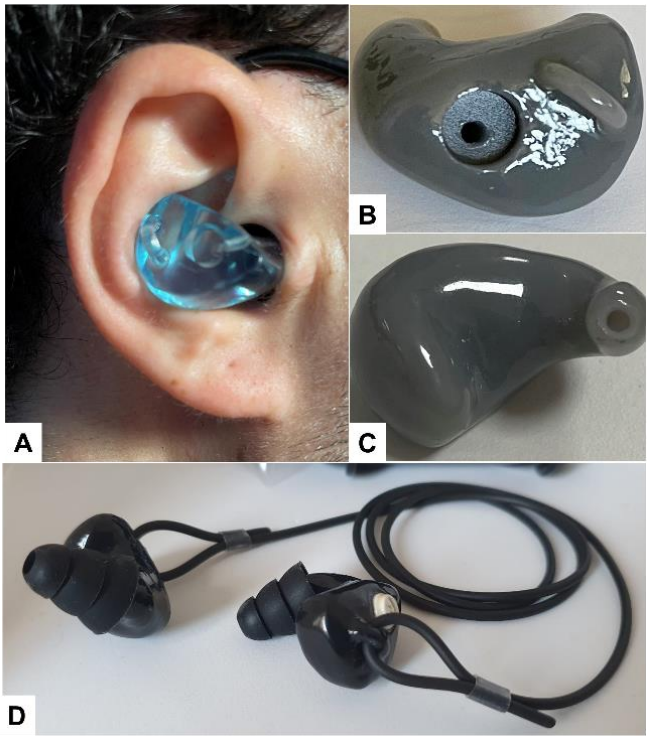

*Figure 26: **A**: Protective earplug worn by a subject; **B**: anterior view of the protective earplug; **C:** posterior view of the protective earplug (without ear tip); **D**: protective earplugs with ear tips.*

4.3 Validation of the acoustic earplug

4.3.1 Experimental testing

The FONIX 7000 electronic ear was chosen to test the performance of the earplug. This testing device allows to characterize the response of hearing aids and earplugs in terms of frequency response, harmonic distortion, equivalent input noise, and compression.
To conduct the test, the device was connected to a 2 cc coupler and placed in a sound chamber. A schematic representation of the experimental setup is shown in Figure 27.
A composite signal was used, which was a continuous real-time, speech-weighted signal composed of 79 different frequencies. This approach provides the advantage of assessing the response to noise in a way that more accurately simulates speech. Specifically, the ANSI speech-weighting setting was chosen. This composite filter, based on the ANSI S3.42 standard, attenuates the high frequencies at a rate of 6 dB per octave, starting with a 3 dB drop at 900 Hz.
Additionally, a noise reduction setting of “4X” was selected. This setting applies a "running average" to the measurements taken while the composite signal is active. In practice, it averages several previous measurements with the current one to generate the next response curve. Selecting “4X” means that the last four measurements are averaged together. When making composite measurements, due to the nature of the moving average, it takes a few seconds for the noise reduction to reach the set value. More noise reduction leads to smoother curves but increases the time it takes the analyser to update the composite measurements.

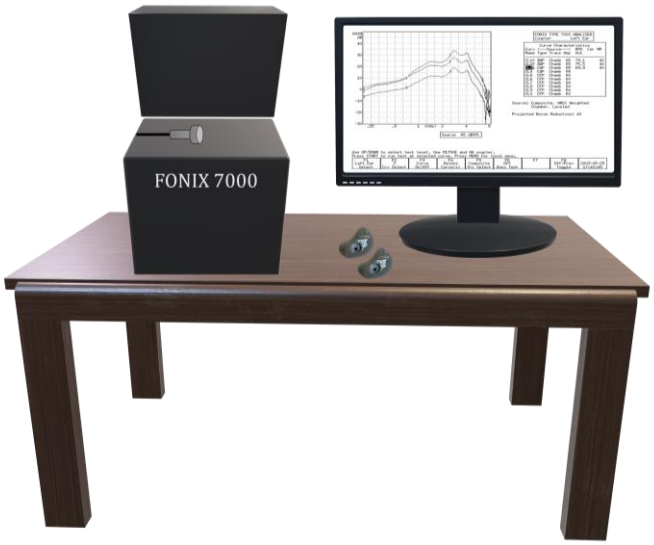

Figure 27: Schematic representation of the experimental setup. The figure shows the FONIX 7000 device with the 2 cc coupler, a PC displaying a representative screen of the software used and the protective earplug.

The test results are shown in Figure 28. The no-earplug line represented the reference value, when no earplug is applied. It was obtained with a sweep taken at 60 dB SPL, following the IEC 118-7 standard. The closed earplug was measured by blocking the protective earplug hole with surgical silicone, resulting in an attenuation greater than 15 dB across all frequencies.

Conversely, the protective earplug, with its open hole, showed a selective amplification of frequencies between 500 Hz and 1000 Hz, ranging from 4 dB to 13 dB, while predominantly reducing frequencies between 4000 Hz and 6000 Hz.

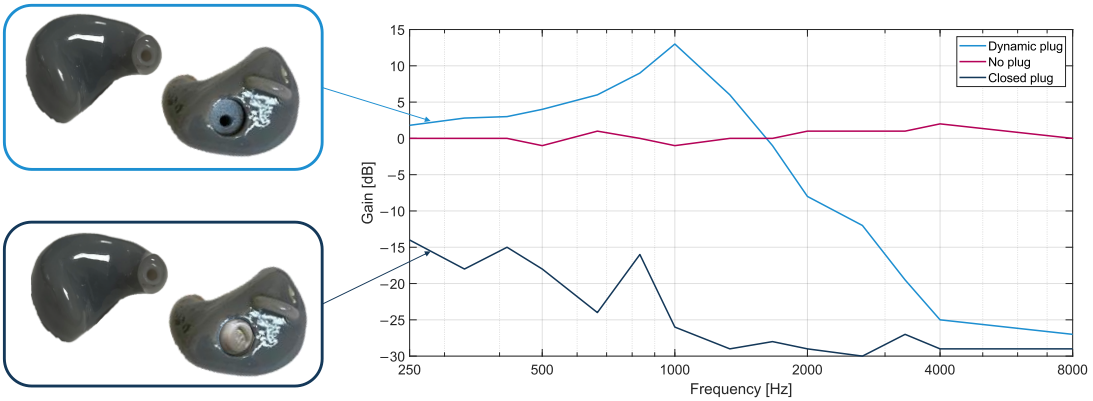

Figure 28: The response curve of the protective earplug closed earplug, and no earplug was inserted.

4.3.2 Use Case: Application for dental practitioners

Among the various professionals chronically exposed to noise, dental practitioners experience constant exposure to high-frequency (ranging from 4000 Hz - 12000 Hz) and high-intensity (65 dBA - 85 dBA) noise [120]–[124]. In this occupational category, NIHL is estimated to reach a prevalence ranging from 5% to 20% of workers [54], [125], [126]. However, dentists are not the only dental professionals who suffer from this disorder, as they are not the only ones working in such an environment. Dental technicians, prosthodontists, dental hygienists, and chairside assistants are also exposed and may need protection. Chronic exposure to noisy sources can lead to short- and long-term consequences, such as difficulty in communication, annoyance, interference in conversation, and difficulty concentrating [122]–[125], [127], [128]. The dental instruments and equipment most used by dentists that emit high-frequency noise are high-speed turbines, aspirators, and ultrasonic scalers. Typically, these dental instruments produce high-intensity noise between 65 dBA and 85 dBA with an average frequency ranging from 4000-12000 Hz [120], [121], [129]. Even though the levels of exposure of modern dental equipment are generally within the limits set by the National Institute for Occupational Safety and Health, which recommends limiting noise exposure to 85 dBA at 40 h per week [130], studies reported that the noise levels of dental equipment may still provoke NIHL [54], [122]–[125]. Indeed, continuous exposure to more than 100 dB for more than 8 hours increases the risk of permanent HL from 94.5% to 99.5% [123], [131]. Prolonged and uninterrupted exposure to noise may impact the professional performance of clinicians, affecting communication with patients and colleagues and potential interruptions in their work. Moreover, long exposure to such noise may result in permanent hearing damage, such as sensorineural NIHL, and the development of tinnitus. Additionally, the enduring consequences of this long-term exposure include reduced concentration and memory capacity and decreased sleep quality. However, short-term consequences also need to be considered, such as headache, nausea, fatigue, hypertension, irritability, and tinnitus [132]. In particular, tinnitus is believed to be highly prevalent in the dental clinician's community, yet only a few studies have evaluated the real prevalence of this condition among them. Among these, a study conducted in South Africa showed a prevalence of 31.85% [133], and similarly, a study conducted in the USA found a prevalence of 31% [125]. A slightly higher prevalence was found in the United Arab Emirates, which was reported to be 37% [134].

Although the presence of NIHL among dentists is well documented, many are still unaware of the immediate and long-term effects that chronic noise exposure can cause on the auditory system, and preventive measures are not widely promoted and used. Dentists are often reluctant to use these ear protection devices as they are perceived as annoying and severely limiting clinical activity, as they reduce the ability to communicate with patients and assistants [122].

Currently, no commercially available hearing PPE is specifically designed for dentists and health care personnel, but earplugs and/or headphones inserted in the pinna may be used. However, these PPE attenuate all sounds indiscriminately, affecting typical speech frequencies. This, of course, can generate difficulties in communication with patients and staff members, so these devices are often abandoned [54].

For these reasons, this population was decided to be the first tested group.

4.3.2.1 Materials and Methods

From January to May 2023, dentists and technical staff who, in everyday clinical practice, are chronically exposed to noise generated from high-frequency dental instruments averaging 4000 Hz - 6000 Hz were enrolled. The inclusion and exclusion criteria are listed in Table 6.

At the beginning of the study, each participant underwent an ENT examination with otoscopy and liminal tonal audiometry, and the following information was recorded:

- profession (e.g., dentist, prosthodontist, dental technician, dental hygienist, dental assistant);
- years of professional activity;
- number of hours of average daily exposure;
- regular use of hearing PPE in clinical practice.

Then, each participant received the protective earplug for an entire work shift (minimum 8 hours).

At the end of the work shift, they were asked to complete a questionnaire, as reported in the literature [135]. A schematic representation of the protocol is shown in Figure 29.

The questionnaire is divided into three parts: the first regarding the device's characteristics, the second the device's usefulness, and the last the critical aspects and benefits of the device. The questions asked of the subjects are reported in Table 7. Before performing the questionnaire, the questions were explained to the included subjects. In particular, concerning the question related to the hearing of patients' and colleagues' voices (questions 2.3 and 2.4), it was explained that they have to understand what they

were saying and not just hear the sound of the voice. Also, regarding the perception of muffled ears (question 1.2) and pain (question 1.5), it was specified that "Excellent" indicated the absence of these sensations.

Data collected from each test have been expressed as a percentage of agreement. The correlation between the results of the first part of the questionnaires questionnaire and years of experience and time of noise exposure was calculated by Pearson's correlation coefficient, while the correlation between part 2 of the questionnaire and the years of experience and time of noise exposure was calculated with the Point-Biserial correlation since the response is binary. A p-value <0.05 was considered statistically significant. Data were analyzed and plotted using MATLAB® by MathWorks.

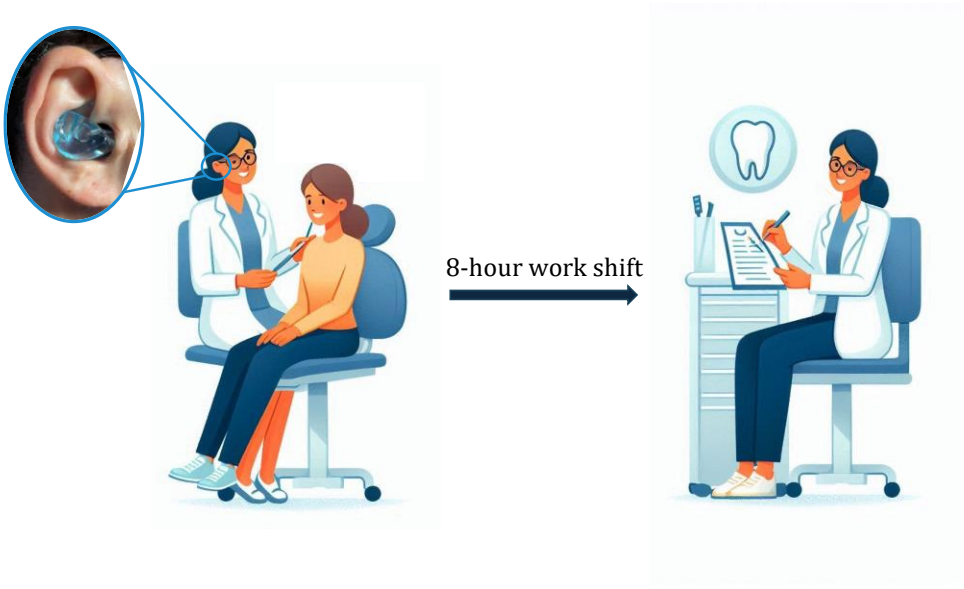

Figure 29: Schematic representation of the experimental protocol followed by the subjects.

Table 6: Inclusion and exclusion criteria.

Inclusion	Exclusion
- Dentists and associated health care personnel aged >18 years old who, in everyday clinical practice, are chronically exposed to high-frequency noise sources (4000 Hz - 6000 Hz). - Normal on otoscopic inspection. - Hearing sensitivity less than 15 dB bilaterally.	- Hearing threshold greater than 15 dB bilaterally for frequencies between 250 Hz - 4000 Hz. - Previous history of ear infection or trauma. - Pathologies affecting the pontocerebellar angle. - Pregnant or lactating women. - History of previous otologic surgery.

Table 7: Questionnaire submitted to participants.

Part 1. Device Characteristics

1.1 Quality of hearing during instrument use	☐ Poor	☐ Fair	☐ Good	☐Very Good	☐ Excellent
1.2 Perception of muffled ear	☐ Poor	☐ Fair	☐ Good	☐Very Good	☐ Excellent
1.3 Stability within the ear canal	☐ Poor	☐ Fair	☐ Good	☐Very Good	☐ Excellent
1.4 Comfort during use	☐ Poor	☐ Fair	☐ Good	☐Very Good	☐ Excellent
1.5 Perception of pain during use	☐ Poor	☐ Fair	☐ Good	☐Very Good	☐ Excellent
1.6 Aesthetic judgment of the device	☐ Poor	☐ Fair	☐ Good	☐Very Good	☐ Excellent
1.7 Ease of insertion of the device into the external ear canal	☐ Poor	☐ Fair	☐ Good	☐Very Good	☐ Excellent

Part 2. The usefulness of the device

2.1 Would you recommend it to other coworkers?	☐ YES	☐ NO
2.2 Would you use it while working?	☐ YES	☐ NO
2.3 Can you hear the voices of co-workers?	☐ YES	☐ NO
2.4 Can you hear patients' voices?	☐ YES	☐ NO

Part 3. Any critical aspects and benefits regarding the use of the device

4.3.2.2 Experimental results

At the end of our selection process, 20 subjects were included (12 males and 8 females), aging (mean ± standard deviation) 47.5 ± 14.4 years old and with 17.4 ± 14.0 years of practice. The study population comprised 13 dentists, 3 dental hygienists, and 4 chairside assistants. The chronic noise exposure recorded was 8.1 ± 1.7 hours. Among the included subjects, 90% (n=18) reported not using hearing protection devices every day.

The questionnaire results were reported in Table 8 as mean ± standard deviation of the scores and in Figure 30 and Figure 31 as percentages of agreement.

The third part of the questionnaire allows subjects to comment on their experience. Among those who would not recommend the earplugs to coworkers or use them while working, two mentioned experiencing a muffled ear sensation, two stated that the dimensions need to be reduced, one noted difficulty in adjusting their speaking volume with the earplugs inserted, and one reported that the earplugs tend to disengage from the ear. The remaining participants did not provide any comments.

Conversely, other participants noted that the overall ergonomics were satisfactory and reported a 50% reduction in mechanical sounds. Finally, one subject mentioned that the earplugs tend to disengage from the ear only when the operator's head is in certain positions, suggesting that this might have been due to improper placement.

Lastly, the correlation between the results of the first part of the questionnaire and years of experience and time of noise exposure was calculated. The results are shown in Table 9; however, no correlation was found, except for a significant correlation between the device's aesthetic judgment and the noise exposure time ($r=0.451$, $p=0.046$). The correlation between the second part of the questionnaire and the years of experience and the number of hours of exposure is reported for the questions related to the use and recommendation. The questions related to hearing the colleagues' and patients' voices led to all positive answers, so it was impossible to calculate the correlation. No correlation was found between these variables (Table 10). No correction for multiple comparisons was applied since all the comparisons, except for one, were already non-significant before applying any correction for multiple testing. Therefore, the adjustment for multiple comparisons would not change the overall conclusions drawn.

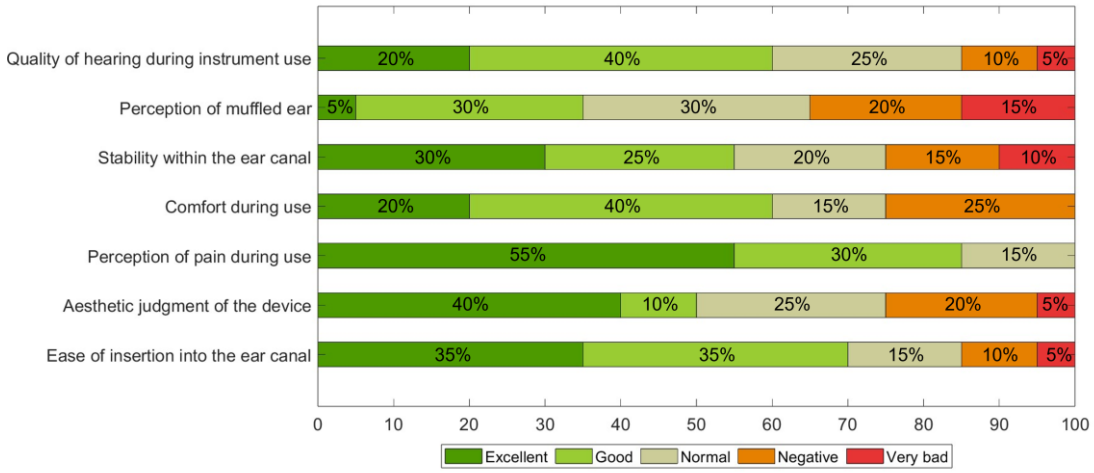

Figure 30: Results of Questionnaire Part 1: Device Characteristics.

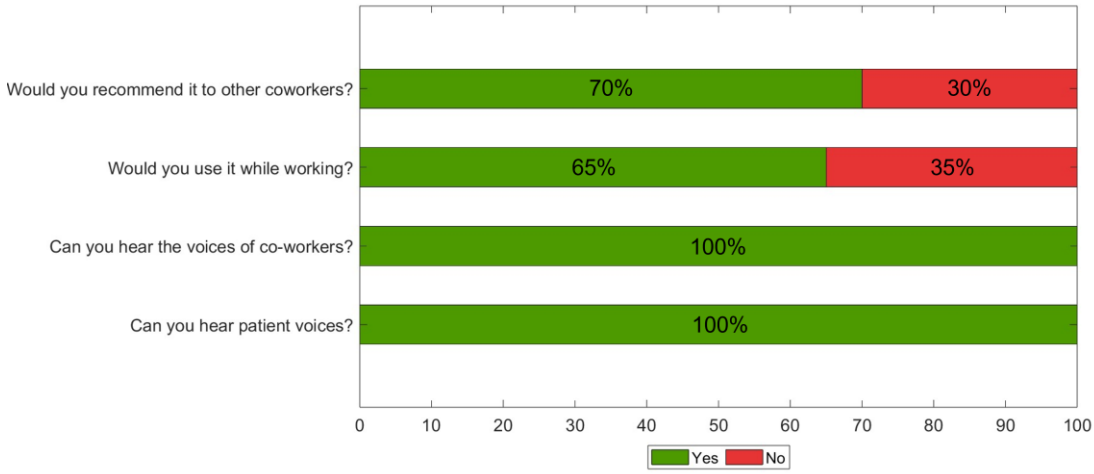

Figure 31: Results of Questionnaire Part 2: Usefulness of the device.

Table 8: Results of Part 1 of the questionnaire.

	Mean ± standard deviation
1.1 Quality of hearing during instrument use	2.40 ± 1.10
1.2 Perception of muffled ear	3.10 ± 1.17
1.3 Stability within the ear canal	2.50 ± 1.36
1.4 Comfort during use	2.45 ± 1.10
1.5 Perception of pain during use	1.60 ± 0.75
1.6 Aesthetic judgment of the device	2.40 ± 1.35
1.7 Ease of insertion of the device into the external ear canal	2.15 ± 1.18

Table 9: Pearson Correlation between Part 1 of the questionnaire and the years of experience, and Part 1 of the questionnaire and the time of noise exposure during the work shift.

	Years of Experience		**Time of Noise Exposure**	
	r	**p-value**	**r**	**p-value**
1.1 Quality of hearing during instrument use	-0.117	0.624	0.347	0.134
1.2 Perception of muffled ear	-0.290	0.215	0.335	0.149
1.3 Stability within the ear canal	0.223	0.346	0.229	0.330
1.4 Comfort during use	0.330	0.158	0.255	0.278
1.5 Perception of pain during use	0.094	0.693	0.148	0.534
1.6 Aesthetic judgment of the device	0.097	0.684	0.451	0.046*
1.7 Ease of insertion of the device into the external ear canal	-0.069	0.772	0.329	0.157

*statistically significant

Table 10: Point-Biserial Correlation between Part 2 of the questionnaire and the years of experience, and Part 2 of the questionnaire and the time of noise exposure during the work shift.

	Years of Experience		**Time of Noise Exposure**	
	r_{pb}	**p-value**	**r_{pb}**	**p-value**
2.1 Would you recommend it to other coworkers?	-0.32492	0.16218	0.23015	0.32897
2.2 Would you use it while working?	-0.34847	0.13214	0.22447	0.34138

4.4 Discussion and Conclusion

Numerous nations mandate that workplaces in all economic sectors adhere to rules aimed at limiting exposure to harmful noise levels and putting in place programs to preserve hearing. Although controlling the source of exposure is the best way to lower risks from workplace hazards, the most popular approach in use today is the distribution of hearing PPEs [111]. The primary frequencies involved in NIHL are mainly the high frequencies (4000 Hz - 6000 Hz), which are processed by nerve endings located in the basal turn of the cochlea, following the cochlea's tonotopic organization [136], [137]. Due to its tonotopic organization, the basis of the cochlea is typically involved in decoding high frequencies. The hair cells of the basal turn of the cochlea are more sensitive to noxa pathogens than the apex [138]. Lesions that occur in the inner ear due to noise exposure can be divided into two main categories: mechanical and metabolic. The earliest mechanical lesions observed following noise exposure include the rupture of the bridges connecting the stereocilia of the hair cells, their reorganization through the repair mechanisms of the ciliary bundles, and the disconnection followed by the restoration of contact between the stereocilia and the tectorial membrane. This varying susceptibility is believed to be due to mechanical reasons: on one hand, there is greater stress imposed on the cilia by the oscillations of the tectorial membrane near the first row; on the other hand, there is lower tolerance of the ciliary bundles of the outer hair cells in this region because they are shorter. Metabolic lesions, on the other hand, depend on different mechanisms, particularly ionic, ischemic, excitotoxic, and oxidative. Basal outer hair cells are also more susceptible to free radical damage because of the lower level of glutathione [137]. For this reason, it is important to protect the hearing from these high frequencies. Among all the working categories, dental workers are at high risk of exposure. Although modern dental equipment generally adheres to the noise limits set by the National Institute for Occupational Safety and Health [130], studies have indicated that dental equipment noise levels can still cause noise-induced HL, leading to an estimated prevalence of up to 20% [54], [122]–[126], [139]–[141]. In the literature, several studies have assessed the effect of NIHL in the field of dentistry. In particular, a recent study conducted on 114 dental students observed that 80% of the students experienced auditory discomfort, while 10% exhibited HL [142]. Also, Al-Rawi et al. [143] and Ma et al. [132] demonstrated a positive correlation between the duration of service and the degree of auditory alterations. Theodoroff and Folmer [122] compared dental clinicians exposed to noise with a group of dental professionals who do not use high-speed

handpieces and a group composed of dental students. The audiometric results for the noise-exposed group revealed a sloping high-frequency HL. On the contrary, the group of workers with minimal noise exposure had hearing thresholds within the normal hearing range; however, their thresholds were poorer than the last group. Lastly, a recent study [54] compared the audiometry results of two groups of dentists: the first one was asked to use the ultrasonic scaler without wearing any protection, while the second one used a hearing protection device. They demonstrated that the noise produced by the ultrasonic scalers can negatively impact the hearing acuity, with an increase in the pure tone audiometry, the acoustic reflex threshold, and a reduced otoacoustic emission value. Indeed, the use of protection devices was effective in reducing the immediate temporary threshold shift. Also, hearing protection devices can reduce the risk of non-auditory effects of high-frequency noise, such as fatigue, nausea, headaches, irritation, tinnitus, and hypertension [128], [132].

Commonly employed hearing PPE includes passive earmuffs, which consist of rigid cups internally lined with sound-absorbing material to enhance sound attenuation; ear inserts designed for insertion into the external auditory canal; and acoustic helmets or headsets, rigid devices that effectively reduce sound transmission through bone. However, these types of PPE attenuate all frequencies equally, including those essential for comprehending spoken language. According to a recent systematic review and meta-analysis [144], three studies showed that wearing hearing PPE did not improve speech perception ability [145]–[147]. The authors tested two passive and two active hearing PPEs commonly used in the military field [145], the MineEars electronic hearing protector and the Bilsom model 847, which is a conventional passive-attenuation earmuff [146], and two types of insert hearing PPEs commonly used in industry, a user-molded foam earplug and a pre-molded triple flange earplug [147]. On the other hand, three studies found that wearing hearing PPE could improve speech perception performance [148]–[150]. Active noise reduction PPE significantly improved speech recognition performance, particularly for hearing-impaired users [148]. Passive noise reduction PPE, on the other hand, has a low noise reduction rating but has demonstrated increased speech intelligibility in the presence of background noise [150]. Manning et al. tested the military communications headsets and reported on the benefits of bone-conduction PPE [149]. Using both air- and bone-conduction PPEs, they performed speech recognition tasks in noisy environments for tinnitus patients, hearing-impaired users, and listeners with normal hearing. According to the authors, in every group, bone-conduction hearing protection performed better than air-conduction protection [149].

Consequently, uniform attenuation may lead to challenges in perceiving conversations, verbal messages, and warning signals, potentially resulting in users abandoning these protective devices. To address this issue, specialized electronic headphones with controlled attenuation are available on the market. These headphones allow users to adjust the amplification of speech frequencies (500 Hz -2000 Hz) while effectively limiting impulsive noises to 82 dBA. However, the electronic tuning system increases the cost of the device and limits its deployment. Notably, there are no hearing protection devices specifically designed for dental workers that effectively address these issues.

In this context, we developed a new hearing protection device called a protective earplug. The device was designed to be universal and low-cost, eliminating the need for electronic filters. It selectively reduces harmful high-frequency noise and amplifies speech frequencies using the physical principle of the resonant tube. Indeed, by modifying the tube length, a specific range of frequencies resonates and is amplified while all the other frequencies are attenuated.

The initial assessment evaluated the device's performance using the "Fonix 7000 Hearing Aid Test System". It was found that the protective earplug effectively filtered out frequencies higher than 4000 Hz, commonly generated by dental instruments, and amplified speech frequencies (500 Hz -1000 Hz) by up to 13 dB. Since modern dental equipment adheres to noise limits, this attenuation can limit the difficulty in communication and concentration caused by prolonged exposure to noise.

After this first analysis, the protective earplug was worn by a group of 20 individuals, including dentists, dental hygienists, and chairside assistants. The participants were instructed to wear the device during an approximately 8-hour workday and provide feedback through the questionnaires previously presented by Spomer et al. in a similar study [135]. First, neither the years of experience nor the noise exposure duration has influenced the answers to the questions. Moreover, the findings of our study can be compared with the ones found by Spomer et al. [135], who tested 4 different types of earplugs: the MP 9-15 Music PRO Electronic Earplugs (Etymotic Research, Inc.), the ETY Plugs High Fidelity Non-Electronic Earplugs (Etymotic Research, Inc.), the Laser-Lite Earplugs (The Safety Zone, LLC distributed by Henry Schein), and the DI-15 High-Fidelity Electronic Earplugs (Dental Innovations, LLC). Our results from the first section of the questionnaire align with the outcomes reported by Spomer et al. For the second section, all participants included in our study reported the ability to hear patients and co-workers clearly. In comparison, the most effective earplugs among the four tested by Spomer et al. achieved an 86.7% success rate for both questions. Regarding the intention

to use the earplugs regularly and recommend them, our earplugs demonstrated superior outcomes to non-electronic earplugs and performed similarly to electronic ones [135].

In conclusion, the protective earplug represents a hearing protection device that selectively filters high-frequency noise and amplifies speech frequencies. Most subjects in the study positively evaluated aesthetics, ease of insertion, comfort, stability, and noise attenuation while using high-frequency dental instrumentation.

This pilot study presents some limitations. Additionally, even though a correlation between the answers and the noise exposure time was not found, long-term monitoring would be desirable to assess its effectiveness over time, eliminating possible bias due to first-time experience. Finally, the lack of a control group using a different hearing protection device, or no device, prevents a direct comparison of the efficacy of the protective earplug with other options. Also, objective assessment of speech understanding through speech audiometry will be carried out in future studies. Future studies will address the drawbacks reported by the subjects, like the perception of ear muffling and a better fit and stability during head movements. Furthermore, the device will be tested on a larger sample of subjects with different occupations, comparing it with a control group.

5 Conclusions

The increasing integration between engineering and medicine leads to continuous progress in the healthcare industry. This collaboration stimulates the development of new technologies to support both diagnosis and medical treatment. Research in this field is guided by the principles of "4P Medicine" - Preventive, Participatory, Personalized, and Predictive. This model focuses on individual well-being and health, aiming to provide more people with access to a tailored and high-quality diagnostic and therapeutic pathway that actively involves the patient.

In this new paradigm, healthcare professionals and patients can share information and data, ensuring constant updates on the individual's health status and preventing diseases. Medicine is no longer limited to hospitals, but it is increasingly becoming available to a broader population reaching people far from big cities and accessible, reaching individuals wherever they are and becoming available to a broader population. A key component of this change is telemedicine, which is becoming increasingly popular in routine medical practice.

Among the various medical specialties, Otorhinolaryngology stands out as one of the fields experiencing rapid and consistent innovation. Specialists in this area address disorders affecting multiple anatomical regions, encountering various medical issues daily—from balance disorders to ear infections, nasal congestion, upper respiratory diseases, and voice disorders. This specialty is characterized by complex anatomy and challenging surgical access, prompting professionals to continually pursue minimally invasive methods to navigate and treat these areas with precision.

Technological advancements have revolutionized this field, evolving from the earliest light-assisted instruments to modern techniques such as endoscopy, microscopy, and robotic surgery. These innovations have significantly enhanced visualization and precision, enabling less invasive approaches and yielding improved patient outcomes.

However, challenges remain. The accuracy of medical assessments still heavily relies on the experience and expertise of physicians, which can lead to diagnostic and therapeutic errors. This is particularly important because otorhinolaryngological diseases are highly prevalent in the general population but are often underestimated due to a lack of awareness about their impact on daily life.

In this context, the present Ph.D. dissertation aims to develop novel technological solutions in the otorhinolaryngology field, addressing the key challenges in the

monitoring of respiratory and sleep-related breathing disorders and the prevention of otological disorders.

The importance of respiratory rate monitoring to assess the health status of the patients is well known, being a predictor of potential clinically severe events such as readmission to an intensive care unit, cardiopulmonary deterioration, pneumonia, pulmonary embolism, obstructive sleep apnea, and overdose. Moreover, changes in respiratory patterns indicate the presence of stressors such as pain, emotional and environmental stress, and cognitive load. For this reason, a wearable system for physiological respiratory monitoring was developed. The SFM, designed during this research, integrates thermistor sensors to estimate RR. These sensors exploit the temperature differences between inhaled and exhaled air, providing a good estimation of the breathing pattern. From the signal acquired by the two thermistors, it is possible to estimate the RR of the subject from the distance of two consecutive peaks in the signal. The performance of the SFM was evaluated in static and dynamic conditions by comparing its measurements with those of a reference system (BH). The results demonstrated high accuracy in estimating RR in static conditions, both during quiet breathing and tachypnoea, with mean MAPE and MAE within acceptable ranges. The Bland-Altman analysis confirmed the agreement between the SFM and the reference device. Similar results were found when testing the SFM in more dynamic conditions, such as walking, showing that the choice of the face mask as support for the sensors is suitable for daily life and occupational settings. The SFM then represents a promising advancement in wearable respiratory monitoring technology, offering a practical and accurate solution for improving respiratory health assessment in diverse scenarios.

Since respiratory disorders can also occur during the night, the research focused on developing a system to monitor Sleep-Related Breathing Disorders. These encompass a spectrum of chronic conditions ranging from snoring, upper airway resistance syndrome, OSA, and central sleep apnea.

A non-invasive method for detecting OSA was developed based on the analysis of snoring sounds recorded via the sound recording application on a tablet. Indeed, the snoring sound follows the breathing pattern of the subject, and from the analysis of this signal, it is possible to visualize an interruption in the breathing caused by an obstruction of the upper airways. Also, snoring is a predictor of OSA, and patients who snore are at high risk of having this disorder. The algorithm's performance was evaluated on subjects with suspected OSA, with the commercial WatchPAT device serving as the reference system. The analysis revealed strong agreement between the audio-based method and the

WatchPAT for simple snorers and mild OSA subjects. For the subject with a severe degree of OSA, the performance of the audio-based algorithm was lower, imposing some limitations on the system. Indeed, it did not detect central respiratory events and missed respiratory events that did not lead to a snoring sound.

However, these findings underscore the system developed as a potentially cost-effective and accessible tool for initial OSA screening by offering a practical solution for early detection and intervention.

Lastly, this Ph.D. research has focused on another important issue that concerns otolaryngologists, which is NIHL. This disorder is very common in occupational settings where prolonged exposure to intensive noises causes damage to the inner ear structures due to hair cell degeneration. Using ear protectors is fundamental to avoid this irreversible damage, but it is often underestimated. Existing hearing protection devices often attenuate all frequencies indiscriminately, including essential speech frequencies, causing communication challenges and discomfort, which leads to low compliance. A new protective earplug was developed by exploiting the principle behind the resonant tube: the device was designed to selectively amplify speech frequencies (500–1000 Hz) up to 13 dB while attenuating harmful high frequencies. Among the professionals who suffer from NIHL, dental practitioners are constantly exposed to high-frequency noise (4000–6000 Hz) from equipment like ultrasonic scalers and turbines. The device was tested on 20 dental professionals during an 8-hour workday. Participants evaluated the performance of the device using a structured questionnaire. Results indicated positive feedback on communication clarity and noise attenuation, with most participants expressing willingness to adopt the device regularly. The limitations pointed out by the subjects included perceived ear muffling and occasional device displacement. The study underscores the device's potential as a low-cost, non-electronic solution for high-frequency noise protection while maintaining speech intelligibility.

In conclusion, this dissertation underscores the impact of technological innovation in addressing unmet clinical needs within the field of otorhinolaryngology. The proposed solutions represent a promising starting point for developments that could significantly influence clinical practice.

References

[1] M. Viscaino, J. C. Maass, P. H. Delano, and F. A. Cheein, "Computer-Aided Ear Diagnosis System Based on CNN-LSTM Hybrid Learning Framework for Video Otoscopy Examination," *IEEE Access*, vol. 9, pp. 161292–161304, 2021, doi: 10.1109/ACCESS.2021.3132133.

[2] "Deafness and hearing loss." https://www.who.int/health-topics/hearing-loss#tab=tab_2 (accessed Dec. 09, 2024).

[3] S. B. Tufik, G. N. Pires, L. Palombini, M. L. Andersen, and S. Tufik, "Prevalence of upper airway resistance syndrome in the São Paulo Epidemiologic Sleep Study," *Sleep Med.*, vol. 91, pp. 43–50, Mar. 2022, doi: 10.1016/J.SLEEP.2022.02.004.

[4] A. V Benjafield *et al.*, "Estimation of the global prevalence and burden of obstructive sleep apnoea: a literature-based analysis," *Lancet. Respir. Med.*, vol. 7, no. 8, pp. 687–698, 2019, doi: 10.1016/S2213-2600(19)30198-5.

[5] A. Malhotra *et al.*, "Metrics of sleep apnea severity: beyond the apnea-hypopnea index," *Sleep*, vol. 44, no. 7, Jul. 2021, doi: 10.1093/SLEEP/ZSAB030.

[6] A. M. Rana and A. Sankari, "Central Sleep Apnea," *StatPearls*, Jun. 2023, Accessed: Dec. 09, 2024. [Online]. Available: https://www.ncbi.nlm.nih.gov/books/NBK578199/

[7] L. M. Donovan and V. K. Kapur, "Prevalence and Characteristics of Central Compared to Obstructive Sleep Apnea: Analyses from the Sleep Heart Health Study Cohort," *Sleep*, vol. 39, no. 7, p. 1353, Jul. 2016, doi: 10.5665/SLEEP.5962.

[8] S. Chowdhuri, S. Pranathiageswaran, H. Loomis-King, A. Salloum, and M. S. Badr, "Aging is associated with increased propensity for central apnea during NREM sleep," *J. Appl. Physiol.*, vol. 124, no. 1, pp. 83–90, Jan. 2018, doi: 10.1152/JAPPLPHYSIOL.00125.2017.

[9] J. Sobiesk and S. Munakomi, *Anatomy, Head and Neck, Nasal Cavity.* StatPearls Publishing, 2024. [Online]. Available: https://www.ncbi.nlm.nih.gov/books/NBK544232/

[10] P. Carinci, E. Gaudio, and G. Marinozzi, *Anatomia umana e istologia*. 2012.

[11] K. Vlahovich and A. Sood, "A 2019 Update on Occupational Lung Diseases: A Narrative Review.," *Pulm Ther.*, vol. 7, no. 1, pp. 75–87, doi: 10.1007/s41030-020-00143-4.

[12] D. Montano, "Chemical and biological work-related risks across occupations in

Europe: a review.," *J Occup Med Toxicol*, 2014, doi: 10.1186/1745-6673-9-28.

[13] T. H. Bhat, G. Jiawen, and H. Farzaneh, "Air pollution health risk assessment (Aphra), principles and applications," *Int. J. Environ. Res. Public Health*, vol. 18, no. 4, pp. 1–29, 2021, doi: 10.3390/ijerph18041935.

[14] Y. Kim and V. Radoias, "Severe Air Pollution Exposure and Long-Term Health Outcomes," *Int. J. Environ. Res. Public Health*, vol. 19, no. 21, 2022, doi: 10.3390/ijerph192114019.

[15] G. Viegi *et al.*, "Health effects of air pollution: a Southern European perspective," *Chin. Med. J. (Engl).*, vol. 133, no. 13, p. 1568, Jul. 2020, doi: 10.1097/CM9.0000000000000869.

[16] F. H. Dominski, J. H. Lorenzetti Branco, G. Buonanno, L. Stabile, M. Gameiro da Silva, and A. Andrade, "Effects of air pollution on health: A mapping review of systematic reviews and meta-analyses," *Environ. Res.*, vol. 201, p. 111487, Oct. 2021, doi: 10.1016/J.ENVRES.2021.111487.

[17] A. Nicolò, C. Massaroni, E. Schena, and M. Sacchetti, "The Importance of Respiratory Rate Monitoring: From Healthcare to Sport and Exercise," *Sensors (Basel).*, vol. 20, no. 21, pp. 1–45, Nov. 2020, doi: 10.3390/S20216396.

[18] H. Liu, J. Allen, D. Zheng, and F. Chen, "Recent development of respiratory rate measurement technologies," *Physiol. Meas.*, vol. 40, no. 7, 2019, doi: 10.1088/1361-6579/ab299e.

[19] D. Pevernagie, R. M. Aarts, and M. De Meyer, "The acoustics of snoring q," *Sleep Med. Rev.*, vol. 14, no. 2, pp. 131–144, 2010, doi: 10.1016/j.smrv.2009.06.002.

[20] Z. Huang *et al.*, "Prediction of the obstruction sites in the upper airway in sleep-disordered breathing based on snoring sound parameters : a systematic review," *Sleep Med.*, vol. 88, pp. 116–133, 2021, doi: 10.1016/j.sleep.2021.10.015.

[21] R. L. Owens *et al.*, "The classical Starling resistor model often does not predict inspiratory airflow patterns in the human upper airway," *J. Appl. Physiol.*, vol. 116, no. 8, pp. 1105–1112, Apr. 2014, doi: 10.1152/JAPPLPHYSIOL.00853.2013.

[22] L. E. Bilston and S. C. Gandevia, "Biomechanical properties of the human upper airway and their effect on its behavior during breathing and in obstructive sleep apnea," *J. Appl. Physiol.*, vol. 116, no. 3, pp. 314–324, Feb. 2014, doi: 10.1152/JAPPLPHYSIOL.00539.2013.

[23] M. W. Johns, "A new method for measuring daytime sleepiness: the Epworth sleepiness scale," *Sleep*, vol. 14, no. 6, pp. 540–545, 1991, doi: 10.1093/SLEEP/14.6.540.

[24] A. Moffa *et al.*, "The Potential Effect of Changing Patient Position on Snoring: A Systematic Review," *J. Pers. Med.*, vol. 14, no. 7, Jul. 2024, doi: 10.3390/JPM14070715.

[25] B. Lechat *et al.*, "Regular snoring is associated with uncontrolled hypertension," *npj Digit. Med. 2024 71*, vol. 7, no. 1, pp. 1–8, Feb. 2024, doi: 10.1038/s41746-024-01026-7.

[26] M. Sowho, F. Sgambati, M. Guzman, H. Schneider, and A. Schwartz, "Snoring: a source of noise pollution and sleep apnea predictor," *Sleep*, vol. 43, no. 6, pp. 1–9, Jun. 2020, doi: 10.1093/SLEEP/ZSZ305.

[27] M. Maurizi, "Clinica otorinolaringoiatrica : basi anatomo-funzionali, patologiche e cliniche delle grandi sindromi e delle malattie," p. 435, 2007, Accessed: Dec. 09, 2024. [Online]. Available: http://www.piccin.it/it/otorinolaringoiatria/1093-clinica-otorinolaringoiatrica-basi-anatomo-funzionali-patologiche-e-cliniche-delle-grandi-sindromi-e-delle-malattie-9788829918430.html

[28] C. Guilleminault and S. Quo, "Sleep-disordered breathing. A view at the beginning of the new Millennium," *Dent Clin North Am*, vol. 45, no. 4, pp. 643–56, 2001.

[29] P. Mayer *et al.*, "Relationship between body mass index, age and upper airway measurements in snorers and sleep apnoea patients," *Eur. Respir. J.*, vol. 9, no. 9, pp. 1801–1809, 1996, doi: 10.1183/09031936.96.09091801.

[30] R. L. Horner, "Contributions of passive mechanical loads and active neuromuscular compensation to upper airway collapsibility during sleep," *J. Appl. Physiol.*, vol. 102, no. 2, pp. 510–512, Feb. 2007, doi: 10.1152/JAPPLPHYSIOL.01213.2006.

[31] R. B. Berry *et al.*, "Rules for scoring respiratory events in sleep: update of the 2007 AASM Manual for the Scoring of Sleep and Associated Events. Deliberations of the Sleep Apnea Definitions Task Force of the American Academy of Sleep Medicine," *J. Clin. Sleep Med.*, vol. 8, no. 5, pp. 597–619, 2012, doi: 10.5664/JCSM.2172.

[32] D. Landzberg and K. Bagai, "Prevalence of objective excessive daytime sleepiness in a cohort of patients with mild obstructive sleep apnea," *Sleep Breath.*, vol. 26, no. 3, pp. 1471–1477, Sep. 2022, doi: 10.1007/S11325-021-02473-2.

[33] T. D. Bradley, A. G. Logan, and J. S. Floras, "Treating Sleep-Disordered Breathing for Cardiovascular Outcomes: Observational and Randomised Trial Evidence," *Eur. Respir. J.*, p. 2401033, Dec. 2024, doi: 10.1183/13993003.01033-2024.

[34] T. Feng, Q. Li, Y. Chen, and R. Duan, "Evaluating the relationship between

obstructive sleep apnea and all-cause and cause-specific mortality in adults with and without metabolic syndrome using real-world data," *Eur. Arch. Otorhinolaryngol.*, 2024, doi: 10.1007/S00405-024-09089-8.

[35] A. M. Osman, S. G. Carter, J. C. Carberry, and D. J. Eckert, "Obstructive sleep apnea: current perspectives," *Nat. Sci. Sleep*, vol. 10, p. 21, 2018, doi: 10.2147/NSS.S124657.

[36] S. C. Veasey and I. M. Rosen, "Obstructive Sleep Apnea in Adults," *N. Engl. J. Med.*, vol. 380, no. 15, pp. 1442–1449, Apr. 2019, doi: 10.1056/NEJMCP1816152.

[37] G. Salzano *et al.*, "Obstructive sleep apnoea/hypopnoea syndrome: relationship with obesity and management in obese patients," *Acta Otorhinolaryngol. Ital.*, vol. 41, no. 2, pp. 120–130, May 2021, doi: 10.14639/0392-100X-N1100.

[38] X. Chen *et al.*, "Racial/Ethnic Differences in Sleep Disturbances: The Multi-Ethnic Study of Atherosclerosis (MESA)," *Sleep*, vol. 38, no. 6, pp. 877–888, Jun. 2015, doi: 10.5665/SLEEP.4732.

[39] H. K. Yaggi and K. P. Strohl, "Adult obstructive sleep apnea/hypopnea syndrome: definitions, risk factors, and pathogenesis," *Clin. Chest Med.*, vol. 31, no. 2, pp. 179–186, Jun. 2010, doi: 10.1016/J.CCM.2010.02.011.

[40] P. Armeni, L. Borsoi, F. Costa, G. Donin, and A. Gupta, "Final report Cost-of-illness study of Obstructive Sleep Apnea Syndrome (OSAS) in Italy," 2019.

[41] T. Young, J. Skatrud, and P. E. Peppard, "Risk Factors for Obstructive Sleep Apnea in Adults," *JAMA*, vol. 291, no. 16, pp. 2013–2016, Apr. 2004, doi: 10.1001/JAMA.291.16.2013.

[42] P. E. Peppard, T. Young, J. H. Barnet, M. Palta, E. W. Hagen, and K. M. Hla, "Increased prevalence of sleep-disordered breathing in adults," *Am. J. Epidemiol.*, vol. 177, no. 9, pp. 1006–1014, May 2013, doi: 10.1093/AJE/KWS342.

[43] J. R. Stradling and R. J. O. Davies, "Sleep. 1: Obstructive sleep apnoea/hypopnoea syndrome: definitions, epidemiology, and natural history," *Thorax*, vol. 59, no. 1, pp. 73–78, Jan. 2004, doi: 10.1136/THX.2003.007161.

[44] P. Lévy *et al.*, "Obstructive sleep apnoea syndrome.," *Nat Rev Dis Prim.*, 2015, doi: 10.1038/nrdp.2015.15.

[45] C. A. Kushida *et al.*, "Practice parameters for the indications for polysomnography and related procedures: an update for 2005," *Sleep*, vol. 28, no. 4, pp. 499–521, Apr. 2005, doi: 10.1093/SLEEP/28.4.499.

[46] A. Moffa *et al.*, "New diagnostic tools to screen and assess a still too underestimated disease: the role of the wrist-worn peripheral arterial

tonometry device—a systematic review," *Sleep Breath.*, no. 0123456789, 2022, doi: 10.1007/s11325-022-02700-4.

[47] "Regulations and Guidance | CMS." https://www.cms.gov/marketplace/resources/regulations-guidance (accessed Dec. 26, 2024).

[48] S. Paruthi *et al.*, "Consensus Statement of the American Academy of Sleep Medicine on the Recommended Amount of Sleep for Healthy Children: Methodology and Discussion," *J. Clin. Sleep Med.*, vol. 12, no. 11, pp. 1549–1561, 2016, doi: 10.5664/JCSM.6288.

[49] "Deafness and hearing loss." https://www.who.int/health-topics/hearing-loss#tab=tab_1 (accessed Dec. 01, 2024).

[50] T. Yamasoba, F. R. Lin, S. Someya, A. Kashio, T. Sakamoto, and K. Kondo, "Current concepts in age-related hearing loss: epidemiology and mechanistic pathways," *Hear. Res.*, vol. 303, pp. 30–38, Sep. 2013, doi: 10.1016/J.HEARES.2013.01.021.

[51] T. N. Le, L. V. Straatman, J. Lea, and B. Westerberg, "Current insights in noise-induced hearing loss: a literature review of the underlying mechanism, pathophysiology, asymmetry, and management options," *J. Otolaryngol. - Head Neck Surg. 2017 461*, vol. 46, no. 1, pp. 1–15, May 2017, doi: 10.1186/S40463-017-0219-X.

[52] I. S. Bhatt, "Determinants of the Audiometric Notch at 4000 and 6000 Hz in Young Adults," *J Am Acad Audiol*, vol. 31, pp. 371–383, 2020, doi: 10.3766/jaaa.19030.

[53] M. Maurizi, *Audiovestibologia clinica*. 2000.

[54] K. M. Mohan, A. Chopra, V. Guddattu, S. Singh, and K. Upasana, "Should Dentists Mandatorily Wear Ear Protection Device to Prevent Occupational Noise-induced Hearing Loss? A Randomized Case-Control Study," *J. Int. Soc. Prev. Community Dent.*, vol. 12, no. 5, pp. 513–523, Sep. 2022, doi: 10.4103/JISPCD.JISPCD_28_22.

[55] R. Sommerstein *et al.*, "Risk of SARS-CoV-2 transmission by aerosols, the rational use of masks, and protection of healthcare workers from COVID-19," *Antimicrob. Resist. Infect. Control*, vol. 9, no. 1, pp. 1–8, 2020, doi: 10.1186/s13756-020-00763-0.

[56] L. Dogbla *et al.*, "Occupational Risk Factors by Sectors: An Observational Study of 20,000 Workers.," *Int J Env. Res Public Heal.*, vol. 20, no. 4, doi: 10.3390/ijerph20043632.

[57] Q. Lu *et al.*, "Intelligent facemask based on triboelectric nanogenerator for

respiratory monitoring," *Nano Energy*, vol. 91, p. 106612, Jan. 2022, doi: 10.1016/J.NANOEN.2021.106612.

[58] M. Simić, A. K. Stavrakis, A. Sinha, V. Premčevski, B. Markoski, and G. M. Stojanović, "Portable Respiration Monitoring System with an Embroidered Capacitive Facemask Sensor," *Biosens. 2022, Vol. 12, Page 339*, vol. 12, no. 5, p. 339, May 2022, doi: 10.3390/BIOS12050339.

[59] D. Lo Presti, M. Zaltieri, R. D'Amato, M. Caponero, C. Massaroni, and E. Schena, "Feasibility assessment of an FBG-based soft sensor embedded into a single-use surgical mask for respiratory monitoring," *2021 IEEE Int. Work. Metrol. Ind. 4.0 IoT, MetroInd 4.0 IoT 2021 - Proc.*, pp. 166–171, Jun. 2021, doi: 10.1109/METROIND4.0IOT51437.2021.9488558.

[60] C. Massaroni, A. Nicolò, D. Lo Presti, M. Sacchetti, S. Silvestri, and E. Schena, "Contact-based methods for measuring respiratory rate," *Sensors (Switzerland)*, vol. 19, no. 4, pp. 1–47, 2019, doi: 10.3390/s19040908.

[61] P. Höppe, "Temperatures of expired air under varying climatic conditions," *Int. J. Biometeorol.*, vol. 25, no. 2, pp. 127–132, 1981, doi: 10.1007/BF02184460.

[62] C. Massaroni *et al.*, "Influence of torso movements on a multi-sensor garment for respiratory monitoring during walking and running activities," *I2MTC 2020 - Int. Instrum. Meas. Technol. Conf. Proc.*, May 2020, doi: 10.1109/I2MTC43012.2020.9128754.

[63] C. Massaroni *et al.*, "Respiratory Monitoring during Physical Activities with a Multi-Sensor Smart Garment and Related Algorithms," *IEEE Sens. J.*, vol. 20, no. 4, pp. 2173–2180, Feb. 2020, doi: 10.1109/JSEN.2019.2949608.

[64] T. Das, N. Subhash, S. Guha, N. Banerjee, and P. Basak, "Development of Thermistor based low cost high sensitive Respiration Rate Measurement System," *Third Int. Conf. Biosignals, Images Instrum.*, 2017, doi: 10.1109/ICBSII.2017.8082283.

[65] J. Lerman *et al.*, "Linshom respiratory monitoring device: a novel temperature-based respiratory monitor," *Can. J. Anesth.*, vol. 63, no. 10, pp. 1154–1160, 2016, doi: 10.1007/s12630-016-0694-y.

[66] V. S. Thippeswamy, P. M. Shivakumaraswamy, S. G. Chickaramanna, V. M. Iyengar, A. P. Das, and A. Sharma, "Prototype development of continuous remote monitoring of ICU patients at home," *Instrum. Mes. Metrol.*, vol. 20, no. 2, pp. 79–84, 2021, doi: 10.18280/i2m.200203.

[67] K. M. R. Rao and B. G. Sudarshan, "Design and Development of Real Time

Respiratory Rate Monitor Using Non-Invasive Biosensor," *Int. J. Res. Eng. Technol.*, vol. 04, no. 06, pp. 437–442, 2015, doi: 10.15623/ijret.2015.0406074.

[68] H. Qudsi and M. Gupta, "Low-cost, thermistor based respiration monitor," *Proc. - 29th South. Biomed. Eng. Conf. SBEC 2013*, pp. 23–24, 2013, doi: 10.1109/SBEC.2013.20.

[69] H. Turnbull *et al.*, "Development of a novel device for objective respiratory rate measurement in low-resource settings," *BMJ Innov.*, vol. 4, no. 4, pp. 185–191, 2018, doi: 10.1136/bmjinnov-2017-000267.

[70] R. Cao *et al.*, "Self-powered nanofiber-based screen-print triboelectric sensors for respiratory monitoring," *Nano Res.*, vol. 11, no. 7, pp. 3771–3779, 2018, doi: 10.1007/s12274-017-1951-2.

[71] M. C. Caccami, M. Y. S. Mulla, C. Di Natale, and G. Marrocco, "Wireless monitoring of breath by means of a graphene oxide-based radiofrequency identification wearable sensor," *2017 11th Eur. Conf. Antennas Propagation, EUCAP 2017*, pp. 3394–3396, 2017, doi: 10.23919/EuCAP.2017.7928355.

[72] F. Güder *et al.*, "Paper-Based Electrical Respiration Sensor," *Angew. Chemie - Int. Ed.*, vol. 55, no. 19, pp. 5727–5732, 2016, doi: 10.1002/anie.201511805.

[73] E. Sifuentes, J. Cota-Ruiz, and R. González-Landaeta, "Respiratory rate detection by a time-based measurement system," *Rev. Mex. Ing. Biomed.*, vol. 37, no. 2, pp. 91–99, 2016, doi: 10.17488/RMIB.37.2.3.

[74] D. E. Hurtado, A. Abusleme, and J. A. P. Chávez, "Non-invasive continuous respiratory monitoring using temperature-based sensors," *J. Clin. Monit. Comput.*, vol. 34, no. 2, pp. 223–231, 2020, doi: 10.1007/s10877-019-00329-5.

[75] J. Dawood, M. Muller, and C. S. Carlson, "'Are you breathing?' – Design, build and testing of a low-cost, portable respiratory rate monitor," *Curr. Dir. Biomed. Eng.*, vol. 8, no. 2, pp. 109–112, Aug. 2022, doi: 10.1515/CDBME-2022-1029/MACHINEREADABLECITATION/RIS.

[76] L. Giorgi *et al.*, "An innovative smart face mask for the estimation of respiratory rate: design, development and feasibility assessment," *2023 IEEE Int. Work. Metrol. Ind. 4.0 IoT, MetroInd4.0 IoT 2023 - Proc.*, pp. 189–193, 2023, doi: 10.1109/METROIND4.0IOT57462.2023.10180151.

[77] L. Giorgi *et al.*, "Assessment of an innovative smart face mask for the estimation of respiratory rate in static and dynamic conditions," *2024 IEEE Int. Work. Metrol. Ind. 4.0 IoT, MetroInd4.0 IoT 2024 - Proc.*, pp. 476–481, 2024, doi: 10.1109/METROIND4.0IOT61288.2024.10584212.

[78] R. S. Figliola and D. E. Beasley, “Theory and design for mechanical measurements,” *Meas. Sci. Technol.*, vol. 7, no. 7, 1996, doi: 10.1088/0957-0233/7/7/016.

[79] J. Martin Bland and D. G. Altman, “STATISTICAL METHODS FOR ASSESSING AGREEMENT BETWEEN TWO METHODS OF CLINICAL MEASUREMENT,” *Lancet*, vol. 327, no. 8476, pp. 307–310, Feb. 1986, doi: 10.1016/S0140-6736(86)90837-8.

[80] J. Clark, S. Kochovska, and D. C. Currow, “Burden of respiratory problems in low-income and middle-income countries,” *Curr. Opin. Support. Palliat. Care*, vol. 16, no. 4, pp. 210–215, Dec. 2022, doi: 10.1097/SPC.0000000000000615.

[81] J. Meghji *et al.*, “Improving lung health in low-income and middle-income countries: from challenges to solutions,” *www.thelancet.com*, vol. 397, 2021, doi: 10.1016/S0140-6736(21)00458-X.

[82] J. Meghji *et al.*, “Chronic respiratory disease in low-income and middle-income countries: From challenges to solutions,” *J. Pan African Thorac. Soc.*, vol. 3, no. 2, pp. 92–97, May 2022, doi: 10.25259/JPATS_10_2022.

[83] J. Zhong *et al.*, “Smart Face Mask Based on an Ultrathin Pressure Sensor for Wireless Monitoring of Breath Conditions,” *Adv. Mater.*, vol. 34, no. 6, pp. 1–9, 2022, doi: 10.1002/adma.202107758.

[84] M. Simić, A. K. Stavrakis, A. Sinha, V. Premčevski, B. Markoski, and G. M. Stojanović, “Portable Respiration Monitoring System with an Embroidered Capacitive Facemask Sensor,” *Biosensors*, vol. 12, no. 5, 2022, doi: 10.3390/bios12050339.

[85] J. A. Dempsey, S. C. Veasey, B. J. Morgan, and C. P. O’Donnell, “Pathophysiology of sleep apnea,” *Physiol. Rev.*, vol. 90, no. 1, pp. 47–112, 2010, doi: 10.1152/physrev.00043.2008.

[86] I. Aiyer, L. Shaik, A. Sheta, and S. Surani, “Review of Application of Machine Learning as a Screening Tool for Diagnosis of Obstructive Sleep Apnea,” *Med. 2022, Vol. 58, Page 1574*, vol. 58, no. 11, p. 1574, Nov. 2022, doi: 10.3390/MEDICINA58111574.

[87] N.-Y. Kuo, H.-J. Tsai, S.-J. Tsai, and A. C. Yang, “Efficient Screening in Obstructive Sleep Apnea Using Sequential Machine Learning Models, Questionnaires, and Pulse Oximetry Signals: Mixed Methods Study.,” *J. Med. Internet Res.*, vol. 26, no. 1, p. e51615, Dec. 2024, doi: 10.2196/51615.

[88] H. Alshaer, R. Hummel, M. Mendelson, T. Marshal, and T. D. Bradley, “Objective

Relationship Between Sleep Apnea and Frequency of Snoring Assessed by Machine Learning," pp. 8–11, 2019.

[89] H. Alshaer, G. R. Fernie, E. Maki, and T. D. Bradley, "Validation of an automated algorithm for detecting apneas and hypopneas by acoustic analysis of breath sounds q," vol. 14, pp. 562–571, 2013.

[90] J. Luo *et al.*, "A novel deep feature transfer-based OSA detection method using sleep sound signals," *Physiol. Meas.*, vol. 41, no. 7, Jul. 2020, doi: 10.1088/1361-6579/AB9E7B.

[91] V. L. Le *et al.*, "Real-Time Detection of Sleep Apnea Based on Breathing Sounds and Prediction Reinforcement Using Home Noises: Algorithm Development and Validation," *J. Med. Internet Res.*, vol. 25, no. 1, p. e44818, Feb. 2023, doi: 10.2196/44818.

[92] S. C. Han *et al.*, "In-Home Smartphone-Based Prediction of Obstructive Sleep Apnea in Conjunction With Level 2 Home Polysomnography," *JAMA Otolaryngol. Head Neck Surg.*, vol. 150, no. 1, pp. 22–29, Jan. 2024, doi: 10.1001/JAMAOTO.2023.3490.

[93] R. Tiron *et al.*, "Screening for obstructive sleep apnea with novel hybrid acoustic smartphone app technology," *J. Thorac. Dis.*, vol. 12, no. 8, pp. 4476–4495, Aug. 2020, doi: 10.21037/JTD-20-804.

[94] H. E. Romero, N. Ma, G. J. Brown, and E. A. Hill, "Acoustic Screening for Obstructive Sleep Apnea in Home Environments Based on Deep Neural Networks," *IEEE J. Biomed. Heal. informatics*, vol. 26, no. 7, pp. 2941–2950, Jul. 2022, doi: 10.1109/JBHI.2022.3154719.

[95] K. Bahr-Hamm, A. Abriani, A. R. Anwar, H. Ding, M. Muthuraman, and H. Gouveris, "Using entropy of snoring, respiratory effort and electrocardiography signals during sleep for OSA detection and severity classification," *Sleep Med.*, vol. 111, pp. 21–27, Nov. 2023, doi: 10.1016/J.SLEEP.2023.09.005.

[96] F. Hajipour, M. J. Jozani, and Z. Moussavi, "A comparison of regularized logistic regression and random forest machine learning models for daytime diagnosis of obstructive sleep apnea," *Med. Biol. Eng. Comput.*, vol. 58, no. 10, pp. 2517–2529, Oct. 2020, doi: 10.1007/S11517-020-02206-9.

[97] M. Sowho, F. Sgambati, M. Guzman, H. Schneider, and A. Schwartz, "Snoring: A source of noise pollution and sleep apnea predictor," *Sleep*, vol. 43, no. 6, pp. 1–9, 2020, doi: 10.1093/sleep/zsz305.

[98] N. Ben-israel, A. Tarasiuk, and Y. Zigel, "Obstructive Apnea Hypopnea Index

Estimation by Analysis of Nocturnal Snoring Signals in Adults," 2012.

[99] A. Azarbarzin and Z. Moussavi, "Snoring sounds variability as a signature of obstructive sleep apnea," *Med. Eng. Phys.*, vol. 35, pp. 479–485, 2013.

[100] M. Halevi, E. Dafna, A. Tarasiuk, and Y. Zigel, "Can we discriminate between apnea and hypopnea using audio signals ?," pp. 3211–3214, 2016.

[101] A. Levartovsky, E. Dafna, Y. Zigel, and A. Tarasiuk, "Breathing and Snoring Sound Characteristics during Sleep in Adults," vol. 12, no. 3, 2016.

[102] M. Sowho, F. Sgambati, M. Guzman, H. Schneider, and A. Schwartz, "Snoring : a source of noise pollution and sleep apnea predictor," no. December 2019, pp. 1–9, 2020, doi: 10.1093/sleep/zsz305.

[103] V. K. Kapur *et al.*, "Clinical Practice Guideline for Diagnostic Testing for Adult Obstructive Sleep Apnea: An American Academy of Sleep Medicine Clinical Practice Guideline," *J. Clin. Sleep Med.*, vol. 13, no. 3, pp. 479–504, 2017, doi: 10.5664/JCSM.6506.

[104] C. H. Sia, Y. Hong, L. W. L. Tan, R. M. van Dam, C. H. Lee, and A. Tan, "Awareness and knowledge of obstructive sleep apnea among the general population," *Sleep Med.*, vol. 36, pp. 10–17, Aug. 2017, doi: 10.1016/J.SLEEP.2017.03.030.

[105] S. L. Walker, D. L. Saltman, R. Colucci, and L. Martin, "Awareness of risk factors among persons at risk for lung cancer, chronic obstructive pulmonary disease and sleep apnea: a Canadian population-based study," *Can. Respir. J.*, vol. 17, no. 6, pp. 287–294, 2010, doi: 10.1155/2010/426563.

[106] O. B. Ozoh, O. O. Ojo, S. O. Iwuala, A. O. Akinkugbe, O. O. Desalu, and N. U. Okubadejo, "Is the knowledge and attitude of physicians in Nigeria adequate for the diagnosis and management of obstructive sleep apnea?," *Sleep Breath.*, vol. 21, no. 2, pp. 521–527, May 2017, doi: 10.1007/S11325-016-1407-Z.

[107] M. Di Pumpo *et al.*, "Multiple-access versus telemedicine home-based sleep apnea testing for obstructive sleep apnea (OSA) diagnosis: a cost-minimization study," *Sleep Breath.*, vol. 1, p. 1, 2021, doi: 10.1007/S11325-021-02527-5.

[108] A. Moffa *et al.*, "A new telemedicine-based sleep service using WatchPAT ® ONE for patients with suspected OSA : what does the patient experience ?," pp. 1–8, 2025.

[109] N. Devani, R. X. A. Pramono, S. A. Imtiaz, S. Bowyer, E. Rodriguez-Villegas, and S. Mandal, "Accuracy and usability of AcuPebble SA100 for automated diagnosis of obstructive sleep apnoea in the home environment setting: An evaluation study," *BMJ Open*, vol. 11, no. 12, pp. 1–10, 2021, doi: 10.1136/bmjopen-2020-046803.

[110] S. Mehrnaz, S. Saha, P. Hadi, F. Rudzicz, and A. Yadollahi, “Snoring Sound Classification from Respiratory Signal,” in *2016 38th Annual International Conference of the IEEE Engineering in Medicine and Biology Society (EMBC)*, 2016, pp. 3215–3218.

[111] T. C. Morata, W. Gong, C. Tikka, A. G. Samelli, and J. H. Verbeek, “Hearing protection field attenuation estimation systems and associated training for reducing workers’ exposure to noise,” *Cochrane Database Syst. Rev.*, vol. 2024, no. 5, 2024, doi: 10.1002/14651858.CD015066.pub2.

[112] N. Natarajan, S. Batts, and K. M. Stankovic, “Noise-Induced Hearing Loss.,” *J. Clin. Med.*, vol. 12, no. 6, p. 12, Mar. 2023, doi: 10.3390/JCM12062347/S1.

[113] K. H. Chen, S. Bin Su, and K. T. Chen, “An overview of occupational noise-induced hearing loss among workers: epidemiology, pathogenesis, and preventive measures,” *Environ. Health Prev. Med.*, vol. 25, no. 1, pp. 1–10, 2020, doi: 10.1186/s12199-020-00906-0.

[114] J. Borell, A. Osvalder, and B. Aryana, “Evaluating the Correct Usage, Comfort and Fit of Personal Protective Equipment in Construction Work,” *Ergon. Des.*, vol. 129, pp. 67–74, 2024, doi: 10.54941/ahfe1004812.

[115] M. C. I. Madahana, J. E. D. Ekoru, B. Sebothoma, and K. Khoza-Shangase, “Development of an artificial intelligence based occupational noise induced hearing loss early warning system for mine workers,” *Front. Neurosci.*, vol. 18, no. March, pp. 1–12, 2024, doi: 10.3389/fnins.2024.1321357.

[116] M. Jeyaraman, N. Jeyaraman, S. Yadav, A. Nallakumarasamy, K. P. Iyengar, and V. Jain, “Impact of Excessive Noise Generation in Orthopaedic Operating Theatres: A Comprehensive Review,” *Cureus*, vol. 16, no. 2, 2024, doi: 10.7759/cureus.54469.

[117] T. C. Wang *et al.*, “Impact of occupational noise exposure on the hearing level in hospital staffs: a longitudinal study,” *Environ. Sci. Pollut. Res.*, vol. 31, no. 16, pp. 24129–24138, 2024, doi: 10.1007/s11356-024-32747-7.

[118] A. Glans, J. Wilén, B. Hansson, Audulv, and L. Lindgren, “Managing acoustic noise within MRI: A qualitative interview study among Swedish radiographers,” *Radiography*, vol. 30, no. 3, pp. 889–895, 2024, doi: 10.1016/j.radi.2024.04.002.

[119] L. E. Kinsler, A. R. Frey, A. B. Coppens, and J. V. Sanders, *Fundamentals of Acoustics, 4th Edition*.

[120] W. Lee and H. B. Kwon, “Vibroacoustic analysis of dental air turbine noise,” *BDJ Open*, vol. 8, no. 1, pp. 1–7, 2022, doi: 10.1038/s41405-022-00117-5.

[121] T. Yamada, S. Kuwano, S. Ebisu, and M. Hayashi, "Statistical Analysis for Subjective and Objective Evaluations of Dental Drill Sounds," *PLoS One*, vol. 11, no. 7, Jul. 2016, doi: 10.1371/JOURNAL.PONE.0159926.

[122] S. Theodoroff and R. Folmer, "Hearing loss associated with long-term exposure to high-speed dental handpieces.," *Gen Dent.*, vol. 63, no. 3, pp. 71–6, 2015.

[123] H. O. Ahmed and W. J. Ali, "Noise levels, noise annoyance, and hearing-related problems in a dental college," *http://dx.doi.org/10.1080/19338244.2016.1179169*, vol. 72, no. 3, pp. 159–165, May 2016, doi: 10.1080/19338244.2016.1179169.

[124] K. Henneberry, S. Hilland, and S. K. Haslam, "Are dental hygienists at risk for noise-induced hearing loss? A literature review," *Can. J. Dent. Hyg.*, vol. 55, no. 2, p. 110, Jun. 2021, Accessed: Jun. 26, 2023. [Online]. Available: /pmc/articles/PMC8219068/

[125] J. Myers, A. John, S. Kimball, and T. Fruits, "Prevalence of tinnitus and noise-induced hearing loss in dentists," *Noise Health*, vol. 18, no. 85, pp. 347–354, Nov. 2016, doi: 10.4103/1463-1741.195809.

[126] K. K. Gulia and V. M. Kumar, "Sleep disorders in the elderly: a growing challenge," *Psychogeriatrics*, vol. 18, no. 3, pp. 155–165, May 2018, doi: 10.1111/PSYG.12319.

[127] H. Moshammer, M. Kundi, P. Wallner, A. Herbst, A. Feuerstein, and H. P. Hutter, "Early prognosis of noise-induced hearing loss," *Occup. Environ. Med.*, vol. 72, no. 2, pp. 85–89, Feb. 2015, doi: 10.1136/OEMED-2014-102200.

[128] C. Tikka, J. H. Verbeek, E. Kateman, T. C. Morata, W. A. Dreschler, and S. Ferrite, "Interventions to prevent occupational noise-induced hearing loss," *Cochrane Database Syst. Rev.*, vol. 2017, no. 7, 2017, doi: 10.1002/14651858.CD006396.pub4.

[129] E. Sorainen and E. Rytkönen, "High-Frequency Noise in Dentistry," *AIHA J (Fairfax, Va)*, vol. 63, no. 2, pp. 231–233, Mar. 2002, doi: 10.1080/15428110208984709.

[130] "Occupational Noise Exposure - Revised Criteria 1998, U.S. DEPARTMENT OF HEALTH AND HUMAN SERVICES."

[131] R. Paramashivaiah and M. L. V. Prabhuji, "Mechanized scaling with ultrasonics: Perils and proactive measures," *J. Indian Soc. Periodontol.*, vol. 17, no. 4, p. 423, Jul. 2013, doi: 10.4103/0972-124X.118310.

[132] K. W. Ma, H. M. Wong, and C. M. Mak, "Dental Environmental Noise Evaluation

and Health Risk Model Construction to Dental Professionals," *Int. J. Environ. Res. Public Health*, vol. 14, no. 9, Sep. 2017, doi: 10.3390/IJERPH14091084.

[133] C. G. Sidley, "Prevalence of tinnitus and hearing loss in South African dentists and investigation into possible connections with noise levels and frequencies in the dental environment," University of Stellenbosch, 2004.

[134] H. M. Elmehdi, "Noise Levels in UAE Dental Clinics: Health Impact on Dental Healthcare Professionals," *J. Public Health (Bangkok).*, vol. 2, no. 4, pp. 189–192, 2013, doi: 10.5963/PHF0204002.

[135] J. Spomer, C. G. Estrich, D. Halpin, R. D. Lipman, and M. W. B. Araujo, "Clinician perceptions of 4 hearing protection devices," *JDR Clin. Transl. Res.*, vol. 2, no. 4, pp. 363–369, 2017, doi: 10.1177/2380084417715599.

[136] S. H. Sha, R. Taylor, A. Forge, and J. Schacht, "Differential vulnerability of basal and apical hair cells is based on intrinsic susceptibility to free radicals," *Hear. Res.*, vol. 155, no. 1–2, pp. 1–8, 2001, doi: 10.1016/S0378-5955(01)00224-6.

[137] M. Casale *et al.*, "Idiopathic sensorineural hearing loss is associated with endothelial dysfunction," *IJC Hear. Vasc.*, vol. 12, pp. 32–33, Sep. 2016, doi: 10.1016/J.IJCHA.2016.05.001.

[138] T. Nakashima *et al.*, "Disorders of cochlear blood flow," *Brain Res. Rev.*, vol. 43, no. 1, pp. 17–28, 2003, doi: 10.1016/S0165-0173(03)00189-9.

[139] G. A. Messano and S. Petti, "General dental practitioners and hearing impairment," *J. Dent.*, vol. 40, no. 10, pp. 821–828, Oct. 2012, doi: 10.1016/J.JDENT.2012.06.006.

[140] M. K. Gurbuz, T. Çatli, C. Cingi, A. Yaz, and C. Bal, "Occupational safety threats among dental personnel and related risk factors," *J. Craniofac. Surg.*, vol. 24, no. 6, Nov. 2013, doi: 10.1097/SCS.0B013E3182A28B80.

[141] B. Willershausen *et al.*, "Hearing assessment in dental practitioners and other academic professionals from an urban setting," *Head Face Med.*, vol. 10, no. 1, Jan. 2014, doi: 10.1186/1746-160X-10-1.

[142] H. O. Ahmed and W. J. Ali, "Noise levels, noise annoyance, and hearing-related problems in a dental college," *http://dx.doi.org/10.1080/19338244.2016.1179169*, vol. 72, no. 3, pp. 159–165, May 2016, doi: 10.1080/19338244.2016.1179169.

[143] N. H. Al-Rawi *et al.*, "Occupational noise-induced hearing loss among dental professionals.," *Quintessence Int.*, vol. 50, no. 3, pp. 245–250, 2019, doi: 10.3290/j.qi.a41907.

[144] C. Kwak and W. Han, "The effectiveness of hearing protection devices: A systematic review and meta-analysis," *Int. J. Environ. Res. Public Health*, vol. 18, no. 21, pp. 1–22, 2021, doi: 10.3390/ijerph182111693.

[145] C. J. Smalt *et al.*, "The Effect of Hearing-Protection Devices on Auditory Situational Awareness and Listening Effort," *Ear Hear.*, vol. 41, no. 1, pp. 82–94, 2020, doi: 10.1097/AUD.0000000000000733.

[146] D. C. Byrne and C. V. Palmer, "Comparison of Speech Intelligibility Measures for An Electronic Amplifying Earmuff and An Identical Passive Attenuation Device," *Audiol. Res. 2012, Vol. 2, Page e5*, vol. 2, no. 1, p. e5, Feb. 2012, doi: 10.4081/AUDIORES.2012.E5.

[147] J. B. Tufts and T. Frank, "Speech production in noise with and without hearing protection," *J. Acoust. Soc. Am.*, vol. 114, no. 2, pp. 1069–1080, Aug. 2003, doi: 10.1121/1.1592165.

[148] C. Giguère, C. Laroche, and V. Vaillancourt, "The interaction of hearing loss and level-dependent hearing protection on speech recognition in noise," *Int. J. Audiol.*, vol. 54 Suppl 1, pp. S9–S18, Feb. 2015, doi: 10.3109/14992027.2014.973540.

[149] C. Manning, T. Mermagen, and A. Scharine, "The effect of sensorineural hearing loss and tinnitus on speech recognition over air and bone conduction military communications headsets," *Hear. Res.*, vol. 349, pp. 67–75, Jun. 2017, doi: 10.1016/J.HEARES.2016.10.019.

[150] M. Karami, M. Aliabadi, R. Golmohammadi, and M. Hamidi Nahrani, "The effect of hearing protection devices on speech intelligibility of Persian employees," *BMC Res. Notes*, vol. 13, no. 1, pp. 4–9, 2020, doi: 10.1186/s13104-020-05374-x.

List of Ph.D. Candidate Publications

Peer-Reviewed Journals

1. **Giorgi L**, Nardelli D, Moffa A, Iafrati F, Di Giovanni S, Olszewska E, Baptista P, Sabatino L, Casale M. Advancements in Obstructive Sleep Apnea Diagnosis and Screening Through Artificial Intelligence: A Systematic Review. *Healthcare*. 2025; 13(2):181. DOI: 10.3390/healthcare13020181
2. Moffa A, Iafrati F, **Giorgi L**, Nardelli D, Carnuccio L, Baptista P, Olszewska E, Casale M. Clinical Evidence of the Use of Mepolizumab in the Treatment of Chronic Rhinosinusitis with Nasal Polyps: A Prospective Observational Study. *Healthcare*. 2025; 13(4):419. DOI: 10.3390/healthcare13040419
3. **Giorgi L,** Moffa A, Mattaroccia M, Lopez MA, Schena E, Casale M. Design, Development, and Testing of a New Device to Prevent High-Frequency Noise-Induced Damage: The "Dynamic Earplug". Inventions. 2025; 10(1):2. DOI: 10.3390/inventions10010002
4. Moffa A, **Giorgi L**, Nardelli D, Ferro A, Capuano MC, Iafrati F, Iannella G, Baptista PM, Casale M. A new telemedicine-based sleep service using WatchPAT® ONE for patients with suspected OSA: what does the patient experience? *Sleep Breath* 29, 47 (2025). DOI: 10.1007/s11325-024-03218-7
5. Moffa A., **Giorgi L.**, Nardelli D., Iafrati F., Iannella G., Magliulo G., Baptista P., Vicini C., Casale M. The Potential Effect of Changing Patient Position on Snoring: A Systematic Review. *J. Pers. Med.* (2024), *14*, 715. DOI: 10.3390/jpm14070715
6. Moffa A, **Giorgi L**, Nardelli D, Iafrati F, Iannella G, Lugo R, Baptista PM, Casale M. Supine or non-supine sleep apnea events: which can be treated better with Barbed Pharyngoplasty? *Sleep Breath* 28, 2107–2115 (2024). DOI: 10.1007/s11325-024-03127-9
7. Moffa A, **Giorgi L**, Nardelli D, Iafrati F, Iannella G, Lugo R, Baptista PM, Vicini C, Casale M. The potential impact of new remodelling intrapharynegal OSA surgery on sleep architecture: a preliminary investigation. *Sleep Breath* 29 (2024). DOI: 10.1007/s11325-024-03222-x
8. **Giorgi L.,** Moffa A., Pericone G., Galantai D., De Benedetto L., Jacobowitz O., Vicini C., Lugo R., Baptista P., Casale M. "Barbed Pharyngoplasty simulation using a 3D-

printed model: design and validation study.", *Sleep and Breathing* (2024). DOI: 10.1007/s11325-024-03067-4

9. Moffa A., Nardelli D., **Giorgi L.**, Di Giovanni S., Carnuccio L., Mangino C., Baptista P., Vacca M., Casale M. Platelet-Rich Plasma for Patients with Olfactory Dysfunction: Myth or Reality? A Systematic Review. *J. Clin. Med.* (2024), *13*, 782. DOI: 10.3390/jcm13030782
10. Casale M, Moffa A, **Giorgi L**, Pierri M, Lugo R, Jacobowitz O, Baptista P. Could the use of a new novel bipolar radiofrequency device (Aerin) improve nasal valve collapse? A systematic review and meta-analysis. *J of Otolaryngol - Head & Neck Surg* 52, 42 (2023). DOI: 10.1186/s40463-023-00644-7
11. Francia C., Lugo R., Moffa A., Casale M., **Giorgi L.**, Iafrati F., Di Giovanni S., Baptista P. Defining Epiglottic Collapses Patterns in Obstructive Sleep Apnea Patients: Francia-Lugo Classification. *Healthcare* (2023), *11*, 2874. DOI: 10.3390/healthcare11212874
12. Sabatino L., Moffa A., Iafrati F., Di Giovanni S., De Benedetto L., **Giorgi L.**, Baptista P., Vicini C., De Vito A., Casale M. A New Lighting System for Surgical Vision Optimization in Barbed Pharyngoplasty for OSA. *J. Pers. Med.* (2023), *13*, 1320. DOI: 10.3390/jpm13091320
13. De Benedetto L., Moffa A., Baptista P., Di Giovanni S., **Giorgi L**., Verri M., Taffon C., Crescenzi A., Casale M. Potential Use of Vivascope for Real-Time Histological Evaluation in Endoscopic Laryngeal Surgery. *J. Pers. Med.* (2023), *13*, 1252. DOI: 10.3390/jpm13081252
14. Baptista P., Moffa A., **Giorgi L**., Casale M. Randomized Clinical Trial to Evaluate the Efficacy and Tolerability of Nebulized Hyaluronic Acid and Xylitol Based Solution after Septoturbinoplasty. *J. Pers. Med.* (2023), *13*, 1160. DOI: 10.3390/jpm13071160
15. Moffa A., **Giorgi L**., Carnuccio L., Lugo R., Baptista P., Casale M. Comparison of Intranasal Steroid Application Using Nasal Spray and Spray-Sol to Treat Allergic Rhinitis: A Preliminary Investigation. *J. Clin. Med.* (2023), *12*, 3492. DOI: 10.3390/jcm12103492
16. Casale M., Moffa A., Pierri M., Baptista P., **Giorgi L.** High-Definition 3D Exoscope-Assisted Barbed Pharyngoplasty for OSAS and Snoring: Better Than Live. *Healthcare* (2023), *11*, 596. DOI: 10.3390/healthcare11040596

17. Moffa A, **Giorgi L**, Carnuccio L, Cassano M, Lugo R, Baptista P, Casale M. Barbed Pharyngoplasty for Snoring: Does It Meet the Expectations? A Systematic Review. *Healthcare* (2023); 11(3):435. DOI: 10.3390/healthcare11030435
18. Moffa A, **Giorgi L**, Carnuccio L, Baptista P, Schena E, Casale M. Effects of New "High Breathability" FFP2 Masks in Healthcare Workers during the "COVID-19 Era". *Journal of Biological Regulators and Homeostatic Agents.* (2022), DOI: 10.23812/j.biol.regul.homeost.agents.20223604.96
19. Moffa A, **Giorgi L**, Carnuccio L, Mangino C, Lugo R, Baptista P, Casale M. New diagnostic tools to screen and assess a still too underestimated disease: the role of the wrist-worn peripheral arterial tonometry device-a systematic review. *Sleep Breath.* (2022) Aug 29. DOI: 10.1007/s11325-022-02700-4.
20. Moffa A, **Giorgi L**, Carnuccio L, Cassano M, Montevecchi F, Baptista P, Casale M. New non-invasive electrical stimulation devices for treatment of snoring and obstructive sleep apnoea: a systematic review. *Sleep Breath.* (2022) Apr 23. DOI: 10.1007/s11325-022-02615-0.
21. Moffa A, **Giorgi L,** Cassano M, Lugo R, Baptista P, Casale M. Complications and side effects after barbed pharyngoplasty: a systematic review. *Sleep Breath.* (2022) Feb 25. DOI: 10.1007/s11325-022-02585-3.
22. Di Pumpo M, Nurchis MC, Moffa A, **Giorgi L**, Sabatino L, Baptista P, Sommella L, Casale M, Damiani G. Multiple-access versus telemedicine home-based sleep apnea testing for obstructive sleep apnea (OSA) diagnosis: a cost-minimization study. *Sleep Breath* 26, 1641–1647 (2022). https://doi.org/10.1007/s11325-021-02527-5
23. Baptista P, Diaz Zufiaurre N, Garaycochea O, Alcalde Navarrete JM, Moffa A, **Giorgi L**, Casale M, O'Connor-Reina C, Plaza G. TORS as Part of Multilevel Surgery in OSA: The Importance of Careful Patient Selection and Outcomes. *J Clin Med.* (2022) Feb 14;11(4):990. DOI: 10.3390/jcm11040990. PMID: 35207264; PMCID: PMC8878188.
24. Casale M, Moffa A, **Giorgi L**, Sabatino L, Pierri M, Lugo R, Baptista P, Rinaldi V. No-cutting remodelling intra-pharyngeal surgery can avoid CPAP in selected OSA patients: myth or reality? *Eur Arch Otorhinolaryngol.* (2022) Oct;279(10):5039-5045. DOI: 10.1007/s00405-022-07261-6.
25. Moffa A, **Giorgi L**, Fiore V, Baptista P, Cassano M, Casale M. Water protection in paediatric patients with ventilation tubes: Myth or reality? A systematic review.

Acta Otorrinolaringol Esp (Engl Ed). (2022) Jul-Aug;73(4):246-254. doi: 10.1016/j.otoeng.2021.05.003. PMID: 35908817.

26. Moffa A, **Giorgi L**, Costantino A, De Benedetto L, Cassano M, Spriano G, Mercante G, De Virgilio A, Casale M. Accuracy of autofluorescence and chemiluminescence in the diagnosis of oral Dysplasia and Carcinoma: A systematic review and Meta-analysis. *Oral Oncol.* (2021) Oct; 121:105482. doi: 10.1016/j.oraloncology.2021.105482. Epub 2021 Aug 13. PMID: 34399191.
27. Moffa A, **Giorgi L**, Cassano M, Rinaldi V, Natalizia A, Bressi F, Guglielmelli E, Casale M. Non-implantable bone conduction device for hearing loss: a systematic review. Journal of Biological Regulators and Homeostatic Agents. 2020 Sep-Oct;34(5 Suppl. 3):97-110. Technology in Medicine. PMID: 33386039.

Peer-Reviewed Conference Proceedings

1. **L. Giorgi**, F. Di Marco, D. Lo Presti, C. Massaroni, C. Romano, A. Moffa, M. Casale, E. Schena "Assessment of an Innovative Smart Face Mask for the Estimation of Respiratory Rate in Static and Dynamic Conditions" *2024 IEEE International Workshop on Metrology for Industry 4.0 & IoT (MetroInd4.0&IoT)*
2. **L. Giorgi**, F. Di Marco, D. Lo Presti, C. Massaroni, C. Romano, A. Moffa, M. Casale, E. Schena "An innovative smart face mask for the estimation of respiratory rate: design, development and feasibility assessment," *2023 IEEE International Workshop on Metrology for Industry 4.0 & IoT (MetroInd4.0&IoT)*, Brescia, Italy, 2023, pp. 189-193, doi: 10.1109/MetroInd4.0IoT57462.2023.10180151.

Book Chapters

1. Casale M, Moffa A, **Giorgi L**, Montevecchi F, Baptista P. “Different Barbed Pharyngoplasty Techniques for Retropalatal Collapse in Obstructive Sleep Apnoea Patients: A Systematic Review.” In: Vicini, C., Salamanca, F., Iannella, G. (eds) Barbed Pharyngoplasty and Sleep Disordered Breathing. *Springer*, Cham. Published 03 September 2022